The Dissertation Committee for Joshua Daniel Rhodes
certifies that this is the approved version of the following dissertation:

Optimal Residential Energy Consumption, Prediction, and Analysis

Committee:

Michael E. Webber, Supervisor

Michael F. Blackhurst

Thomas F. Edgar

Carey King

Atila Noveselac

Optimal Residential Energy Consumption, Prediction, and Analysis

by

Joshua Daniel Rhodes, B.S., M.S., M.S.E

DISSERTATION

Presented to the Faculty of the Graduate School of

The University of Texas at Austin

in Partial Fulfillment

of the Requirements

for the Degree of

DOCTOR OF PHILOSOPHY

The University of Texas at Austin

May 2014

Dedicated to my father Daniel Wayne Rhodes, PhD, whose never ending and vocal confidence in my ability to do anything is the reason I am writing such a document today. Thanks for teaching me long division when I was 7 and inspiring the confidence in myself that got me this far. I'd also like to thank my mother, who never let me quit and did her best to make sure that I would have a life long interest in learning. Also a huge thanks to my wife, Jessie, for putting up with being so poor for so long.

Acknowledgments

There are so many people that have helped make this possible. Thanks to my advisor Dr. Michael E. Webber for taking a chance on me years ago, for giving me such academic freedom and trust, for being so open and honest, for there being no doubt that he wanted me to succeed in and out of school, and for sending me all over North America to learn. Thanks to Brent Stephens for helping me get through my first journal and conference paper and helping me get started on this type of writing. A big thanks to Charlie Upshaw for not only working on so many things with me and becoming a business partner, but becoming such a good friend. Thanks to Wesley Cole for working together on so many different projects and providing great feedback. Thanks to Pecan Street Inc., esp. Suzanne Russo, for helping me through the early times with the data and trusting me with so much of it. Thanks to Chris Holcomb for helping me understand the data and also being a friend. Thanks to David Walling (for answering all my simple questions) and Paul Navratil and the Texas Advanced Computing Center for help with their truly impressive super computers. And God, thank you for the genetics and the environment that are by far better than most get and I deserve.

I'd also like to acknowledge those who funded my student career at UT: ASHRAE, the Doris Duke Charitable Foundation, Pecan Street Inc., the Department of Energy, and the Webber Energy Group, thanks to you all.

Optimal Residential Energy Consumption, Prediction, and Analysis

Joshua Daniel Rhodes, Ph.D.
The University of Texas at Austin, 2014

Supervisor: Michael E. Webber

In the United States, buildings are responsible for 40.36 Quads (40.36×10^{15} BTU) of total primary energy consumption per year, 22.15 of which are used in residential buildings (reference year 2010). Also, the United States residential sector is responsible for about 20% of United States carbon emissions or about 4% of the world's total. While there are over 130 million residential units in the United States, only 0.1% of R&D is spent in the residential sector. This means the residential sector represents an underinvested opportunity for energy savings. Tackling that problem, this dissertation presents work that is focused on assessing, analyzing, and optimizing how residential buildings use and generate energy.

This work presents an analysis of a unique dataset of 4971 energy audits performed on homes in Austin, Texas in 2009–2010. The analysis quantifies the prevalence of typical air-conditioner design and installation issues such as low efficiency, oversizing, duct leakage, and low measured capacity, then estimates the impacts that resolving these issues would have on peak power demand and cooling energy consumption. It is estimated that air-conditioner use in single-family residences currently accounts for 17–18% of peak demand in Austin, and that improving equipment efficiency alone could save up to 205 MW, or 8%, of peak demand. It was also found

that 31% of systems in this study were oversized, leading to up to 41 MW of excess peak demand. Replacing oversized systems with correctly sized higher efficiency units has the potential for further savings of up to 81 MW. Also, the mean system could achieve 18% and 20% in cooling energy savings by sealing duct leaks and servicing air-conditioning units to achieve 100% of nominal capacity, respectively.

A different dataset of measured whole-home electricity consumption from 103 homes in Austin, TX was analyzed to 1) determine the shape of seasonally-resolved residential demand profiles, 2) determine the optimal number of normalized representative residential electricity use profiles within each season, and 3) draw correlations to the different profiles based on survey data from the occupants of the 103 homes. Within each season, homes with similar hourly electricity use patterns were clustered into groups using the *k-means* clustering algorithm. The number of groups within each season was determined by comparing 30 different optimal clustering criteria. Then probit regression was performed to determine if homeowner survey responses could serve as explanatory variables for the clustering results. This analysis found that Austin homes typically fall into one of two seasonal groups. Because these groups differ in temporal energy use and the wholesale electricity price is temporal, homes in one group use more expensive electricity than others. The probit regression results indicated that variables such as whether or not someone worked from home, the number of hours of television watched per week, and level of education have significant correlation with average profile shape, but that significant indicators of profile shape can vary across seasons. Also, these results point to markers of households that might be more impacted by time-of-use (TOU) or real time price (RTP) electricity rates and can act as predictors as to how changing local demographics can change local electricity demand patterns.

This work also considers the effect of the placement (azimuth and tilt) of fixed solar PV systems on their total energy production, peak power production, and economic value given local solar radiation, weather, and electricity market prices and rate structures. This model was then used to calculate the output of solar PV systems across a range of azimuths and tilts to find the energetically and economically optimal placement. The result of this method, which concludes that the optimal placement can vary with a multitude of conditions, challenges the default due-south placement that is conventional for typical installations. For Austin, TX the optimal azimuth to maximize energy production is about 187–188°, or 7–8° west of south, while the optimal azimuth to maximize economic output based on the value of the solar energy produced is about 200–230° or 20–50° west of south. The differences between due south (which is the conventional orientation) and the optimal placement were on the order of 1–7%. For the rest of the US and for most locations the energetically optimal solar PV azimuth is within 10° of south. Considering the temporal value of the solar energy produced from spatially-resolved market conditions derived from local time-of-use rates, the optimal placement shifts to a west-of-south azimuth in attempt to align solar energy production with higher afternoon prices and higher grid stress times. There are some locations particularly on the west coast that have west-of-south energy optimal placements, possibly due to typical morning clouds or fog. These results have the potential to be significant for solar PV installations: utilities might alter rate structures to encourage solar generation that is more coincident with peak demand, utilities might also use west-of-south solar placements as a hedge against future wholesale electricity price volatility, building codes might encourage buildings to match roof azimuths with local optimal solar PV generation placements, and calculations of the true value of solar in optimal and non-optimal placements can be more accurate.

This analysis also uses a dataset of whole home electricity consumption to consider the role of small distributed fuel cells in managing energy and thermal flows in the home. The analysis determines that the average home in Austin, TX could utilize a 5.5 kW fuel cell either for total generation or backup, and the average home could operate as its own micro-grid while not sacrificing core functionality. Matching the thermal output of a possibly smaller fuel cell, used in combined heat and power mode (CHP), to an absorption refrigeration system in place of traditional space cooling further reduces the needed capacity. Lastly, it is estimated that the system efficiency could possibly double by transporting natural gas to the end user to be converted into electricity and heat as compared with traditional methods of using natural gas for power generation followed by electricity delivery.

Results from two regression analyses of total energy use and energy use reductions following energy efficiency retrofits are also presented. The first model shows that home size and age were positively correlated with total yearly energy use, but there is significant correlation of reduced yearly energy use with increased energy and water knowledge. This result might lend some support for increased energy and water education campaigns. The second model (retrofit analysis) also provided results that utilities can use to assess the value of residential retrofit rebates as compared to the cost of acquiring energy on the wholesale market. The second model indicates that the current level of rebates is cost effective for the utility (on a $ per kWh offset basis) for all three considered retrofits (air-sealing, attic insulation, and air-conditioner replacement) and the rebates could be increased while still being below the cost of acquiring electricity on the wholesale market. Considering an average of $0.113/kWh for residential electric service, both the air-sealing and increased attic insulation seem to make economic sense for the homeowner given current rebate structures.

Table of Contents

List of Tables

List of Figures

Chapter 1

Introduction

1.1 Purpose and motivation

This dissertation presents work that is focused on assessing, analyzing, and optimizing how residential buildings use and generate energy. The work within attempts to assess the amount of efficiency to be gained through improvements in residential energy systems, the drivers behind residential electric demand profiles, and optimal strategies for renewable residential distributed generation systems.

In the United States, buildings are responsible for 40.36 Quads (40.36×10^{15} BTU), or about 40% of total primary energy consumption per year, 22.15 Quads or about 22% of which are used in residential buildings [3]. Also, the United States residential sector is responsible for about 20% of United States carbon emissions or about 4% of the world's total [4]. While there are over 130 million residential units in the United States, only 0.1% of R&D is spent in the residential sector [5]. This means the residential sector represents an underinvested opportunity for energy savings. Residential structures are unique in form, build, and use. Even tract homes built by the same builder in the same time period can be similar in outward appearance, but vary greatly in terms of efficiency and energy use. Residential air-conditioning systems are particularly disruptive to the electric grid and create significant swings in demand. In Texas, 7.7 million households (both single-family and multi-family units) use approximately 43 TWh of electricity for air-conditioning annually [6] – about 13% of total electricity use in Texas. The percentage of electrical load on the

Electric Reliability Council of Texas (ERCOT) electric grid attributed to residential users increases from about 20% in the spring to 48% in the summer of 2010 (400% real increase, 6,139 vs. 30,735 MW in 2010), mostly due to the operation of residential air-conditioning systems [7].

Numerous studies have evaluated the energy savings associated with increasing the energy efficiency of the United States residential building stock [8–22]. Many studies have focused on various aspects of residential buildings such as heating, ventilation, and air-conditioning (HVAC) equipment, façade, air tightness, insulation levels, duct leakage, and construction type. Evidence suggests that there is significant value in intensive energy commissioning and monitoring of buildings [23] and that significant numbers of residential buildings built to energy codes are non-compliant [24, 25]. Although many residential efficiency standards exist [26,27], few studies [13] can estimate residential resource consumption and savings for a large, statistically significant portion of a local residential building stock because of a lack of data, particularly for a hot and humid cooling climate such as Austin, Texas. This dissertation proposes to do that analysis through the assessment of residential energy audits.

While the drivers of macro-level, aggregate energy use are current topics of study [28], the factors affecting residential energy use at finely-resolved timescales are poorly understood. This work seeks to fill part of that knowledge gap by identifying correlations between electric customer survey data and electricity use profiles. Understanding temporally-resolved electricity consumption patterns and their influencing factors could potentially lead to more robust energy modeling, more precise demand forecasts, and more effective energy conservation and peak reduction campaigns. One relatively new method of electricity profile analysis involves clustering like profiles. Clustering analysis has currently been limited to generating typical load profiles, grouping like customers, or finding outliers [29–35]. This analysis seeks to take the body of knowledge a step further by leveraging the comprehensive data set available from a local smart grid demonstration project [36] and explore the drivers behind the derived groups of electricity customers.

Knowing what to measure or ask in order to quantify and predict resource demands of residential buildings will be a significant contribution of this dissertation. Few studies have analyzed real measured energy use, audit data, and/or survey data for more than a few homes [37–40]. Some recent work has correlated the effect of surveys and audit data to total annual residential electrical energy usage in a heating climate [38] and narrowed the number of field questions and measurements from 60 to 8. This type of analysis will be helpful in developing the framework from which to assess the most important factors that contribute to temporal residential electric demand profiles, which to date (to the best of my knowledge and literature search), has not been studied. Given that the typical grid load curve in Texas is significantly affected by residential energy consumption [7], knowledge of the most important factors that contribute to residential electric demand profiles would be helpful in shaping policy tools directed at reducing electric grid strain. This dissertation will strive to provide this novel analysis.

While it is better to increase the energy efficiency of homes before installing energy generation systems [41, 42], low carbon energy sources such as rooftop solar PV systems are becoming popular. There has been some research on the strategic placement of residential solar for the stability of the grid [43–45], for the economic benefit of the homeowner [46–48], as well as the correlation [49] and the impact [50] of solar production to electricity spot prices. However, there is a lack of analysis using real data that ties these concepts together to show the impact of placement of residential solar PV on temporal generation and how that aligns with the grid as a whole and the price signals that the utility receives. This dissertation proposes to fill that knowledge gap.

To that end, this analysis considers the effect of the placement (azimuth and tilt) of fixed solar PV systems on their total energy production, peak power production, and the economic value of that energy production. Solar energy production is important for a multitude of reasons including reduced carbon emissions; the fuel is free, renewable, domestic and distributed; it contributes to energy equity; and because the prices of solar panels are falling [51–54]. However, since solar energy production curves do not always precisely align with maximum home or electricity grid load, even placements that might be non-optimal from an energy production basis might be optimal on an economic or peak power production basis [55,56]. Most studies have been limited to either calculations of incident solar radiation on an optimal plane or limited to a small location [57, 58]. This analysis extends the body of knowledge by not only considering the amount of solar radiation hitting the optimal collector plane, but estimating the amount of energy and value of the energy produced through fixed solar PV systems, which can depend on environmental and system aspects, such as the temperature of the solar PV system itself and which prices are considered. As the realized price of solar energy gets closer to grid parity, new home builders might choose to orient homes such that sections of the roof are optimally aligned for solar generation or local municipalities might mandate it. The 2015 Austin Energy Code mandates that all new homes in Austin must be net-zero energy capable. Thus since solar placement matters for energy and temporal power production, this analysis could possibly inform that process, including variable rebates for more valuable solar placements. This analysis also extends the consideration of the value of solar energy produced by using time-of-use rates throughout the continental US as a proxy for average local grid conditions.

Common types of distributed generation include rooftop solar PV and small wind electric power generation. These types of generation, while carbon friendly, are not dispatchable, meaning that the amount of power they produce is not controllable like a typical power plant. Therefore, a grid that relies more on distributed generation of these types would benefit from electricity storage or firming power (such as from dispatchable generating units on stand-by), to provide continuous service even with the added variability. This analysis considers small-scale fuel cells for that purpose. Numerous computer models and prototype units have been built to test the ability of small-scale fuel cells to perform in residential-specific situations [59–63]. While most analyses consider the potential for fuel cells to match average loads or ramp with dynamic loads, this analysis uses real data to optimize the size of the fuel cell needed to provide power and keep the home thermally comfortable.

Engineering calculations of energy saved from residential energy retrofits often give optimistic predictions, but rebound effects can reduce those savings [64]. Many times these interventions are prescriptive-based, not performance based, (i.e. insulation is brought up to a certain level, a building envelope is air tightened, etc.), but there is little measurement and verification (M&V) for how retrofits actually perform. The last analysis in this dissertation provides some actual energy reduction results from homes that have gone through one of Austin Energy's residential energy retrofit programs, along with the associated cost to the homeowner and utility in $/kWh saved.

This dissertation has the following four objectives:

1. *Explore the residential electricity consumption and common air-conditioner design and installation parameters of homes in Austin, Texas,*

2. *Determine the key correlations between homeowners and their temporal energy use in Austin,*

3. *Determine the optimal placement of residential-based solar PV systems for Austin and the greater US, and*

4. *Explore the efficiencies associated with firm distributed generation and residential energy retrofits.*

1.2 Scope and organization

Three research chapters (2-4) explore objectives 1-3 above, and chapter 5 presents work that is related to the three. Each chapter contains an introduction, background/literature review, methods, results, and discussions/conclusions section.

Chapter 2 uses an expansive set of energy audits from Austin Energy's Energy Conservation and Disclosure (ECAD) ordinance to assess the total energy and peak power demand implications of inefficiencies associated with poor energy aspects of homes, including air-conditioning systems. This chapter uses the industry standard Manual J calculation for "right-sizing" air-conditioning units and considers the improvements (energy and peak power demand) that would be associated with aggressive participation in residential energy retrofit programs.

Chapter 3 explores the correlations between homeowner survey results and seasonal, temporal (hourly) power demand profiles. A probit regression model built from the data is used to give insight into the types of profiles that one might expect from a given demographic of persons inhabiting a home in Austin.

Chapter 4 considers the effect of solar radiation and economics toward the optimal placement of solar PV systems. A fundamental model of a generic solar

PV system was constructed and optimized for various locations and prices including wholesale market prices and electricity rates. The model considers multiple Austin inputs and then is extended to over 1,000 locations across the US.

Chapter 5 has two preliminary sections that 1) look at the ability of a residential-sized natural gas fuel cell to provide distributed firming power for non dispatchable generation sources such as solar PV and reduce distributed electricity demand by generating electricity and providing waste heat for absorption cooling and 2) estimate the costs and measured energy use difference (before and after) of residential energy retrofits on daily energy use for homes in Austin, TX.

This dissertation also includes Appendix A, which is a complementary analysis that compares the output of commercially available residential energy simulation software to actual use in various scenarios including the impacts of various weather data files, thermostat set-point temperatures, and simplified home geometries. This analysis also considers the error associated with homes that use significantly more or less energy per home area than the average and lastly considers the ability of the model to predict inter-daily energy use patterns.

1.3 Major high-level findings from this body of work

The major findings from this body of work include:

1. Single-family residential air-conditioning systems account for about 17-18% of summer peak power demand in Austin, TX.

2. Increasing the efficiency of single-family residential air-conditioning systems could save as much as 205 MW of peak power demand.

3. Right-sizing oversized residential air-conditioning systems could avoid up to 81 MW of peak power demand.

4. Austin Energy could almost double their maximum residential efficiency retrofit rebates and still be at price parity with building new power generation.

5. There are typically two groups of residential power demand profiles in each season, one of which tends to use more expensive power than the other.

6. Demographic variables (if persons work from home, how many hours of TV are watched per week, and the amount of computing devices inside the home) can be indicators of what type of power demand profile a home will have.

7. A due south orientation is not always the energy optimum placement for solar PV systems.

8. Temporal pricing schemes such as time-of-use rates and real-time pricing scenarios affect the optimal economic placements for solar PV systems, generally pushing placements to west-of-south.

9. West-of-south solar PV placements could be used as a hedge for utilities against volatile wholesale electricity markets in cooling climates.

10. Small distributed firm combined heat and power generation such as residential sized fuel cells can significantly increase the primary energy efficiency of homes.

11. Homes whose inhabitants scored higher on general energy and water knowledge questions had reduced yearly electricity use.

12. The average "rebate cost" ($/kWh reduced) incurred by Austin Energy (the electric utility for Austin, TX) for residential energy retrofit rebates cost less than yearly average wholesale electricity costs.

13. The average "customer cost" ($/kWh saved) incurred by Austin Energy customers for some residential energy retrofits (air-sealing and attic insulation) cost less than purchasing retail electricity.

The findings listed above are explored further in the following chapters.

Chapter 2

Using energy audits to investigate the impacts of common air-conditioning design and installation issues on peak power demand and energy consumption in Austin, Texas

2.1 Introduction

Air-conditioning* has become ubiquitous in buildings in the developed world [14, 65] and is typically one of the largest summer electrical loads in residential buildings, particularly in cooling climates such as the southern United States. In Texas, 7.7 million households (both single-family and multi-family units) use approximately 43 TWh of electricity for air-conditioning annually [6], and load in Electric Reliability Council of Texas (ERCOT) attributed to residential users increased from 20% (6,139 MW) in the spring to 48% (30,735 MW) in the summer of 2010, mostly due to the seasonal operation of residential air-conditioning systems [7].

*Part of the analysis in this chapter has been published as a journal article [8]:

Rhodes, J.D., Brent Stephens, Michael E.Webber, "Using energy audits to investigate the impacts of common air-conditioning design and installation issues on peak power demand and energy consumption in Austin, Texas", Energy and Buildings 43 (11) (2011) 32713278, DOI: 10.1016/j.enbuild.2011.08.032

and part as a conference paper [9]:

Rhodes, J.D, Brent Stephens, Michael E. Webber, Energy audit analysis of residential air-conditioning systems in Austin, Texas, ASHRAE Transactions 118 (1) (2012) 143150.

Co-authors included Drs. Brent Stephen and Michael E. Webber (supervisor) – their contributions included editing the manuscript.

There is a lack of statistically relevant recent data about the installed base of air-conditioning systems, which leaves a knowledge gap about current air-conditioning operation in the residential sector even though it is particularly important in hot climates. This work uses a database of 4,971 recently performed energy audits on single family homes in Austin, Texas to fill that knowledge gap by 1) investigating the prevalence of the most common air-conditioning system design and installation issues that lead to excess power draw and energy consumption, and 2) estimating the impacts that these issues have on aggregate peak power demand, 3) quantifying the likely distribution of achievable energy savings from retrofits in individual residences, and 4) assessing the potential savings from mass participation in energy retrofit programs. Additionally, several shortcomings in the audit database are identified and recommendations are made of some additional energy audit procedures that can be implemented in order to improve the database.

2.2 Background

Several widespread design and installation issues associated with residential air-conditioning systems have been shown to contribute to these loads in the U.S. by increasing both energy consumption (e.g. sub-optimal airflow rates, low refrigerant charge, and excess duct leakage) and peak power demand (e.g. improper equipment sizing and low equipment efficiency) [13, 22, 66–69]. Duct sealing is a common residential retrofit that has been shown to be an effective means of energy conservation for space conditioning [1, 2, 70]. Some researchers have predicted that sealing duct leaks could also reduce peak power draw of residential air-conditioning units [71], although others have failed to produce this result [72]. Low measured capacity has been identified in several previous studies, e.g. [14], and may be indicative of low airflow rates [67], improper refrigerant charge [68], and excess duct leakage [73].

Previous investigations of these issues have focused on various sample sizes and levels of detail. Some have been case studies using detailed measurements in small samples of residences. James et al. (1997) [66] compared the installed air-conditioner capacity of 368 Florida homes to their Manual J calculation (industry-standard residential HVAC sizing metric) and found that over half were sized to be over 120% of their Manual J calculation. They also found that oversized systems had a 13% increase in peak demand cooling, but no noticeable difference in overall runtimes. Proctor et al. (1997) [67] analyzed 28 residential air-conditioning systems in Phoenix and found substantial defects in their installations – only 18% of systems were correctly charged, airflow across the coils was on average 14% below specification, and the average system was 48% oversized. Stephens et al. (2011) [14] considered 17 residential and light commercial air-conditioning systems and found that all were out of recommended air flow range and that the systems were one average only operating at 62–67% of rated cooling capacities.

Other studies have analyzed large regional mixed residential and commercial data [13,69]. Downey and Proctor (2002) [13] studied a database of 13,000 residential and commercial air-conditioning diagnostic reports from a commercial HVAC computer aided diagnostic tool. They found that 67% of systems needed repair, 57% were improperly charged, and 21% had improper air flow rates. Mowris et al. (2004) [69] analyzed the results of 4,168 air-conditioner field tests in California and found that 72% had improper refrigerant charge and 44% had suboptimal airflow. They found that realized measured efficiency (realized EER) gains for fixed air-conditioners were 17 – 21%. However, only a few previous studies have sample sizes large enough and diverse enough to scale to the utility level. Neme et al. (1999) [22] in a meta analysis of studies found that aggressive energy efficiency upgrades to HVAC systems in the US could yield a national savings of 15,000 TWh, 40 GW of peak demand, and 12 million metric tons of avoided CO_2 per year.

2.3 Energy audit database

Austin, Texas, is unique in that it is one of the few cities in the U.S. that requires an energy audit to be performed on a home before it can be sold. This mandate is part of the City of Austin's Energy Conservation Audit and Disclosure (ECAD) ordinance [74, 75]. A home may be exempted from this ordinance under several conditions, including its participation in utility-sponsored energy efficiency programs within the previous 10 years of the sale of the home, if it is a condominium or manufactured home, or if the change of ownership occurs under a variety of extenuating legal conditions (e.g. foreclosure, exercise of eminent domain, or property settlements). The program hopes to induce investment that increases the energy efficiency of existing homes and also aims to address part of the Austin Climate Protection Plan, which includes avoiding 800 MW of new generating capacity.

There are over 200 companies in the greater Austin area permitted to conduct official ECAD audits. Each auditor receives training by Austin Energy (the local municipally-owned electric utility) and is given a detailed handbook explaining the steps necessary to conduct an official ECAD audit. Individual audits typically cost between $200 and $300 and audit results are all submitted on a uniform document to Austin Energy who then supplies the completed audit to prospective buyers. Auditors' results are internally checked against similar home audits to determine authenticity [76], and non-compliance with the ordinance is a Class C misdemeanor for the party selling the home. Because of the rarity of Austin's energy audit requirements, the recentness of the audits, and the size of the sample, this information forms a unique dataset in terms of scope, size, and content.

While the ECAD ordinance applies to both residential (single and multi-family) and commercial buildings, this analysis considers only single-family residences. This work presents an analysis of a database of 4971 energy audits that were performed on single-family detached homes under the mandatory ECAD ordinance between January 2009 and December 2010. To the best of the authors' knowledge, these audits are the first of their kind for southern climates and this analysis is the first with such an extensive data set. While the results are not directly applicable to other climates, it is expected that some of the findings will have relevance for other southern states, and the methods are general to any climate region.

2.4 Methodology

2.4.1 Energy audit procedure

The ECAD handbook provides instructions to auditors to gather information about the homes, including details related to the cooling and/or heating systems and ductwork, window types and shading, attic insulation, obvious pathways of air infiltration, and the number and types of appliances. Thus, information obtained from the energy audit database was used first to describe general building and system characteristics in the audited homes, including building age, floor area, window type, and attic insulation; age, nominal capacity, and manufacturer-rated efficiency of the primary air-conditioning system; and several other HVAC system parameters, including estimates of system airflow rates, measurements of duct leakage, and measurements of temperature differences across cooling coils. While some parameters were directly measured, many were simply recorded by visual inspection of equipment and building details by the auditors. For example, attic insulation levels were estimated by multiplying the depth of existing insulation in the attic by R-values provided to the auditors for typical insulation types found in homes built over the past century in

Austin (e.g. fiberglass batts, blown-in cellulose, or spray-foam). System airflow rates were not actually measured during the energy audits, but were estimated by using manufacturer's data for the blower or were assumed to be 193 m^3 hr^{-1} per kW of rated capacity (400 ft^3 min^{-1} per ton). Duct leakage measurements were made by installing a calibrated fan at a return grille of the system or an access panel of the air handling unit, taping the remaining supply registers and return grille(s), and measuring the airflow rate required to depressurize the duct system to -25 Pa. These leakage measurements thus represent total duct leakage (supply and return) to both interior and exterior spaces. Additionally, the temperature difference across the cooling coil was measured at the return air intake and immediately after the evaporator coil after the system had been operating at least 15 minutes.

Relevant calculations for four parameters of interest are described in the following sections, including 1) installed nominal air-conditioning system efficiency, 2) air-conditioning system oversizing, 3) excess duct leakage, and 4) measured vs. rated system capacity. After quantifying several parameters for the audited homes in the database, the actual (or estimated) performance of the buildings and their air-conditioning systems was compared against design or nominal values of the same parameters. Differences between the two were used to estimate the impacts on peak demand attributed to common design and installation issues present in the homes, and to estimate the potential energy savings of remedying some of these issues in individual homes. Finally, some of these estimates were scaled to represent the entire single-family residential building stock in Austin, Texas.

2.4.2 Estimating energy impacts of common problems

2.4.2.1 Installed nominal air-conditioning system efficiency

The outdoor condenser-compressor unit and indoor blower fan of a residential air-conditioning system typically accounts for 80–85% of the total power draw of the system [14]. Because the database contained values of nominal system capacities (BTU hr^{-1}) and rated energy efficiency ratios (EER[†], in BTU hr^{-1} W^{-1}), the power draw of the outdoor condenser-compressor units, P, during operation under rated conditions was estimated by Equation 2.1:

$$P = \frac{CAP \times 12 \times (1 + CF)}{EER} \tag{2.1}$$

where P is the peak power draw (kW), CAP is the nominal capacity of the unit (tons), 12 is the unit conversion factor (BTU kW $\mathrm{hr}^{-1}\mathrm{tons}^{-1}\mathrm{W}^{-1}$), EER is the rated efficiency of the unit (BTU hr^{-1} W^{-1}), and CF is the consumption factor used to account for increased power draw at outdoor conditions during the peak hour in Austin that are likely higher than rated conditions. The total maximum power draw that all of the units in the database could theoretically demand if operating at the same time is simply the sum of the individual power draw values. To achieve more realistic estimates of aggregate demand during the peak period it was assumed that 70% of these systems operate during the summer peak hour (best estimate using the high end of hourly runtimes reported in 8 residential air-conditioning systems in Austin in Stephens et al. [14]). Additionally, systems are typically rated at indoor and outdoor temperatures of 26.7°C and 35°C, respectively [77], but the outdoor temperature in Austin is typically higher during the summer peak hour. Thus, rated

[†]SI equivalent = coefficient of performance, or COP – the useful refrigerating effect per power supplied, $\mathrm{kW}_{thermal}$ kW_{power}^{-1}

power draws were scaled to approximately 10% over rated conditions to match a peak summer temperature of 40.6°C [78], using an increase of 1.8 ± 0.8% per °C rise in outdoor temperature, as observed in Stephens et al. [14].

Scenarios were explored where all the homes in the audit database were upgraded to either 12 EER (COP 3.5) and 14 EER (COP 4.1) air-conditioning units, which is consistent with Austin Energy's energy efficiency rebate program. The low and high ranges of improved efficiency were chosen to reflect the requirements of the US Environmental Protection Agency's and US Department of Energy's ENERGY STAR program (which requires a minimum EER of 12, COP 3.5) and the upper end of efficiency available on the market in 2011 (EER 14, COP 4.1). Also the possible reductions in peak power demand from replacing all oversized units (estimated using methods in the subsequent section) with correctly sized units of higher efficiency, either EER 12 (COP 3.5) or EER 14 (COP 4.1) were explored.

2.4.2.2 Air-conditioning oversizing

A custom spreadsheet program was used to perform the Manual J sizing calculations. The Manual J method allows for two different design scenarios: 1) a peak cooling load procedure and 2) an average load procedure. The latter design scheme is typically used for sizing residential HVAC equipment and is used in this analysis. A portion of the calculation is based on the design temperature difference between the inside and outside of the home. The interior conditions were assumed to be 23.9 °C and 50% relative humidity (RH), which is a standard industry assumption [27] and is in the middle of the human comfort zone. Outdoor design conditions for Austin, 35.6 °C and 50% RH, are included in the Manual J literature and were used in the calculations (Manual J is designed to meet the demand of 97.5% of summer cooling hours). The resulting estimated design system capacities (referred to as "correctly sized") were compared to the installed rated capacities in order to determine the prevalence of oversized systems in the audited homes. An installed unit with a capacity that is greater than or equal to 120% of the Manual J calculation is considered oversized for the purposes of this investigation, which is consistent with previous studies [66, 79].

Only houses that contained one central air-conditioning unit were included in this oversizing analysis (19% had more than 1 air-conditioner), but there is evidence that homes with multiple air-conditioners are just as, if not more, oversized [67]. Also, only houses between 46.5 and 325 m^2 (500 and 3500 ft^2) of floor area were considered (4% were out of this range). Homes that were missing audit data, such as installed system capacity and attic R-values, were also excluded. Missing audit information was not correlated with any specific auditor and is most likely the result of the difficulty of obtaining some information (e.g. nameplates missing from air-conditioning units).

Several home characteristics were not assessed at all in the energy audits, and some reasonable assumptions were made in their absence. For example, wall insulation R-values were not included in the energy audits, as that level of inspection would require significant equipment or penetration of the façade. Thus, wall insulation levels were assumed to meet the City of Austin building codes that coincided with the year of construction of each home: pre-1983 code required RSI of 0.53 m^2 K W^{-1} (R-3) and post-1983 code requires RSI 2 m^2 K W^{-1} (R-11). Because infiltration rates were not measured in the homes, the default "leaky" infiltration values that are provided in the Manual J workbook were used for all homes. Also, the number of occupants was not noted by the auditors, so the value was assumed to be one more than the number of bedrooms, the thermal contribution of individual occupants is generally small and not expected to significantly affect the results [27]. Windows were classified as either single- or double-paned in the audits, so U-values for generic single- and double-paned windows provided in the Manual J literature were used (3.18 and 5.57 W m^{-2} K^{-1}, respectively). The area of windows was missing from the audit database, so it was assumed that the percentage of windows per floor surface area was 16.8% for every home, based on the average of previous investigations of single-family residences in the U.S. [66].

The assumptions for wall insulation levels (that every home meets code and no homes have greater insulation than code requirements) and infiltration rates (that every home is "leaky") should over-estimate cooling loads and required cooling capacities overall, which should provide a conservative estimate of the extent of equipment oversizing. Ultimately, for the analysis of the effect of residential air-conditioner oversizing on peak power demand, the rated power draws of oversized installed units were compared to correctly sized systems of the same efficiency. Again, rated power draws were scaled to increase approximately 10% over rated conditions, as previously described.

2.4.2.3 Duct leakage

Because supply duct leaks should not alter return air temperatures and return leaks should not increase entering air temperatures enough to drastically alter the power draw of outdoor units [73], it was assumed that the only impact that widespread duct sealing would have on peak demand would be a potential reduction in individual system runtimes, which when aggregated across the building stock, might reduce the likelihood that multiple systems are operating concurrently during hours of peak demand. However, because work investigating system runtimes with varying leakage conditions could not be found, the duct retrofit analysis was limited to the technical energy savings in the individual homes.

To estimate the impacts of sealing duct leaks on cooling energy consumption in individual homes, data were used from two field studies that measured actual reductions in cooling energy after duct retrofits [1, 2]. A linear regression model was built relating cooling energy savings relative to the absolute reduction in the total duct leakage fraction. The slope of that regression was used to estimate how much cooling energy could be saved if each system with a duct leakage fraction greater than 10% was reduced to 10% (as recommended by Austin Energy and other efficiency programs).

2.4.2.4 Measured vs. rated air-conditioning system capacity

Because airflow rates were estimated and temperature differences across cooling coils were measured, the actual cooling capacity of the systems in the audit database were estimated, and compared those values to the nominal cooling capacity of the units. Actual sensible capacity of the audit homes was estimated using Equation 2.2:

$$q_s = Q \times \rho \times C \times \Delta T \tag{2.2}$$

where q_s is the estimated sensible capacity (kW_{cap}), Q is the system airflow rate (m^3 s^{-1}), ρ is the air density (assumed constant, 1.2 kg m^{-3}), C is the specific heat of air (assumed constant, 1.012 kJ kg^{-1} K^{-1}), and ΔT is the temperature difference across the cooling coil (K). Nominal installed sensible capacity was estimated as 80% of the nominal total capacity identified on each unit by the auditors, which is consistent with a typical sensible heat ratio (SHR) of 0.80 in residential systems [14, 73]. Systems with measured capacities less than rated capacities were assumed to operate longer and consume more energy at a rate directly proportional to the difference between the two values, which is a common assumption, although experimental justification was not found in the literature.

2.4.3 Estimating energy impacts enrolling all homes in Austin Energy's Power Saver Program – Home Performance with ENERGY STAR

The potential peak power demand reductions were estimated from various levels of participation in the Home Performance with ENERGY STAR (HPwES) program. HPwES is a joint program between the US Department of Energy and the US Environmental Protection Agency. According to the HPwES website, the program is a "comprehensive, whole-house approach to improving energy efficiency and home comfort, while helping to protect the environment" [80]. Austin Energy is the local sponsor, and has garnered over 7000 participants since 1998. Homeowners participate in the program by first contacting an approved home energy company to perform an energy audit on their home and offer recommendations on improving the efficiency of the home in the following areas: duct sealing and repair, attic insulation, upgrading windows, caulking, weather stripping, radiant barriers, and correctly sizing the air-conditioner or heat pump to a unit with a EER of 12 (COP-3.5). The participant decides which improvements they would like to have performed, and Austin Energy reviews the proposal for work. Once approved, the homeowner has two options, 1) receive a rebate of up to 20% of the cost of repairs, up to $1575 or 2) apply for a low or 0% interest, unsecured loan through Austin Energy.

To establish a "best case" scenario of improved homes, each home in the database was modified with the most commonly performed improvements in the HP-wES program, and then each air-conditioning system was resized. The power demand savings of a resized air-conditioning unit, as compared to the installed unit at the time of the home audit, in each home were then summed and multiplied by a scaling factor to estimate the peak power consequences at the utility scale. For all homes in the database, attic insulation was brought to code (R-38 hr ft^2 °F BTU^{-1}, RSI-6.7 m^2 K W^{-1}), caulking and weather-stripping was assumed to increase air tightness to 0.35 ACH [27], leaky ducts were sealed, and windows were upgraded (if single-paned) to a generic double-paned window (U-value of 0.56 BTU hr^{-1}ft^{-2} °F^{-1}, 0.97 W m^{-2} K^{-1}). Although nearly 5000 homes underwent energy audits as part of a sales transaction as required by the ECAD ordinance, it is assumed that no home energy improvements were implemented in these homes, post audit. Thus, it is assumed that the home characteristics as listed in the ECAD database are an accurate reflection of the homes today, as well as the rest of the single-family homes in Austin.

To assess peak power improvements, the optimal air-conditioner capacity for each improved home in the audit database was estimated by performing a Manual J calculation, the industry standard sizing calculation for residential air-conditioning systems [26]. The calculated unit size (EER 12, COP 3.5) was then compared to the installed unit size (installed EER) and the difference in peak power demand was calculated. Peak power demand was estimated in both cases by dividing equipment nominal capacity by rated EER and adjusting for likely operating conditions, as shown in Equation 2.1.

2.4.4 Scaling analysis to represent the residential building stock in Austin

There are approximately 332,000 residential buildings in Austin Energy's service area, 41.7% (156,000) of which are single-family detached units (US Census, 2009). Thus, this database of 4971 energy audits represents over 3% of all single-family homes in Austin, making it a statistically relevant representation of the building stock (a Wilcoxon signed-rank test yielded no statistical difference in the distributions of year built between the two databases, $p > 0.05$). Because the audits available from the ECAD database were for single-family detached homes, the results of the analysis were extrapolated to all single-family units in Austin.

2.5 Findings from the energy audit database

This section first summarizes building and system characteristics of homes in the audit database. Figure 2.1 shows the distribution of the year that each home in the database was built. The majority (99%) of homes in the audit database were built prior to 2000, with a mean and median year built of 1972 and 1976, respectively. Figure 2.1 gives a distribution of the year built of the homes in the dataset. The mean floor area of the homes in the audit database was approximately 1798 ft^2 (167 m^2) (standard deviation (σ) = 764 ft^2, 71 m^2), with a median value of 1615 ft^2 (150 m^2).

Figure 2.2 shows the measured attic insulation levels for ECAD homes. Austin Energy recommends an attic R-value of 38 hr ft^2 °F/Btu (RSI-6.7 m^2 K/W) for homes in the Austin area, although the majority of homes in the audit database (92%) fall below this recommendation. Homes in the audit database had an average attic insulation R-value of 21.5 hr ft^2 °F/Btu ($\sigma = 9.5$) (RSI-3.8 m^2K/W; $\sigma = 1.7$). High thermal conductivity between conditioned spaces and attic spaces increases cooling demand in the summer, as the temperature difference between the attic and conditioned space can be greater than 54°F (30°C) [19].

Table 2.1 describes selected characteristics for the primary air-conditioning systems in the homes in the audit database, and the subsequent sections describe selected measured (or estimated) air-conditioning system parameters. Only a negligible fraction ($< 0.2\%$) of homes did not have central air-conditioning.

Figure 2.3 shows the distribution of total duct leakage across the audit homes, measured as the leakage airflow rate at -25 Pa, normalized to the estimated system airflow rates. Duct leakage fractions include the combined supply and return leakage

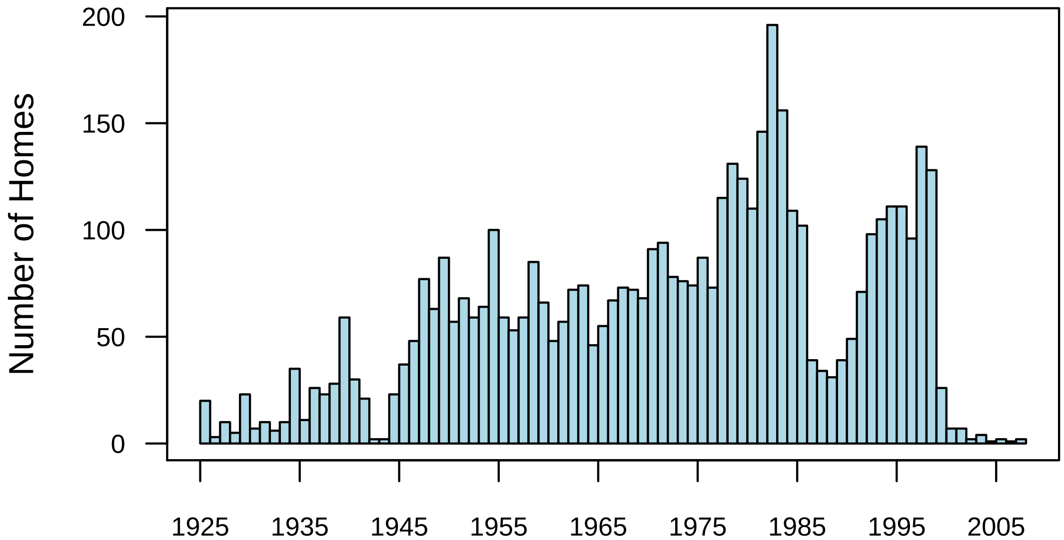

Figure 2.1: Distribution of year built of the homes in the ECAD audit database (N = 4893).

Table 2.1: Air-Conditioning System Characteristics

Parameter	Mean	Median	Standard Deviation	Number of Units
Nominal Capacity (kW)	11.00	10.60	2.80	4763
Airflow Rate (m^3/s)	0.61	0.56	0.31	4714
Rated Efficiency (COP)	2.90	2.90	0.50	3818
Floor Area/Capacity (m^2/kW)	13.30	13.20	2.40	4693
Unit Age (years)	10.80	11.00	5.70	3480

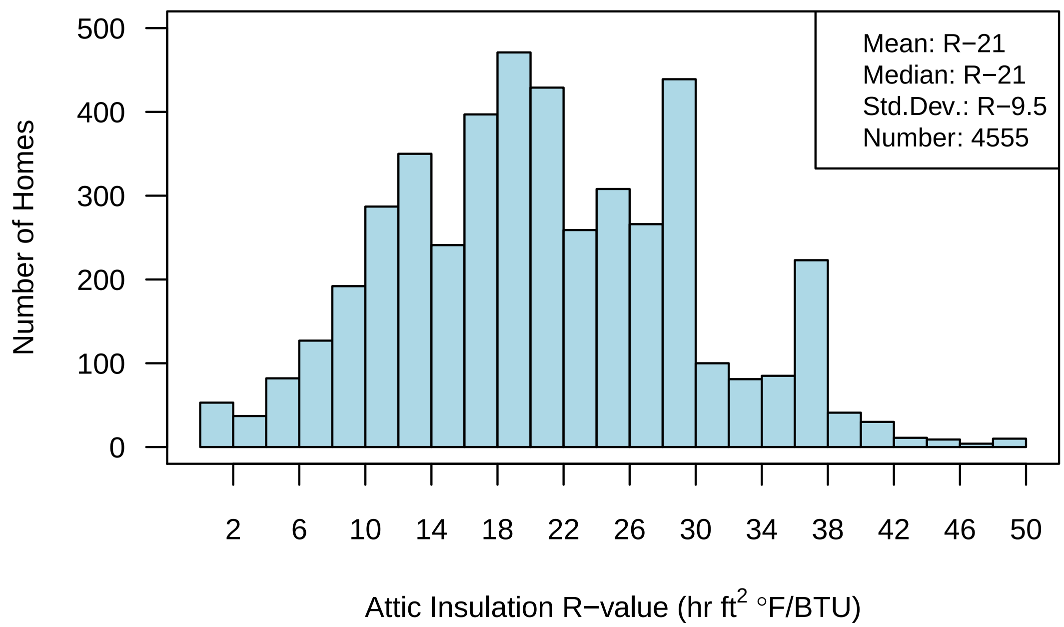

Figure 2.2: Distribution of Attic insulation levels of homes in the ECAD audit database.

to both interior and exterior spaces. The majority of homes (approximately 77%) had duct leakage that would typically require sealing (greater than 10%), although there is considerable uncertainty associated with both the leakage measurements and the estimated system airflow rates. The mean duct leakage fraction was 19% (σ = 13%), with a median of 16% and an interquartile range of 10-24%. The mean duct leakage airflow rate, measured at -25 Pa, was approximately 234 ft^3 min^{-1} (0.108 m^3 s^{-1}), which was at the low end of Neme et al. [22], who summarized 19 duct studies that yielded a range of 193-396 ft^3 min^{-1} (0.091-0.187 m^3 s^{-1}) at -25 Pa.

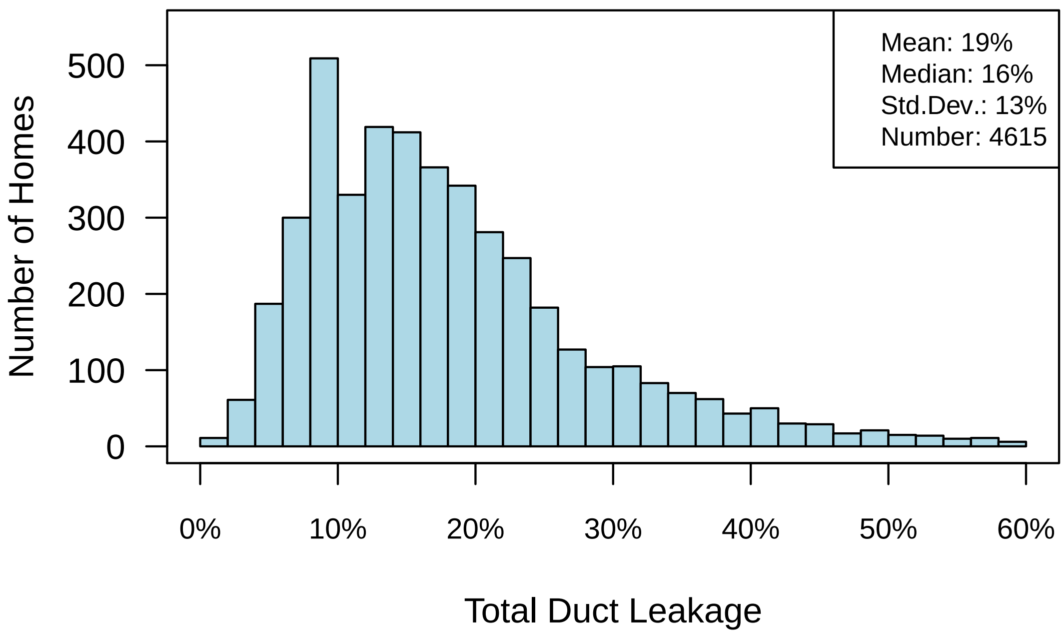

Figure 2.3: Distribution of duct leakage as a fraction of total duct flow for homes in the database.

The temperature difference across the cooling coil is another parameter measured in the audit homes and is an important indicator of how well the system is functioning. Figure 2.4 shows the distribution of temperature differences measured across the audit homes. The mean temperature difference was 17.1°F (9.5°C) (σ = 5.9°F (3.3°C), N = 3687). Austin Energy recommends that the temperature difference across the cooling coil be in the range of 15-20°F (8.3-11.1°C). About 47% of the systems were operating outside of the recommended range, split approximately equally between too high (24%) and too low (23%). Temperatures that are below this range might be indicators of low airflow rates, fouled coils, or improper refrigerant charge, all of which can reduce the cooling capacity of the unit [67]. Excessive temperature differences may be indicators of improper sizing or overcharging, but can be an indication of increased sensible capacity.

Additionally, the distribution of rated EER of the installed units is presented in Figure 2.5, in units of cooling output (BTU/hr) per electrical power input (W). The installed unit efficiency has a direct impact on the energy consumption and power draw of the air-conditioning unit. Approximately 86% of homes had systems with a rated EER less than Austin Energy's recommendation of EER 12 (COP 3.5), and less than 2% exceeded EER 14 (COP 4.1).

2.6 Results

This section describes the effect of the previously mentioned common air-conditioner design and installation issues in the audit homes and estimates the impacts they have on peak power demand and energy consumption.

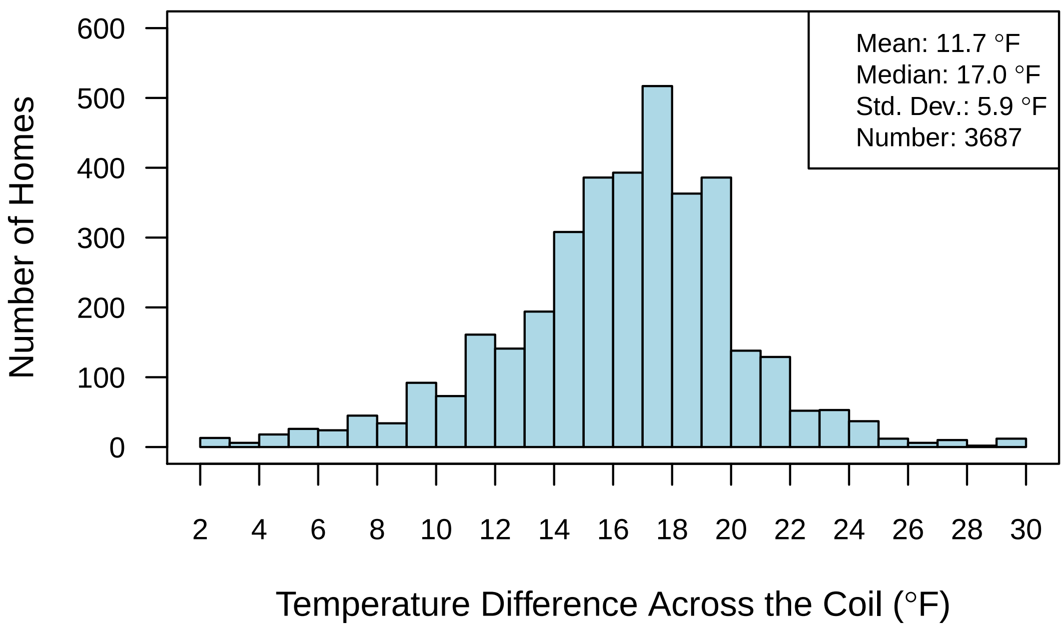

Figure 2.4: Distribution of temperature difference across the evaporator coil for homes in the ECAD audit database.

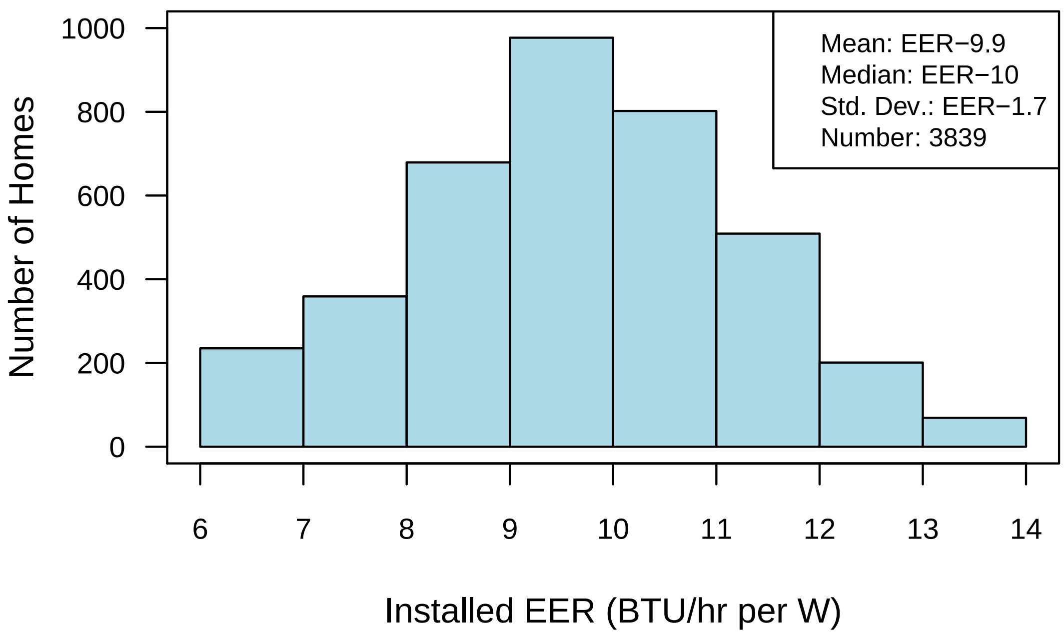

Figure 2.5: Distribution of the installed efficiency of air-conditioning units in the ECAD audit database.

2.6.1 Installed system efficiency

Because new commercially available air-conditioning units continue to increase in efficiency over time, it was attempted to quantify the excess energy consumption and peak power demand associated with older inefficient systems across the homes in the audit database. The estimated distribution of rated power draws for homes in the audit database is shown in Figure 2.6.

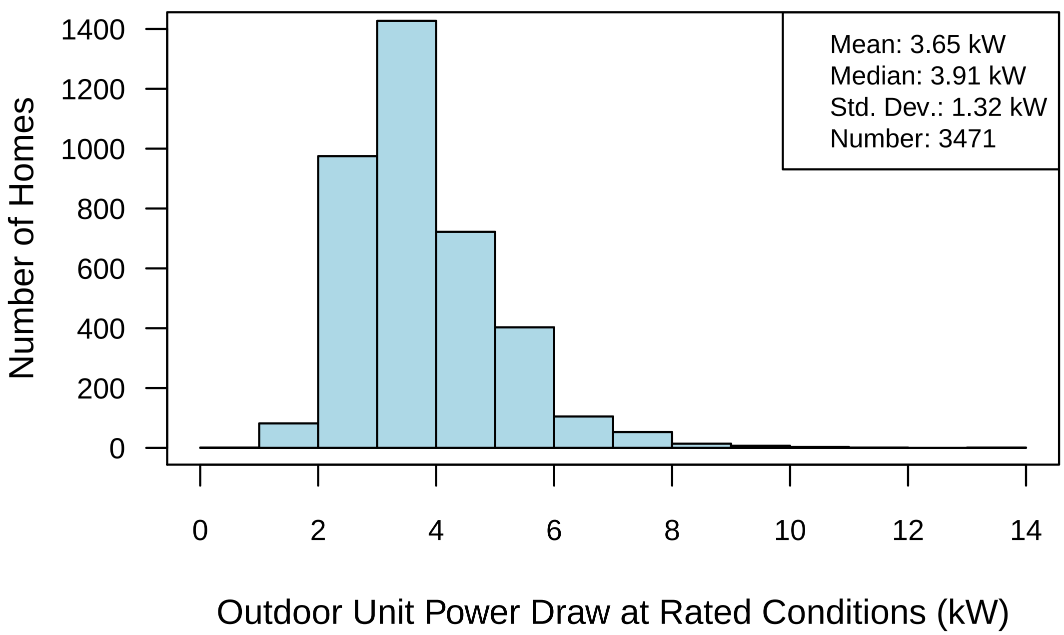

Figure 2.6: Distribution of estimated power draw at rated conditions for homes in the ECAD audit database, in increments of 0.5 kW, where N is the number of individual systems.

The average system in the audit database had an EER of 9.9 (COP 2.9) ($\sigma =$ 1.7, COP 0.5) and the average power demand was 3.9 kW ($\sigma = 1.3$ kW). This average is likely a low estimate for summer peak power demand, as the outdoor temperature during the summer peak hour can exceed 40 °C (104 °F). Again using an increase in outdoor unit power draw of 1.8 $\pm$ 0.8% per °C rise in outdoor temperatures [14], the average peak power demand is estimated as 4.3 kW (σ = 1.4 kW). The best estimate of the uncertainty in this value is approximately 5%, taken as the standard deviation of the high, medium, and low bounds of the estimated increase in power draw over rated conditions that were calculated using the above reference. Scaling to the approximately 156,000 single-family units in Austin, and assuming this dataset is roughly representative of the distribution all single-family detached homes in Austin, this estimate leads to a total peak power demand of approximately 663 $\pm$ 33 MW for air-conditioning (or approximately 464 $\pm$ 23MW if it is assumed that 70% of air-conditioners are operating during the peak hour). For reference, 464 MW represents approximately 17–18% of Austin's highest recorded peak demand of 2628 MW in August 2010.

If every system was upgraded to at least an EER 12 (COP 3.5), it is estimated that the collective peak power draw of single-family detached homes in Austin could decrease by 132 MW to 532 MW (or 372 MW assuming 70% of systems operating at peak). This reduction would be approximately 5% of Austin's highest peak demand and approximately 17% of the city's 800 MW peak reduction goal. Similarly, if every system was upgraded to at least EER 14 (COP 4.1), it is estimated that peak demand could be reduced by 205 MW, or almost 8% of Austin's peak demand, and almost 26% of its peak reduction goal.

Holding all else constant, increasing the efficiency of a unit should directly affect the amount of power draw required to meet the same cooling load but should not alter system runtimes, as the system still has the same capacity to remove heat from the airstream. Thus, it is estimated that increasing the EER of the average system from 9.9 to 14 (COP 2.9 to COP 4.1) would yield an average reduction in household cooling energy consumption of approximately 29%. Thus, approximately 70% of homes in the database could save at least 25% in cooling energy by upgrading their air-conditioners to 14 EER (COP 4.1) units.

2.6.2 Oversizing

Air-conditioning systems were also analyzed to determine the appropriateness of their sizing. This analysis was restricted to homes in the audit database that have a single air-conditioner, have a floor area between 46.5 m^2 and 325.2 m^2, and that had enough audit information to facilitate a Manual J calculation; 74% of the homes in the database met these requirements (N = 3669). There did not appear to be any systematic reason for missing data, and so it is expected that this smaller subset is still representative of the Austin housing stock.

Figure 2.7 compares "correct" cooling capacities estimated using Manual J calculations and the actual installed capacities as found in the audits. Each circle represents an installed unit in the database. Because manufacturers only provide air conditioning units in certain size intervals, usually in 1.76 kW ($\frac{1}{2}$ ton) increments, design capacities recommended by Manual J calculations were rounded up to the nearest 1.76 kW. The rounded values are used for all percentages stated for oversizing, as well as calculations involving aggregated peak power demand; the pre-rounded Manual J values are left in Figure 2.7 for clarity.

Manual J calculations showed that 31% of the installed units to be sized at least 120% of necessary capacity (units to the left of the dotted line in Figure 2.7), and 66% were at least 100% of necessary capacity (units to the left of the solid line in Figure 2.7). These results are in general agreement with previous studies on

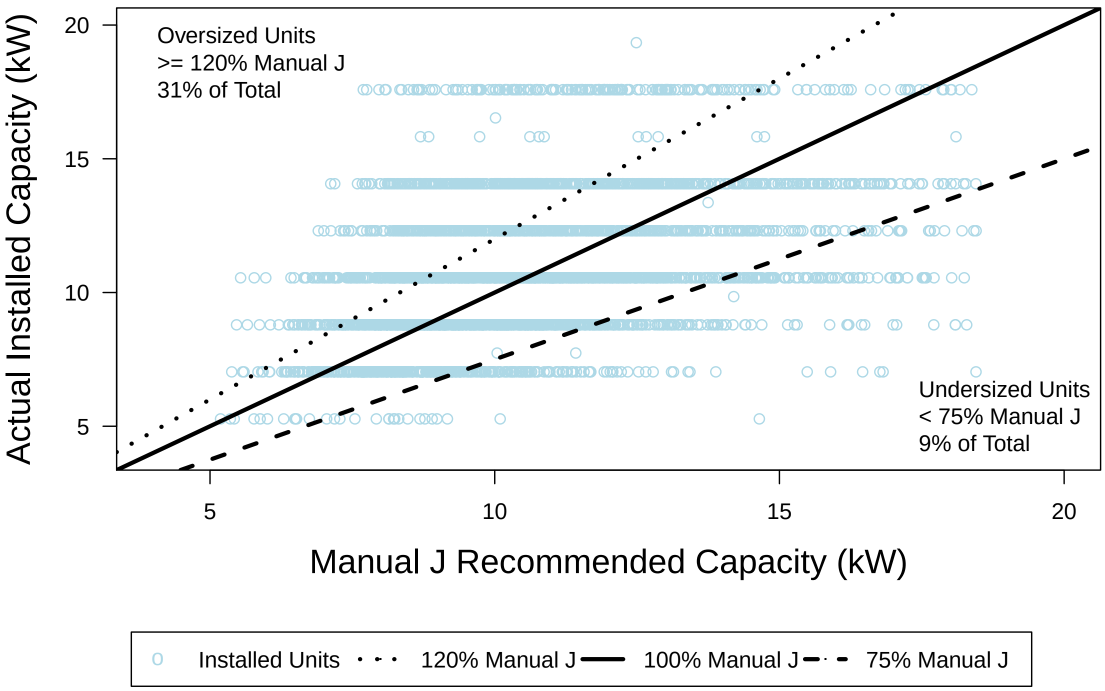

Figure 2.7: Distribution of the actual installed air-conditioner capacities vs. calculated (Manual J) capacities for homes in the audit database (N = 3669 homes). Because of the large size of the data set, it is difficult to clearly see each point, but the seemingly solid horizontal lines are closely spaced individual units.

residential air-conditioner oversizing [66, 67]. In addition, approximately 9% were undersized (below the dashed 75% line). Figure 2.8 shows a cumulative distribution of the installed units vs. percent of Manual J capacity.

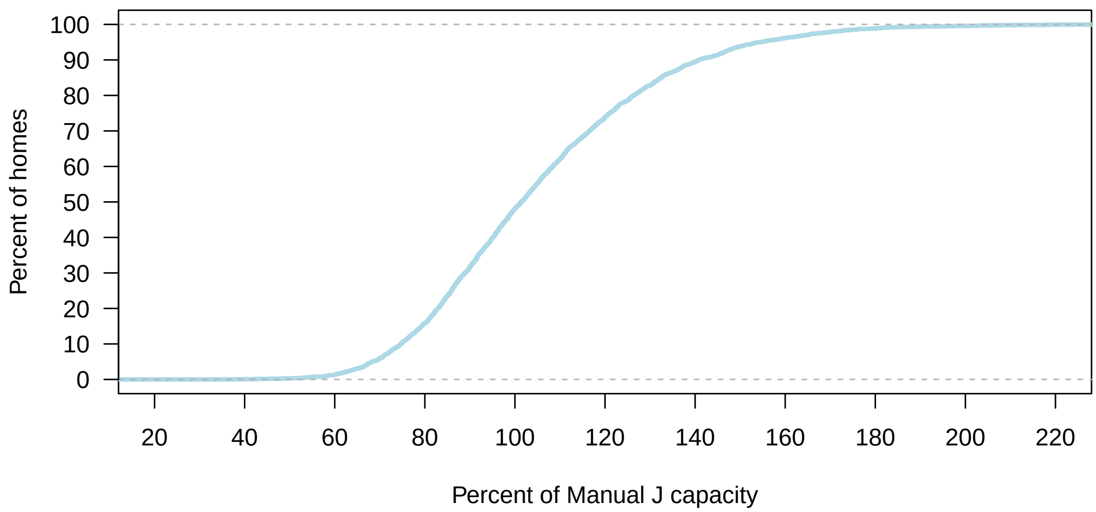

Figure 2.8: Cumulative distribution of the installed units vs. percent of Manual J capacity showing the percent of homes above various levels of oversizing.

The average power draw of oversized (≥120% Manual J) units is 4.86 kW ($\sigma =$ 1.45 kW, N = 923), compared to 3.54 kW ($\sigma = 0.97$ kW, N = 923) for correctly sized units, both calculated at 5.6 °C above rated conditions. If 31% of all single-family residential units in Austin are considered to be oversized, and it is assumed that 70% of these systems are operating during the summer peak hour, with a 10% increase in power draw with a 5.6 °C temperature increase over rated conditions [14], it is estimated that the aggregated excess peak power demand due to all oversized single family residential air-conditioner units is as much as 41 MW (or approximately 1.6% of Austin's peak demand). Furthermore, if each oversized unit was replaced with a correctly sized unit that is also upgraded to an EER of 12 (COP 3.5) or 14 (COP 4.1), that would yield a peak power reduction of 67 MW or 81 MW, respectively (or 2.5% and 3.1% of peak). If the undersized units in Figure 2.7 were simultaneously upgraded in size and efficiency (EER 14, COP 4.1), extrapolated to the entire single-family housing stock, the aggregated peak power demand increase would be approximately 1 MW.

The aggregated peak power demand of residential air-conditioners depends on how many are operating concurrently and it is important to note that smaller, correctly sized air-conditioning units should actually run longer to meet the same cooling load in a building. In the only two studies (of which the author is aware) that measured the additional runtime caused by correctly sizing over-sized air-conditioning units, Pigg [81] measured an average increase in runtime of 32% ($\sigma = 21\%$) in three homes in Wisconsin after reducing unit sizes by approximately 30% and Sonne et al. [82] measured increases in runtimes of 57 $\pm$ 19% and 33 $\pm$ 17% in two homes in Florida after reducing the units' sizes by one-third. Thus it is reasonable to assume that there is a greater likelihood of multiple units across the building stock operating more often during the peak hour (i.e. more than the assumption of 70%), and that the potential reductions in peak power due to correctly sizing units may not actually be realized without the incorporation of utility-controlled thermostat cycling programs [83]. However, a recent analysis by the author looking at the air-conditioner runtimes of 14 green built homes in Austin found that 85% of units were running during summer peak hours [84].

The energy impacts of correctly sizing systems in individual residences are not as clear. Smaller systems will draw less power when operating, but because cooling loads do not change, the amount of energy (all else equal) required to condition the space will remain the same. One would expect that decreasing the size of a residential system would lead to longer runtimes and ultimately observe little change in overall energy use. This phenomenon has been observed in field studies in both Wisconsin [81] and Florida [82]. Additionally, James et al. [66] observed that systems sized 120% greater of Manual J increased overall cooling energy use by just under 4% and by 13% during the peak hour in the summer in Florida. Although the overall energy impacts of correctly sizing systems are unclear, occupants might benefit from added comfort, as correctly sized systems that operate for longer periods of time should provide more dehumidification [72], thus possibly allowing for a higher dry bulb temperature while remaining in the human comfort zone [27].

2.6.3 Duct leakage

Because there was not enough information to support a detailed model of the ductwork in the homes, values of energy savings from previous studies of duct retrofits were relied on. Figure 2.9 shows actual reductions in cooling energy use measured in two previous field investigations of the impact of sealing duct leaks in residential buildings [1,2]. As previously mentioned, a linear regression was performed on these data to estimate the average cooling energy savings achievable from a reduction in total duct leakage fractions [1,2]. Three outliers from Jump et al. [2] were ignored to achieve some reasonable certainty (slope = 1.47, R^2 = 0.73, 95% CI = 1.16-1.77), as shown in Figure 2.9. The regression output means that, for example, if duct retrofits achieve a 20% reduction in total leakage (e.g. from 30% to 10%), approximately 30% savings in cooling energy can be achieved. For comparison, Cummings et al. [1] reduced mean total leakage in 23 homes from 16% (std dev. 10%) to 5% (std dev. 4%), which yielded mean cooling energy savings of 18% (σ = 11%) [1].

Assuming a target duct leakage of 10%, approximately 76% of the homes in

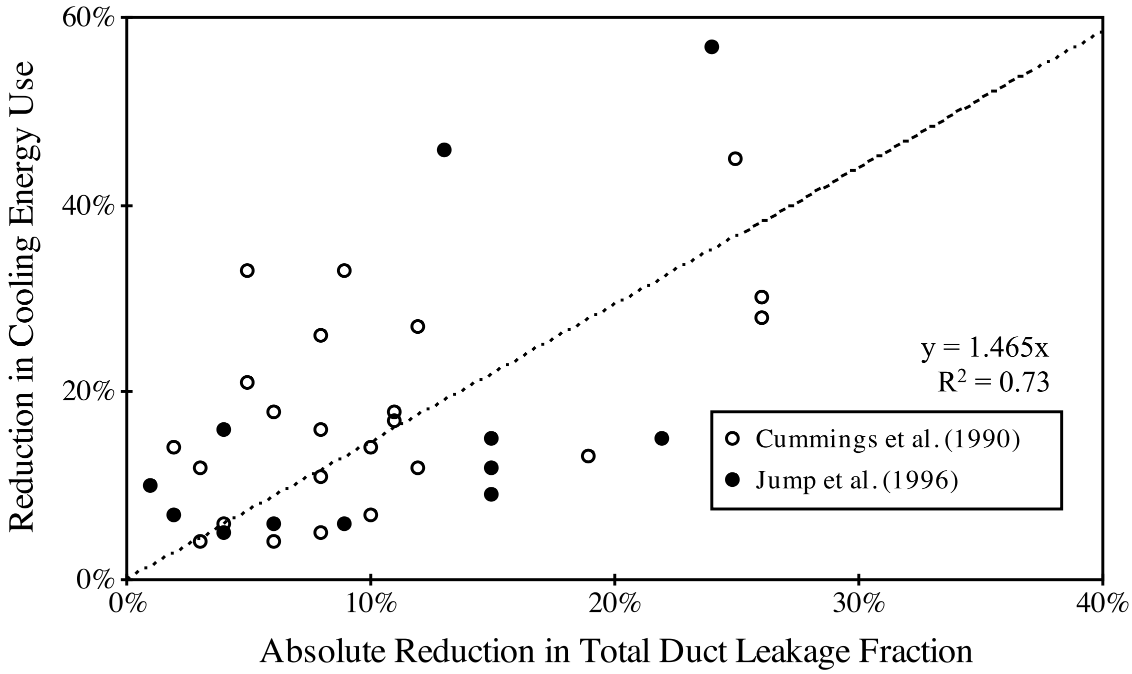

Figure 2.9: Estimations of the reduction in cooling energy use associated with reductions in total duct leakage. Plot generated with data taken from [1, 2], and ignoring three outliers from Jump et al. [2].

the database would require duct sealing (mean sealing required = 13%, σ = 13%). The required duct sealing values (in absolute terms) was multiplied by the slope in Figure 2.9 to yield the likely cooling energy savings achievable by sealing ducts in each eligible home. The distribution of achievable energy savings is shown in Figure 2.10. The amount of energy savings is capped at 60% because of data limitations in Figure 2.9 and likely invalid values of duct leakage fractions entered at the extreme ends in the audit database.

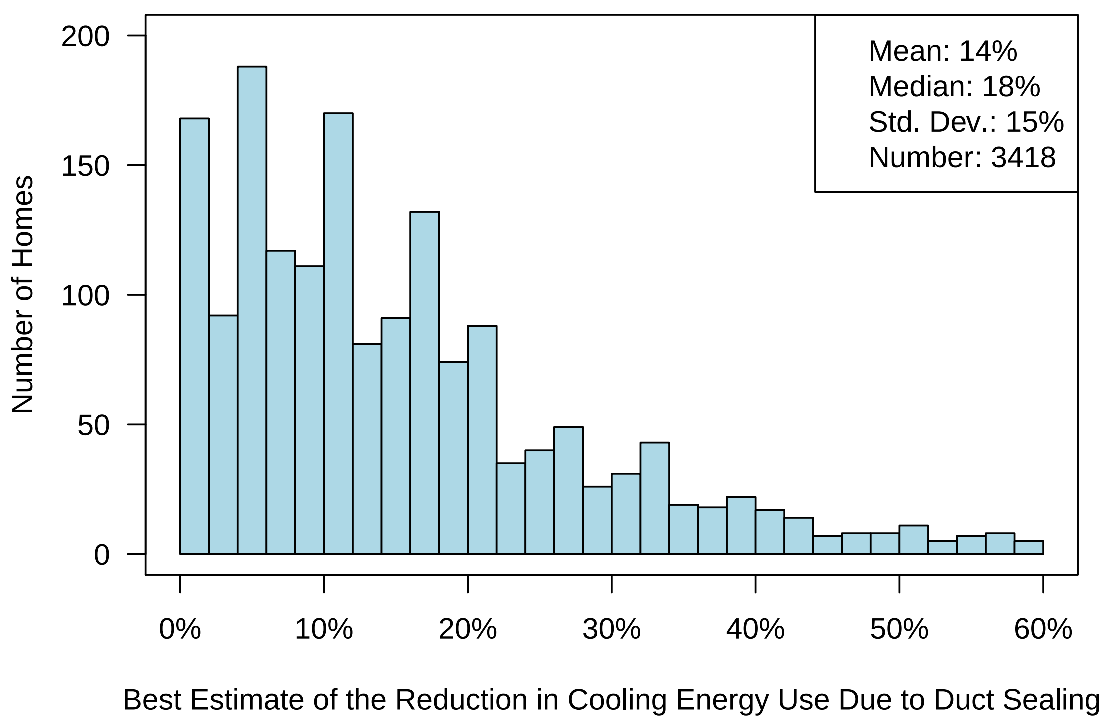

Figure 2.10: Distribution of the estimated reduction in cooling energy consumption achievable by sealing duct leaks in the audit homes (N = 3418 homes).

Repeating the calculations using the confidence intervals for the slopes of the regression line in Figure 2.9, it is estimated that the mean system could achieve 14–22% in cooling energy savings by sealing duct leaks. The best estimate of the mean cooling energy savings (using only the slope from Figure 2.9) is 18% ($\sigma = 15\%$), with a median savings of 14% and an interquartile range of 7–23%. Unfortunately, the values of peak reduction cannot extrapolate absolute from these data because of lack of information about individual system runtimes, although it can be estimated that more than 75% of homes in the audit database (and thus single-family homes in the city of Austin) could benefit from sealing duct leaks, with an average cooling energy savings of approximately 18%.

2.6.4 Measured vs. nominal capacity

Because system airflow rates were estimated and temperature differences across cooling coils were measured, the operating sensible capacity could be compared to the estimated rated sensible capacity. The average system was estimated to be operating at approximately 77% of rated sensible capacity ($\sigma = 21\%$). Approximately 10% of systems were operating under 50% of rated capacity and approximately 10% were operating over 100% of rated capacity, respectively, as shown in Figure 2.11.

Low operating capacity has a direct impact on energy consumption and system runtime, as systems that remove less energy than they are rated for should operate longer. If a linear relationship is assumed between deficiencies in delivered capacity and increases in runtime [72], the average homeowner could save up to 23% in cooling energy by servicing their air-conditioning units to achieve 100% of rated sensible capacity (although there is some evidence that this relationship may be nonlinear and the savings may be smaller; for example, Stephens et al. [15] reported that residential air-conditioning systems that observed a 4% decrease in sensible capacity due to the installation of high-efficiency filters did not lead to an increase in total

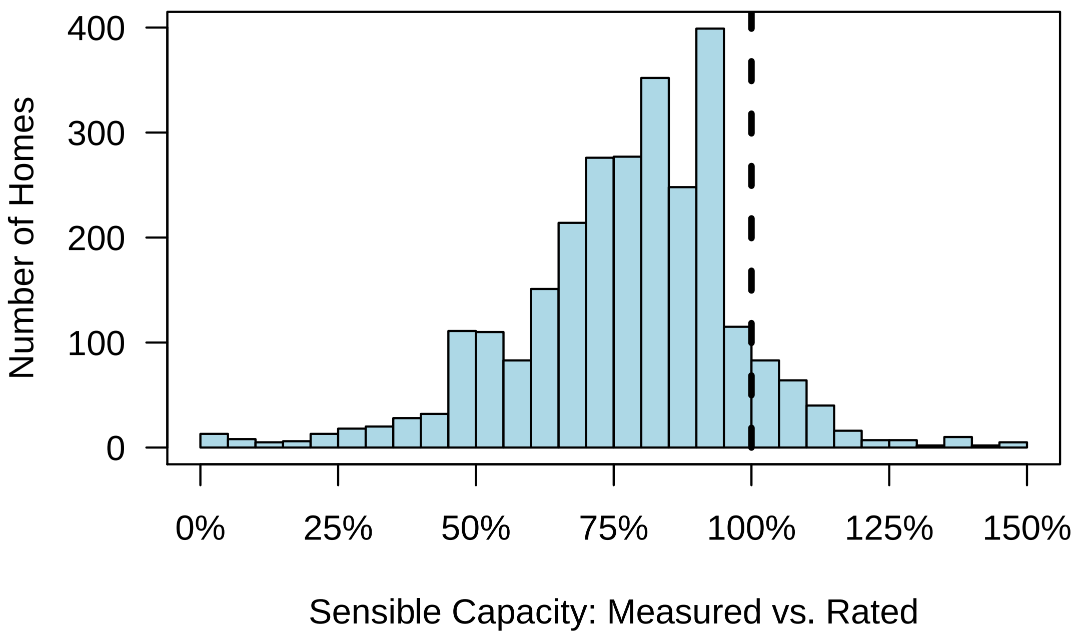

Figure 2.11: Distribution of the estimated operating sensible capacity relative to the rated sensible capacity, assuming a sensible heat ratio (SHR) of 0.8 (N = 2886 homes) showing that the mean system was operating at approximately 77% of rated sensible capacity (σ = 21%).

energy consumption). Although there are no estimates of the uncertainty of these measurements, these values should be taken as rough estimates because there is a considerable amount of uncertainty in the airflow measurements/estimates, the measured temperature differences, and the assumed SHR = 0.8 [14, 73]. Sensible heat ratios typically range from 0.7 to 0.8 in residential settings [85]. If a SHR = 0.7 is assumed, the mean system would be operating at 88% of rated capacity (σ = 23%), and the average energy savings of tuning equipment would decrease to 12%. Finally, although this analysis focuses on the energy savings to residents achievable by increasing system cooling capacities, reductions in peak demand might be realized due to reduced system runtimes. There is not enough information to quantify this impact.

2.6.5 Increasing the efficiency of the homes with the Home Performance with ENERGY STAR Program

Enrolling all the homes in the audit database in the HPwES program (increasing attic insulation levels, tightening the building envelope, sealing ducts, and upgrading windows) and replacing oversized units with new correctly sized units would reduce cooling demand. For the audit homes that go through the program, the mean unit size in the database would decrease from 11 kW (σ = 2.8 kW) to 7.7 kW (σ = 1.8 kW), which would allow the average home to realize a peak power demand reduction of approximately 1.8 kW (σ = 1.2 kW) with an EER 12 (COP 3.5) unit. Results indicate that more than 97% of the homes in the audit database would benefit from this program. Aggregated across all 156,000 single-family detached homes in Austin, it is estimated that the application of HPwES retrofits could reduce Austin Energy's peak power demand by as much as 200 MW, or almost 8% of peak demand in 2008.

The estimate of the potential peak power savings of HPwES retrofits assumes that the fraction of systems operating simultaneously during the peak hour does not change after correctly sized units are installed, although this fraction could potentially increase as smaller systems will generally operate for longer periods of time to meet the same cooling load. Oversized systems often cycle on and off frequently, which can help reduce the aggregate instantaneous demand for a utility. If the fraction of air-conditioning systems operating during the peak hour increased from 70% to 100%, the peak savings would be reduced to 86 MW. However, it is not expected that air-conditioners will all operate continuously at peak times because other HPwES retrofits would also decrease cooling loads. The aggregation of air-conditioning units drawing less power because of their decreased size, increased efficiency, and reduced cooling loads from improvements to the efficiency of the home, should still enable substantial reductions in peak power demand [22].

2.7 Discussion

Several common design and installation issues that have been found in previous studies were also found in the homes in the audit database. For example, air-conditioning units were inefficient overall, with an average EER of 9.9 (COP 2.9), compared to the ENERGY STAR minimum requirement of EER 12 (COP 3.5), increases peak power demand and overall cooling energy consumption. Additionally, approximately 31% of the units are estimated to be oversized by at least 120% relative to Manual J calculations. The analysis finds that over 75% of the systems in the audit database had excessive duct leakage and that the average home could reduce cooling energy consumption by up to 18% by repairing ducts. The average system was operating at approximately 77% of rated sensible capacity, suggesting widespread problems with low airflow rates, fouled cooling coils, or suboptimal refrigerant charge and over 97% of homes would benefit from energy efficiency upgrades. Because less than 0.2% of the homes in the original data set (N = 4971 homes) did not have air-conditioning, all of these issues are likely widespread across Austin.

It is a common misconception that “bigger” air-conditioners will perform “better” and many air-conditioning contractors have an incentive to oversize residential HVAC units because they will make more money. In a survey of HVAC contractors, over 75% reported that customers wanted larger size units, that the homes they designed for required oversizing, or that bigger was “simply better” [86]. One of the main concerns of HVAC contractors is that if they do not oversize units, the customer will not feel as if the unit cools the space in a timely manner. If this is the case, the contractor might receive a callback and be required to install a larger unit. However, Rudd et al. [79] showed that even systems as low as 73% of Manual J suggested capacity were able to meet the cooling load and maintain temperatures in homes during the summer of 1999 in Tucson, AZ. Austin typically has a larger latent load than Tucson, so units may not be able to be undersized to this extent, but the analysis shows that significant peak power savings may be achieved by correctly sizing residential air-conditioning systems in Austin.

2.7.1 Comparison of the costs of efficiency upgrades to the costs of peaking power plant acquisitions

This analysis suggests that 200 MW of peak demand can potentially be avoided with aggressive investments in home energy efficiency improvements. Reducing peak demand in Austin might offset the need for Austin Energy to obtain additional peak generation units. A generic 160 MW conventional natural gas combustion turbine is estimated to cost $685 per kW (CAPEX, overnight costs), or approximately $110 million, with $2 million in fixed O&M costs per year [87]. Assuming that fuel costs are $75.60 per MWh, depending on the generating unit and prevailing market prices for natural gas [88], 200 hours per year of operation, and a 5% yearly rise in fuel prices, the total fuel cost for 20 years would be about $80 million. Thus, considering a 20-year life span, the total cost associated with a 160 MW natural gas peaking unit could be approximately $230 million (or $1438 per kW of generation).

The maximum rebate from Austin Energy to homeowners enrolled in HPwES is currently $1575. Considering an average peak power reduction of 1.8 kW per home, the cost per kW (savings) to Austin Energy is approximately $865 per kW, or only 60% of the cost of a new peaking generation plant. With these assumptions, Austin Energy could even increase the maximum rebate to approximately $2600 per home and the cost of savings would still be at parity with the cost per kW of generation. This increased maximum rebate is over half the average cost (approximately $5000) to homeowners for enrolling in the program [89]. Although there are other more cost-effective methods to reduce peak demand on electric utilities, such as direct load control and critical peak pricing [83], this analysis is limited to building retrofits using HPwES, which are more cost-effective than new plant acquisitions while simultaneously benefiting homeowners by reducing their energy bills.

2.7.2 Energy audit recommendations

Although the energy audit procedures detailed herein provide a unique dataset for study, steps can be taken to improve the quality of information provided by the audits. To aid future analysis, it is recommend that detailed window characteristics, such as the area and orientation, be included in the audits. This practice would not add a significant burden to the auditor and would provide an improved characterization of the audit homes. Additionally, air leakage testing using calibrated fans (e.g. blower doors) should be required to establish a baseline value for air infiltration. Airflow rates and duct leakage were not measured using the most accurate and informative methods [90], and given the importance of air-conditioning in a cooling climate like Austin, they could be improved to provide for better home characterizations overall. These measurements would be a helpful addition to the audits and would possibly allow for a better and more accurate understanding of the link between the typical system issues described herein and overall energy performance [68]. Finally, because energy audits have been shown to be highly variable between audit companies [91], steps should be taken to fully detail audit procedures in order to minimize uncertainty.

2.8 Conclusions

This section of work analyzed a database of 4971 energy audits on single-family homes in Austin, Texas. The analysis led to a conclusion similar to previous studies: residential air-conditioning systems are generally operating in poor condition. The inefficiencies associated with poor residential air-conditioning performance aggregated across a city can be significant, especially during peak periods. Mitigation of typical design and installation issues could result in significantly decreased peak power demands on utilities, and because air-conditioning often constitutes the largest single residential energy demand, the reductions in overall energy consumption for individual homeowners could be significant. Single-family residential air-conditioning systems are estimated to account for approximately 17-18% of peak summer electricity demand in Austin. Furthermore, the analysis concludes that efficiency improvements alone (upgrading all systems to EER 14, COP 4.1) could reduce peak power demand by as much as 205 MW, which would achieve almost 26% of Austin's Climate Protection Plan's goal of an 800 MW peak reduction by 2020. Similarly, this analysis suggests that accurately sizing residential air-conditioning equipment could displace as much as 41 MW of peak demand, or nearly the equivalent of one natural gas peaking plant. Additionally, replacing oversized units with higher efficiency units (EER

14, COP 4.1) could increase those peak savings to 81 MW. This research also indicates that Austin Energy could substantially increase energy efficiency rebate levels for home energy retrofits and still be at parity with the cost of building new generating capacity.

While this analysis relies on data from Austin the approach can be applied to other cities. Implementation of initiatives similar to Austin's ECAD ordinance would produce valuable information and the methods used herein can be applied to analyze other databases in other climates. This information would lead to better-informed decisions when assessing energy efficiency programs and climate protection plans.

Chapter 3

Clustering analysis of residential electricity demand profiles

3.1 Introduction

Electricity generation is responsible for 40% of primary energy use in the US [92], and while significant information is available about its generation, much less is known about its end use, particularly on an inter-daily temporal scale. Current smart meter and smart grid deployments are vastly increasing the amount of energy use information being created, curated, and analyzed. These deployments, which typically have 15-minute or 1-hour granularity, increase the amount of available energy use information by orders of magnitude over once-per-month reads. This recently available abundance of data allows for analyses not previously possible. In particular, it allows for temporal assessment of electricity use, which is important because it holds the potential to reveal non-obvious insights about electricity consumption and the behavioral and technological drivers of that consumption. Also, the temporal aspect of electricity use is significant because electricity is hard to store and thus must be produced at the rate of consumption. This balance that must occur in the wholesale market can cause the price for electricity to be volatile, especially during peak demand times typically due to lack of excess capacity and transmission congestion.

Residential power demand can range in magnitudes from a few hundred watts (W) to the low tens of kilowatts (kW), especially in regions where residential air-conditioning units are ubiquitous. Inter-season differences for residential total grid power demand in cooling climates can change by over 400% from non-cooling to cooling periods [7]. Residential electrical use patterns fluctuate differently during the day due to space-conditioning set points, time of year, weather, occupant behavior and schedules. In a similar way, the electric grid load and net carbon emissions change temporally due to changes in demand, temperatures, and generation mixes, which are also dynamic with daily and seasonal timescales [93, 94].

The drivers of macro-level, aggregate energy use are current topics of study [28], but the factors affecting residential energy use at finely-resolved timescales are poorly understood. This work seeks to fill part of that knowledge gap by identifying correlations between electric customer survey data and electricity use profiles. Understanding electricity consumption patterns and their influencing factors could potentially lead to more robust energy modeling, more precise demand forecasts, and more effective energy conservation and peak reduction campaigns. While beyond the scope of this paper, these results might also inform analysis of behavior-related tradeoff calculations such as the environmental impacts of telecommuting [95].

Clustering analysis of temporally-resolved electricity use has currently been limited to generating typical load profiles, grouping like customers, or finding outliers. This analysis seeks to take the analysis a step further by leveraging the comprehensive data set available from a local smart grid demonstration project [36] and explore the drivers behind the derived groups of electricity customers*.

3.2 Background

Clustering is an effective tool for analyzing static data or time series data, such as electricity usage [29, 30]. For example, Chicco [31] used a variety of clustering

*This chapter has been submitted as an original research article to the journal *Energy Policy*.

techniques to analyze 400 load patterns of non-residential, medium voltage consumers during a weekday in Italy. The electricity data were in 15-minute intervals and were normalized by the minimum and maximum value of the daily load pattern so that all normalized load profiles were between 0 and 1. He found that choosing the best clustering algorithms depended on whether or not the purpose was to identify the outliers or to assign all the load profiles to a specific category.

Kim et al. [32] performed a similar analysis by clustering electricity usage from high voltage consumers in South Korea to determine typical load profiles using 15-minute data. They had 3,183 high voltage customers from the Korea Electric Power Corporation (KEPCO) whose meter data were used for this study. They found the hierarchical clustering technique to be the most effective in determining typical load profiles.

Räsänen et al. [33] performed clustering of hourly electricity usage over a more diverse consumer base in Finland. The study included 3,989 consumers in the following categories: 80% residential, 8% public sector, 6% services, 5% agriculture, and 1% industry. To perform the clustering, they reduced the size of the dataset, so they performed the clustering based on 489 randomly chosen time points throughout the year (489 represents 5% of the year). Their data-driven clustering technique provided more accurate load forecasts than the current methods used by the utility.

Zhou et al. [34] and Panapakidis et al. [35] used smaller datasets for their clustering analyses of electricity loads. Zhou et al. used 72 load profiles from six different consumers in China and Panapakidis et al. used a mix of 150 residential, commercial, and industrial consumers in Greece. Panapakidis et al. notes that a consumer's electricity costs might also be helpful to consider when performing clustering.

3.3 Methods

This analysis employed a data-driven approach to 1) create average seasonal curves for each home in the analysis, 2) determine the number of representative residential electricity demand profiles within their respective seasons, and 3) attempt to draw correlations to the different profiles based on data from the same homes. Initial data averaging, grouping, and home curve derivations were performed using the Texas Advanced Computer Center's data applications resource Corral [96]. Corral is a collection of storage and data management resources available to researchers at the University of Texas at Austin. Data analytics and clustering were performed using the statistical program R (version 3.0.2). Figure 3.1 provides a flowchart of the analysis progression.

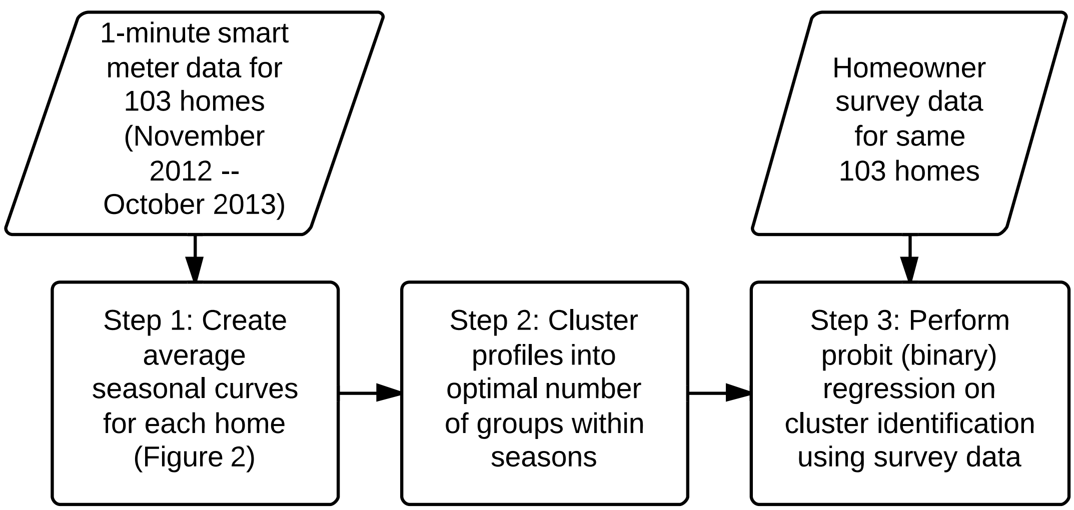

Figure 3.1: This flowchart shows the datasets and sequence of steps for the analysis.

3.3.1 Creating average seasonal curves

The data used in this analysis are collected as part of a smart grid demonstration project located in Austin, TX and operated by the Pecan Street Research Institute [36]. The subset of data analyzed was power consumption in watts measured every 1 minute for 103 homes in Austin from November 2012 to October 2013. The 1 minute data were used to create a representative electricity use profile for each home for every season of the year. The data were first averaged over each hour to create hourly profiles. For example, electricity use data from 14:01 – 15:00 were averaged and assigned to the value 15:00 (interval ending). This yielded a 24-element vector for each day of the year. Figure 3.2 shows a 10 day sample of 1 minute data for a single home. The left plot shows the raw 1 minute data and the right plot shows the same data averaged to 1 hour profiles, with the average of the hourly profiles (for all the days of this month – May 2013) in bold.

This bold curve, which is a home's representative electricity use profile for a season is the curve or profile referred to throughout this analysis. This curve is described in Equation 3.1:

$$curve_j = \begin{pmatrix} w_{j0} \\ w_{j2} \\ \vdots \\ w_{jh} \\ \vdots \\ w_{j23} \end{pmatrix}, \tag{3.1}$$

where $curve_j$ is the representative curve for home j and w_{jh} is described in Equation 3.2:

$$w_{jh} = \sum_{m,h} P_{jm}/60 \tag{3.2}$$

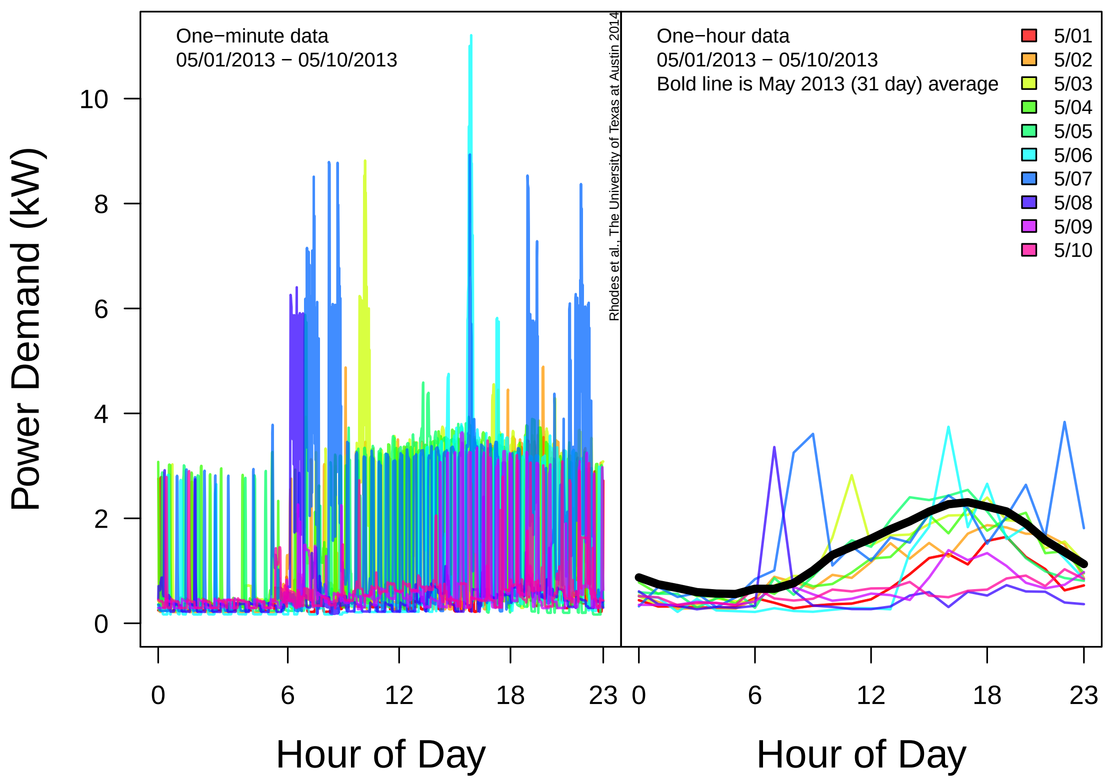

Figure 3.2: Figure showing a sample (10 days worth, May 01, 2013 – May 10, 2013) of the initial, raw 1 minute data from a single home on the left, averaged 1 hour profiles (same days) on the right with the bold line showing the average of the hourly curves for the entire month of May 2013. The raw data (left panel) show the great variability in the demand profiles, whereas the hourly averages and averaged profile (right panel) show the general diurnal variation for consumption.

where P_{jm} is the measured average power draw for home j over minute m of hour h.

The primary focus of this research was temporal variation in electricity use (i.e., profile shape), rather than magnitude, which has been considered in other analyses [36]. When profiles were clustered with magnitude still included, magnitude, not shape dominated the cluster arrangement. Therefore each raw, hourly usage curve was then normalized by its largest value so that all home profiles would be on a fractional 0 to 1 scale. The minimum value was not subtracted from the curve so as not to exacerbate the difference between minimum and maximum electricity use. For example, some homes, on average reduced their usage to almost zero during certain parts of the day while others never dropped their average usage below 40% of their average peak usage. Normalization of the curves could introduce some bias in that even if a home is using less normalized electricity during peak times, it might be using much more (in absolute terms) that others that are using more normalized electricity during peak times. However, homes that are "high users" are likely to be larger [28, 36, 97] and will likely have a larger base load as well as a larger space conditioning load.

The normalized seasonal curves are then used as inputs to the optimal clustering algorithm discussed in the next section.

3.3.2 Determining distinctive clusters within seasons

After creating average curves for each home for each season, the curves were put into groups via a *k-means* clustering analysis. *K-means* is an iterative process that attempts to partition each curve (the seasonal average curve – a 24-valued vector) into groups such that the sum of squares (Euclidean distance) from each group member to its group center is minimized [98]. After each step, the centers are recalculated and the curves are redistributed until the process converges. In this approach, as in most clustering analyses, the number of clusters is pre-specified, so prior knowledge of the number of groups is required. There are tests that attempt to determine the optimal number of clusters in the complete dataset, but different tests can give slightly different results. In this analysis, the *R* function *NbClust* was used to determine the optimal number of clusters. The function *NbClust* performs 30 tests for determining the optimal number of clusters in the complete group of data. The function returns each of the tests optimal number of clusters, and the most-picked number of clusters was chosen as the number to use in the *k-means* clustering analysis. The test of the number of optimal clusters was performed for each season separately.

The temporal shape of the electricity use profile is important because even though residential customers typically pay a constant rate per kWh for electricity, the wholesale electric market price can fluctuate orders of magnitude in less than an hour. These dynamics are particularly observed during the summer peak in the Electric Reliability Council of Texas (ERCOT) grid – the electric grid that services most of Texas, including Austin. For a given season, the average value of the cluster's electricity use can be defined by Equation 3.3:

$$E_{value,z} = \frac{\sum^{h}(C_{z,h} \times SPP_h)}{kWh_z}, \tag{3.3}$$

where $E_{value,z}$ is the average value of cluster z's electricity use (\$/kWh), $C_{z,h}$ is the average (non-normalized) electricity use for cluster z at hour h, SPP_h is the average price of wholesale market electricity at hour h, and kWh_z is the average total kWh of electricity used per day by cluster z.

3.3.3 Binary regression analysis of clustering results

Once clusters of profiles were created for each season, survey data from the homes were used to see if there were any significant correlations between survey responses and cluster identification. A probit regression model (*R*, *probitmfx* [99]) was chosen to test the significance of any marginal effects of explanatory variables on cluster identification. A marginal effect of an explanatory variable, x, is the partial derivative, with respect to x, of the prediction function (in this case the normal cumulative probability density function) with all the other explanatory variables at their average value. Because this method is based on the partial derivative, the marginal effect can be greater than one even though the probability is between 0 and 1. The probit model is a binary classification model where the dependent variable (y_j) can only take on a value of 0 or 1. In this case, the model attempted to estimate the inclusion in a certain cluster (1 if included and 0 if not). The model is given by Equation 3.4:

$$Pr(y_j = 1) = \Phi(X_j\beta), \tag{3.4}$$

where Pr is the probability, y_j is the outcome (response) variable (0 or 1 for home j), Φ is the normal cumulative distribution function with mean 0 and standard deviation 1, X_j is the set of explanatory variables, and β is the set of fit coefficients (usually decided by maximum likelihood) [100].

The *R* function *probitmfx*, with robust standard errors, was chosen to build the model. This function is convenient because the coefficients (β) returned are the marginal effects of the explanatory variables (X_i) on the probability of y_i being equal to 1. Each β is interpreted as the effect of each variable at the average value of the others.

Explanatory variables in the model included: *workday* (whether or not someone worked from home for more than 20 hours per week during the day time); *males* (the number of males living in the home); *females* (the number of females living in the home); *num_kids* (the number of children under 18 living in the home); *education* (the highest education level of the occupants); *income* (the income bracket of the home); *hours_tv* (the number of hours spent watching television per week); *num_computers* (the number of desktop computers, laptops, tablets, and other computing devices in the home); *vehicles* (the number of vehicles in the home); *quiz_total* (the number of questions correctly answered in the survey that referred to general energy and water knowledge); *pv* (wether or not a home had a solar PV system); *bayes* (how the homeowner answered a question on happiness [36]); *ev* (wether or not the home has an electric vehicle (EV)); *greenbuilt* (whether the home was a new green-built home); *retrofit* (wether or not the home has had any major retrofits); *smart_therm* (wether or not the home has a smart thermostat); *pv:greenbuilt* (the interaction term of being a new green-built home and having a solar PV system – most homes with solar PV systems were also green-built); and *ev:in_greenbuilt* (the interaction term of being a new green-built home and having an EV – most homes with EVs were also green-built).

The model was validated by the Wald χ^2 statistic [101] and by checking the percentage of times that it could correctly predict the inclusion in a given cluster. The Wald χ^2 statistic checks if at least one of the explanatory variables (β) in the model is non-zero.

3.4 Results and Discussions

3.4.1 Creating average seasonal curves

Seasonal curves were created for each home for each of the four seasons. Figures 3.3 – 3.6 show box plots of the pre-normalized curves for all the homes with a distribution for each hour of the day. The graphs provide distributions of electric power demand for every hour of the day in each season for all the homes in this analysis. The seasons have varying levels of magnitude with the difference likely driven by residential air-conditioning use [8, 9], which is a function of climate and homeowner preference.

In all four figures, the solid line in the middle of the box plot refers to the median value for that hour for all the curves. The length from the median to the bottom of the box is the second quartile (25% of values) and the distance from the median to the top of the box is the third quartile. The length to the bottom of the box to the bottom whisker is the shorter of 1.5 times the inter-quartile range (top of the box to the bottom) or the distance from the bottom of the box to the lowest data point for that hour and the length to the top of the box to the top whisker is the shorter of 1.5 times the inter-quartile range or the distance from the top of the box to the highest data point for that hour. Any circles are data points that are beyond 1.5 times the inter-quartile range from the bottom or top of the box.

These results highlight the difference in residential inter-seasonal electricity use caused by weather-driven space conditioning loads. The seasons were then used to dissect the data further in search of inter-seasonal variations between homes' usage profiles.

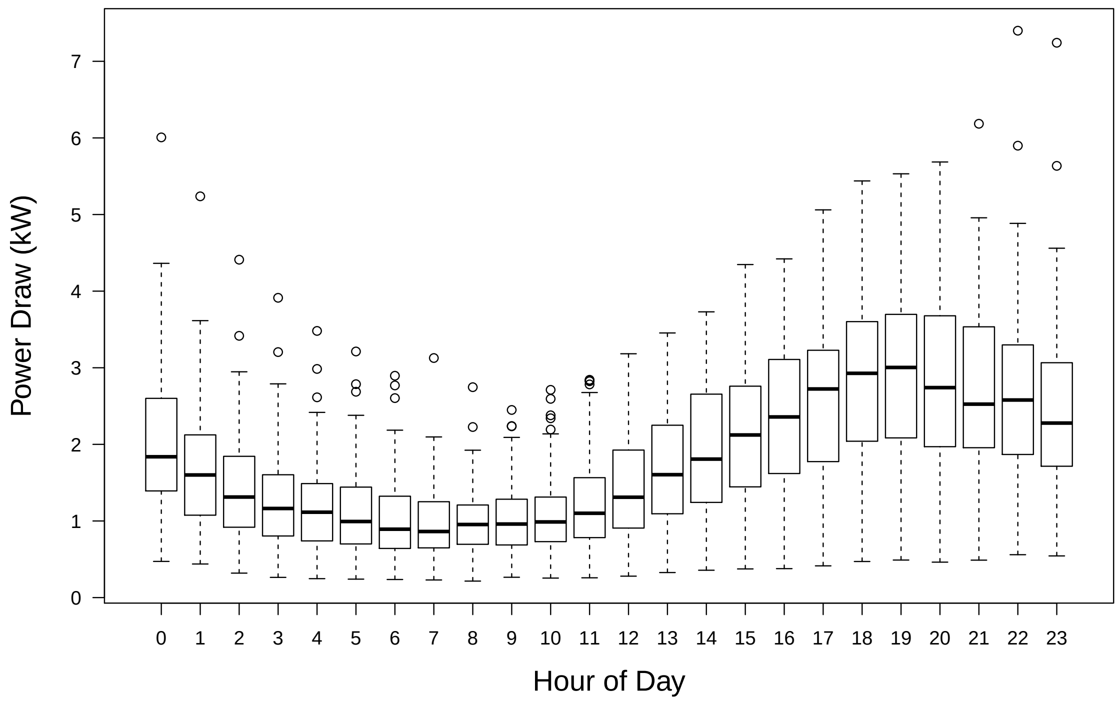

Figure 3.3: Box-and-whisker plot of the raw (pre-normalization) curves for all homes for the summer (June 2013 – August 2013) season. The box-and-whisker shows the 4 quartiles of the data and the circles are data points above or below 1.5 times the interquartile range from either the top or bottom of the box.

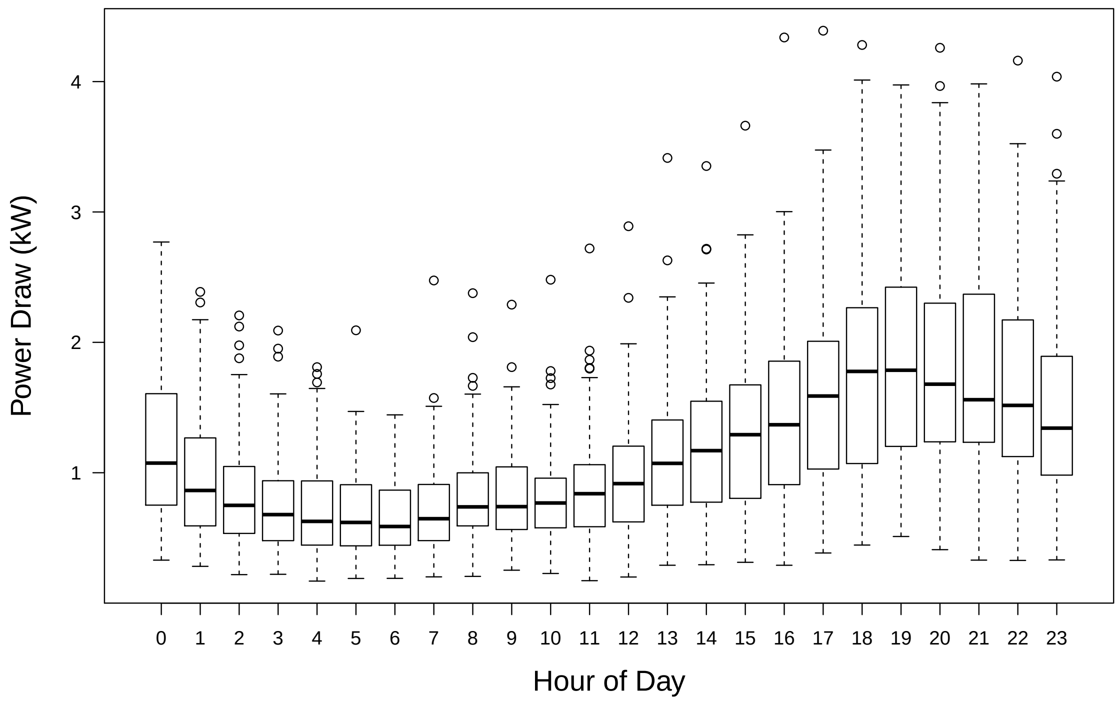

Figure 3.4: Box-and-whisker plot of the raw (pre-normalization) curves for all homes for the fall (September 2013 – October 2013 + November 2012) season. The box-and-whisker shows the 4 quartiles of the data and the circles are data points above or below 1.5 times the interquartile range from either the top or bottom of the box.

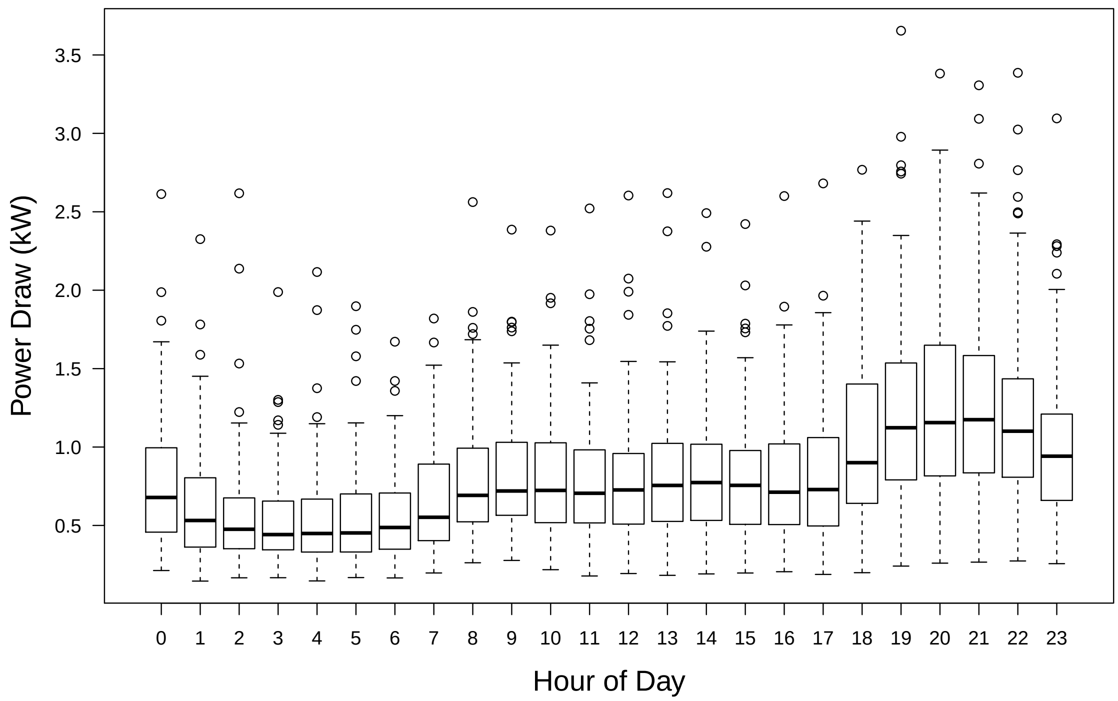

Figure 3.5: Box-and-whisker plot of the raw (pre-normalization) curves for all homes for the winter (December 2012 – February 2013) season. The box-and-whisker shows the 4 quartiles of the data and the circles are data points above or below 1.5 times the interquartile range from either the top or bottom of the box.

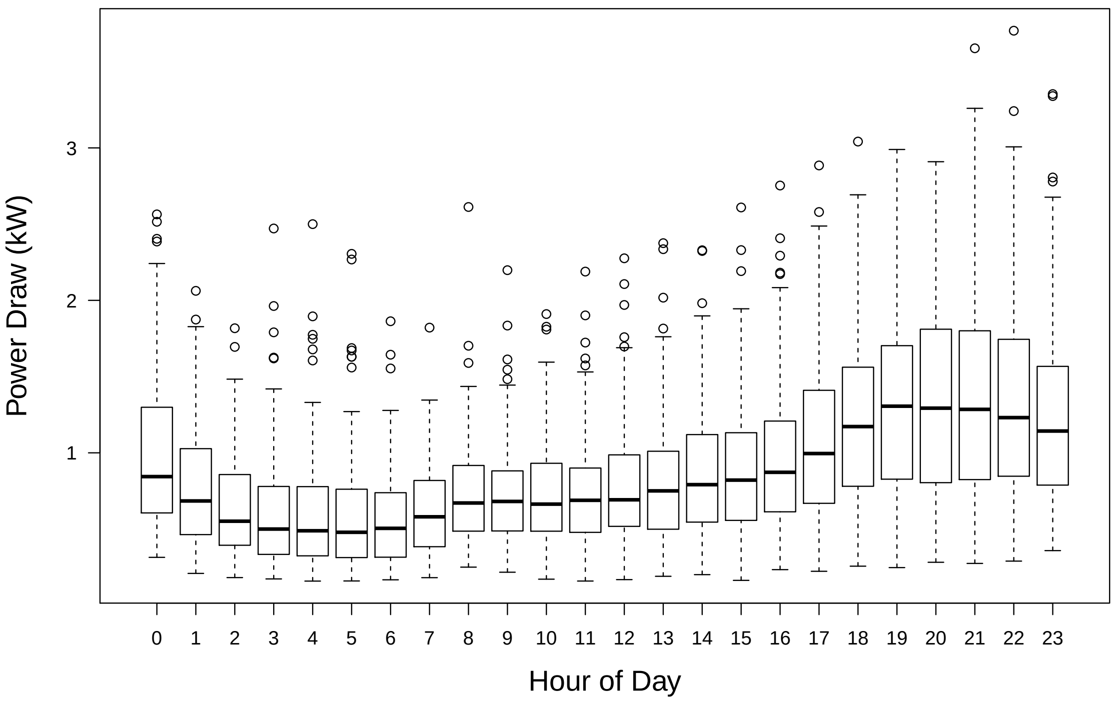

Figure 3.6: Box-and-whisker plot of the raw (pre-normalization) curves for all homes for the spring (March 2013 – May 2013) season. The box-and-whisker shows the 4 quartiles of the data and the circles are data points above or below 1.5 times the interquartile range from either the top or bottom of the box.

3.4.2 Determining optimal distinctive clusters within seasons

It was determined that each season has two definitive clusters that represent seasonal household electricity demand. Figures 3.7 – Figure 3.10 show the normalized profiles clustered into groups as well as the cluster mean.

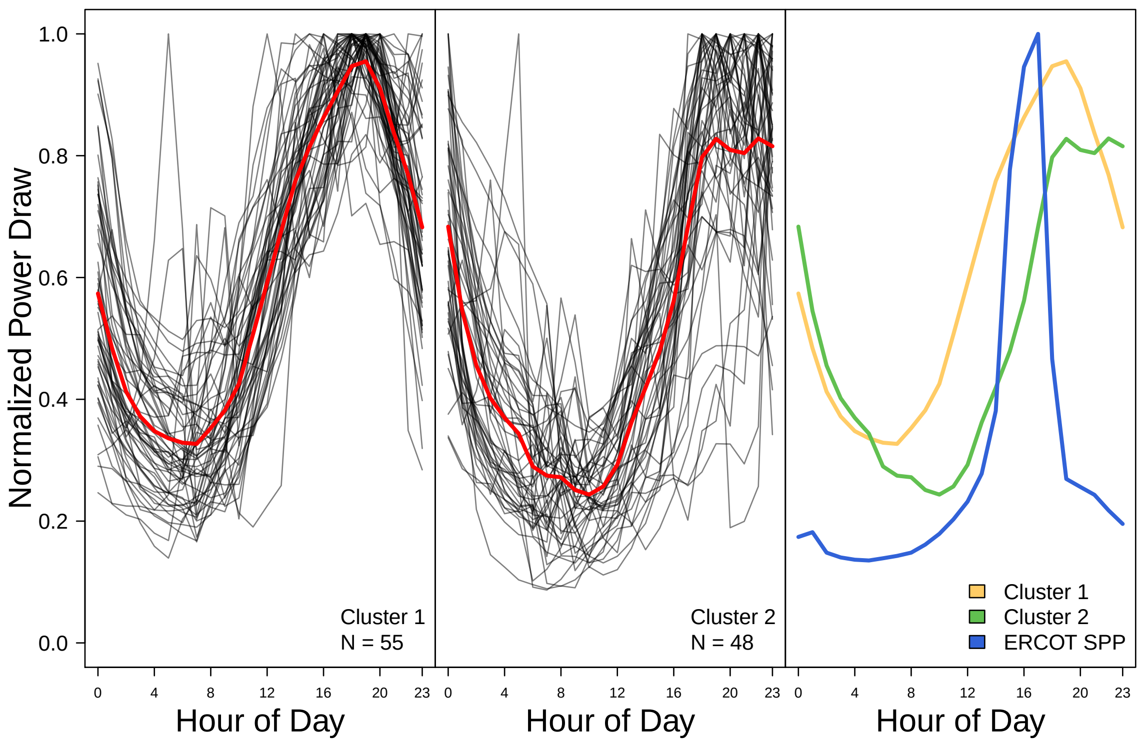

Figure 3.7: Plot showing (left and center) the breakout of summer clusters including the cluster averages in red and (on the right) both cluster averages in the same plot with the normalized ERCOT SPP for the same time period.

Summer cluster 1 (Figure 3.7 left) included homes that (on average) tended to have a wide range of early morning usage that reduces until about 07:00 and then increases to an afternoon peak around 19:00, and then reduces. Summer cluster 2 (Figure 3.7 center) included homes that (on average) start with high usage which decreases until about 10:00 and then increases until about 19:00 at which the homes maintained an average level of power draw for the rest of the day. Summer cluster 1 is tighter than cluster 2 with an average within cluster sum of squares of 0.31 and 0.50, respectfully. Figure 3.7 (right) also includes the average summer cluster profiles on the same plot as the normalized average ERCOT SPP. The normalized summer average ERCOT SPP curve peaked at 17:00. The ERCOT SPP peaks at relatively high prices in the afternoon summer hours with 16 of 24 hours at a price less than 25% of the peak price. Even though individual homes could be peaking coincident with the ERCOT peak, when the summer ERCOT SPP peaks, the cluster 1 average is at 91% of its maximum and the cluster 2 average is at 68% of its maximum. Based on ERCOT's SPP, the average summer value (Equation 3.3) of cluster 1's electricity use is about 10% higher than from cluster 2 (0.0528 verses 0.0480 \$/kWh).

Fall cluster 1 (Figure 3.8 left) included homes that (on average) tended to have a wide range of early morning usage that reduces until about 04:00 and then increases to an afternoon peak around 18:00, and then reduces. Fall cluster 2 (Figure 3.8 center) included homes that (on average) start with high usage which decreases until about 06:00, increases for 2 hours, reduces again, and then increases until about 21:00 at which the homes maintained a roughly average level of power draw before dipping the last hour of the day. Fall cluster 1 is tighter than cluster 2 with an average within cluster sum of squares of 0.35 and 0.46, respectfully. Figure 3.8 (right) also includes the average fall cluster profiles on the same plot as the normalized average ERCOT SPP. The normalized fall average ERCOT SPP curve peaked at 17:00. The ERCOT SPP peaks is less severe than the summer time peak probably due to less residential air-conditioning demand and the greater availability of low-cost wind generation on the grid [102]. Similar to the the summer clusters, when the fall ERCOT SPP peaks, the cluster 1 average is at 88% of its maximum and the cluster 2 average is at 55% of its maximum. Based on ERCOT's SPP, the average fall value (Equation 3.3) of

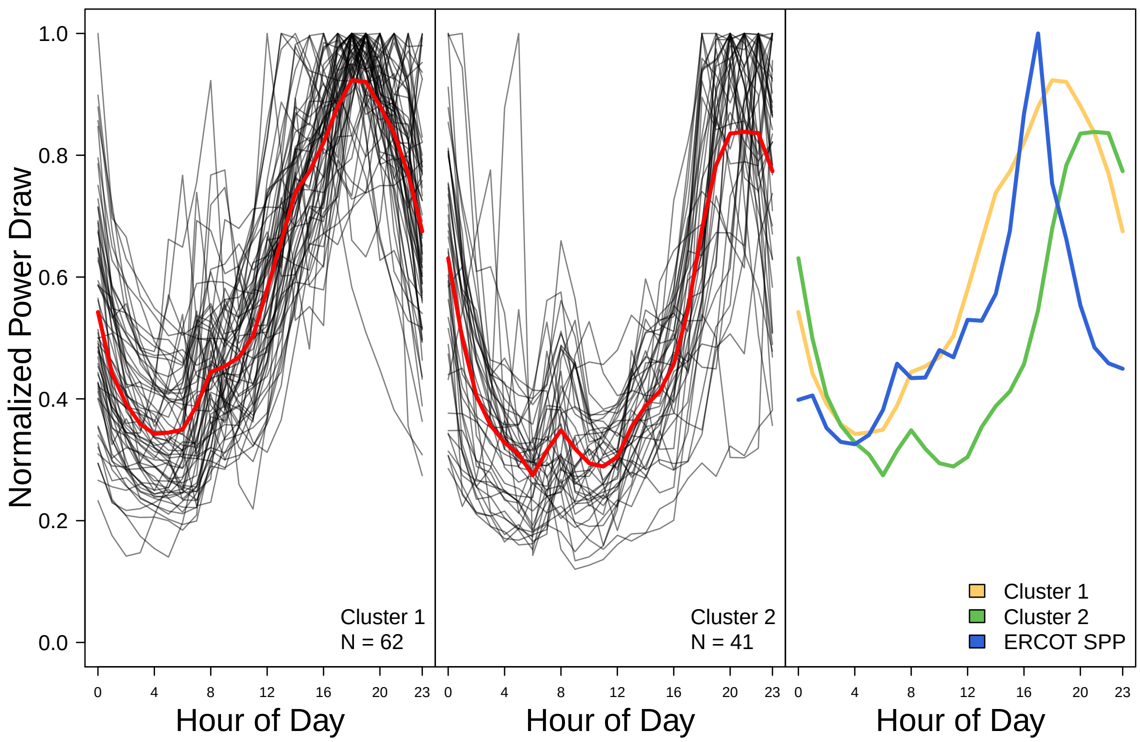

Figure 3.8: Plot showing (left and center) the breakout of fall clusters including the cluster averages in red and (on the right) both cluster averages in the same plot with the normalized ERCOT SPP for the same time period.

cluster 1's electricity use is about 5% higher than from cluster 2 (0.0333 verses 0.0317 $/kWh).

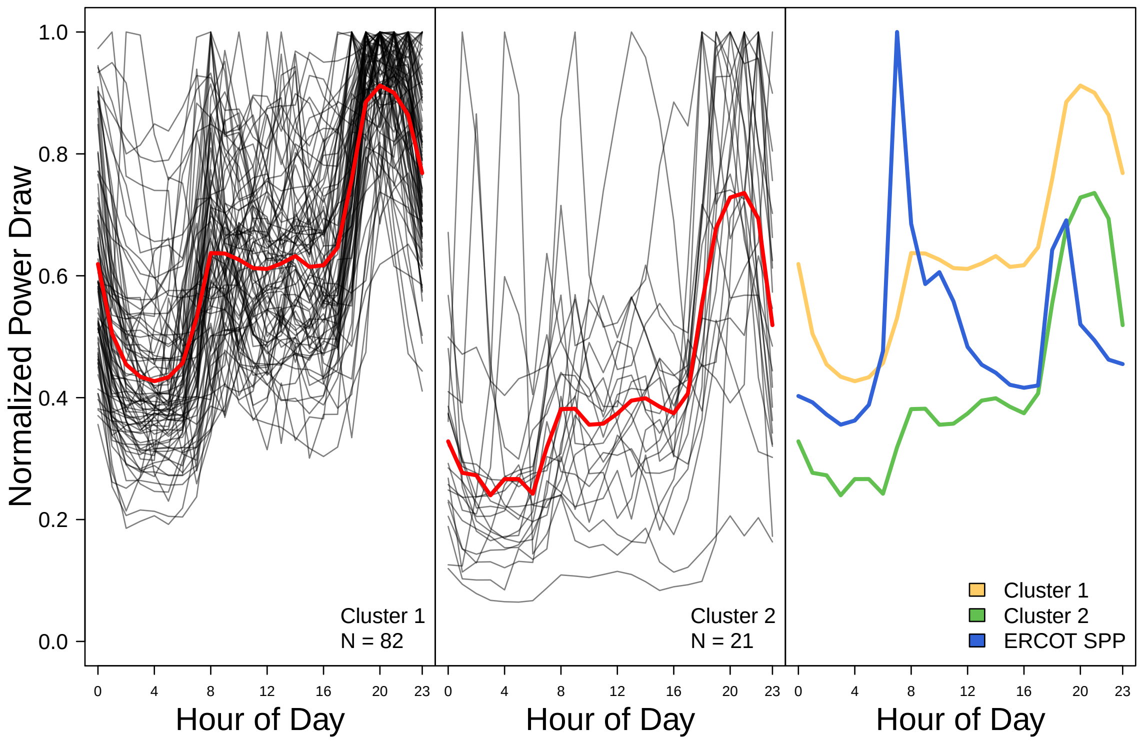

Figure 3.9: Plot showing (left and center) the breakout of winter clusters including the cluster averages in red and (on the right) both cluster averages in the same plot with the normalized ERCOT SPP for the same time period.

Winter cluster 1 (Figure 3.9 left) included homes that (on average) tended to have a wide range of early morning usage that reduces until about 04:00 and then increases to around 08:00, levels off until 18:00, increases until 20:00 before reducing. Cluster 2 (Figure 3.9 center) included homes have a wide range of usage that (on average) roughly follows that of cluster 1. However, cluster 2 included homes that had higher peaks than homes in cluster 1, thus the lower relative usage during most of the day – this will be further discussed in the next section. The curves are similar except for less of a dip in the early morning. Winter cluster 1 is tighter than cluster 2 with an average within cluster sum of squares of 0.49 and 0.81, respectfully. Figure 3.9 (right) also includes the average winter cluster profiles on the same plot as the normalized average ERCOT SPP. The normalized winter average ERCOT SPP has a double peak with the higher at 07:00 and the lower at 19:00. The ERCOT SPP peaks is again less severe than the summer time peak and the early morning peak is probably explained by electric resistance heating or electric heat pumps in many homes in ERCOT [6], and the fact that the relative difference between the morning and evening usage is much less in the winter. Because the mild differences in the winter ERCOT SPP, the average value of cluster 1 and cluster 2's electricity use was essentially the same.

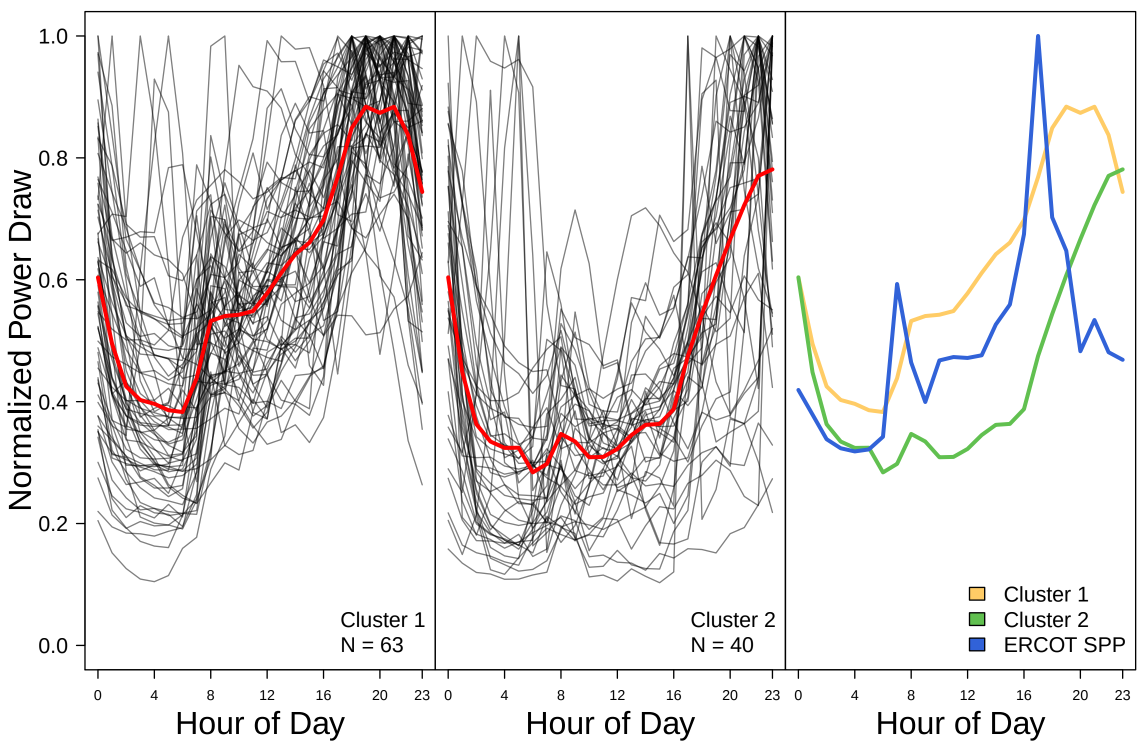

Figure 3.10: Plot showing (left and center) the breakout of spring clusters including the cluster averages in red and (on the right) both cluster averages in the same plot with the normalized ERCOT SPP for the same time period.

Spring cluster 1 (Figure 3.10 left) included homes that (on average) tended to have a wide range of early morning usage that reduces until about 06:00, increases rapidly until 09:00 then increases at a slower rate until peaking around 19:00 and then reducing at 22:00. Cluster 2 (Figure 3.10 center) included homes that (on average) start with higher usage which decreases until about 02:00 and then holds steady until about 18:00 then continues increasing throughout the day peaking at 23:00. Spring cluster 1 is tighter than cluster 2 with an average within cluster sum of squares of 0.52 and 0.74, respectfully. Figure 3.10 (right) also includes the average spring cluster profiles on the same plot as the normalized average ERCOT SPP. The normalized spring average ERCOT SPP has a double peak with the lower at 07:00 and the higher at 17:00. The peaks are probably a result of a combination of heating and cooling putting stress on the grid as the season transitions from winter to summer. Based on ERCOT's SPP, the average summer value (Equation 3.3) of cluster 1's electricity use is about 4% higher than from cluster 2 (0.0296 verses 0.0286 $/kWh). The results from the clustering analysis are summarized in Table 3.1.

Table 3.1: Clustering analysis results showing tightness of clusters and the average seasonal value of electricity used by each cluster.

Season	Cluster	Tightness	Cost($/kWh)	Hour of Peak
Summer	1	0.31	0.0528	19:00
	2	0.5	0.0480	19:00
Fall	1	0.35	0.0333	18:00
	2	0.46	0.0317	21:00
Winter	1	0.49	0.0274	20:00
	2	0.81	0.0275	21:00
Spring	1	0.52	0.0296	19:00
	2	0.74	0.0286	23:00

3.4.3 Binary regression analysis of clustering results

Binomial probit regression was used to determine if there were any significant correlations affecting the probability of a home being in a certain cluster. The output from the analysis of the effect of survey variables on the prediction of a home being in cluster 1 during the summer season is given in Table 3.2. Because there are only two outcomes (cluster 1 or cluster 2) the regression output is the same for the effect of variables prediction of a home being in cluster 2 except the signs on the coefficient estimates are reversed and interpreted as having the opposite effect.

Table 3.2: Probit regression results for summer profiles showing marginal effects (dF/dx) of each explanatory variable (β) on the probability of being in cluster 1, at the average of all the others. Summer cluster 1 is the left box of Figure 3.7.

Explanatory Variable	Coefficient (dF/dx)	Robust Std. Error	z-value	Two-tailed P-test	95% Confidence Interval	
workday	0.552	0.105	5.257	0.000	(0.342 , 0.763)	***
males	–0.243	0.193	–1.259	0.212	(–0.629 , 0.143)	
females	–0.366	0.207	–1.770	0.080	(–0.779 , 0.048)	.
num_kids	0.187	0.205	0.913	0.364	(–0.223 , 0.597)	
education	–0.230	0.121	–1.906	0.060	(–0.471 , 0.011)	.
income	–0.107	0.056	–1.904	0.060	(–0.219 , 0.005)	.
hours_tv	0.100	0.029	3.407	0.001	(0.041 , 0.159)	**
computers	0.132	0.047	2.809	0.006	(0.038 , 0.226)	**
vehicles	0.132	0.121	1.088	0.280	(-0.110 , 0.374)	
quiz_total	–0.017	0.034	–0.493	0.624	(–0.085 , 0.051)	
pv	–0.430	0.398	–1.081	0.283	(–1.225 , 0.365)	
bayes	0.249	0.193	1.294	0.199	(–0.136 , 0.635)	
ev	–0.502	0.368	–1.364	0.176	(–1.238 , 0.234)	
greenbuilt	0.266	0.227	1.174	0.244	(–0.187 , 0.720)	
retrofit	0.427	0.113	3.764	0.000	(0.200 , 0.654)	***
smart_therm	0.156	0.188	0.829	0.409	(–0.220 , 0.533)	
pv:greenbuilt	0.649	0.326	1.992	0.050	(–0.003 , 1.300)	*
ev:greenbuilt	0.017	0.547	0.030	0.976	(–1.078 , 1.111)	

$\chi^2 = 30.3$, n = 103, Significance codes: 0 '***' 0.001 '**' 0.01 '*' 0.05 '.' 0.1 ' ' 1

The variables *workday*, *hours_tv*, *computers*, *retrofit*, and the interaction term *pv:greenbuilt* are all significant using a confidence interval of 95% and the variables *females*, *education*, and *income* are significant using a confidence interval of 90%. The coefficient estimates are calculated as the direct marginal effect (dF/dx) of the explanatory variable on the probability of a home being in cluster 1 with all other explanatory variables at their average value. Thus, if a home contains a person that regularly works from home (*workday*), that home is 55% more likely to be in cluster 1. Each additional hour of television watched per week (*hours_tv*) corresponds to a 10% greater chance of being in cluster 1 (this variable has also been shown to be significant in macro-level studies of electricity use [28]). Each additional computing device (*computers*) in the home leads to a 13% increase in the probability of being in cluster 1. Also, if the home has had recent energy retrofits, it is 42% more likely to be in cluster 1. Lastly, if the home has solar PV *and* is green-built it is 64% more likely to be in cluster 1. The variables *females*, *education*, and *income* were negatively correlated with being in cluster 1, although with less certainty. The χ^2 value of 30.3 indicates that the model is significant compared to the null model (all $\beta = 0$). Because cluster 1 consumes relatively more electricity when prices are higher (see Figure 3.7), the regression results indicate that people who work from home are more likely to be negatively impacted by time-of-use or real-time pricing schemes (all else equal), which are often more prevalent in the summer season.

The model was able to predict the correct summer cluster about 77% of the time. Regression texts typically suggest methods for removing explanatory variables based on the expected sign of the coefficient, significance (z or t-scores), and knowledge of the underlying data and population [100]. Little was known about how certain variables would intuitively affect which cluster a home was likely to be in with the exception of the variable *workday*. Thus, all variables were left in the model.

The results for the fall probit regression are given in Table 3.3.

Table 3.3: Probit regression results for fall profiles showing marginal effects (dF/dx) of each explanatory variable (β) on the probability of being in cluster 1, at the average of all the others. Fall cluster 1 is the left box of Figure 3.8.

Explanatory Variable	Coefficient (dF/dx)	Robust Std. Error	z-value	Two-tailed P-test	95% Confidence Interval	
workday	0.35	0.12	2.89	0.00	(0.11 , 0.59)	**
males	–0.14	0.16	–0.91	0.37	(–0.45 , 0.17)	
females	–0.17	0.16	–1.05	0.30	(–0.49 , 0.15)	
num_kids	0.05	0.16	0.33	0.74	(–0.27 , 0.38)	
education	–0.07	0.10	–0.65	0.52	(–0.28 , 0.14)	
income	–0.06	0.05	–1.36	0.18	(–0.16 , 0.03)	
hours_tv	0.05	0.02	1.95	0.05	(0.00 , 0.10)	.
computers	0.07	0.04	1.73	0.09	(–0.01 , 0.15)	.
vehicles	0.08	0.12	0.67	0.51	(–0.16 , 0.32)	
quiz_total	–0.02	0.03	–0.62	0.53	(–0.08 , 0.04)	
pv	0.09	0.40	0.22	0.83	(–0.71 , 0.89)	
bayes	0.10	0.16	0.61	0.55	(–0.23 , 0.43)	
ev	–0.37	0.41	–0.91	0.37	(–1.18 , 0.44)	
greenbuilt	0.19	0.21	0.89	0.37	(–0.23 , 0.60)	
retrofit	0.22	0.15	1.43	0.16	(–0.09 , 0.52)	
smart_therm	0.14	0.17	0.86	0.39	(–0.19 , 0.48)	
pv:greenbuilt	0.25	0.42	0.60	0.55	(–0.59 , 1.10)	
ev:greenbuilt	–0.14	0.47	–0.31	0.76	(–1.08 , 0.80)	

$\chi^2 = 29.1$, n = 103, Significance codes: 0 '***' 0.001 '**' 0.01 '*' 0.05 '.' 0.1 ' ' 1

For the fall clusters, the variable *workday* was significant using a confidence interval of 95% and the variables *hours_tv* and *computers* were significant using a confidence interval of 90%. Thus, if a home contains a person that regularly works from home (*workday*), that home is 35% more likely to be in cluster 1. The variables *hours_tv* and *computers* were positively correlated with being in cluster 1, although with less certainty. The χ^2 value of 29.1 indicates that the model is significant compared to the null model (all $\beta = 0$). Overall, the model was able to predict the correct summer cluster only about 65% of the time.

The results for the winter probit regression are given in Table 3.4.

Table 3.4: Probit regression results for winter profiles showing marginal effects (dF/dx) of each explanatory variable (β) on the probability of being in cluster 1, at the average of all the others. Winter cluster 1 is the left box of Figure 3.9.

Explanatory Variable	Coefficient (dF/dx)	Robust Std. Error	z-value	Two-tailed P-test	95% Confidence Interval	
workday	0.14	0.08	1.67	0.10	(–0.03 , 0.30)	.
males	0.11	0.11	0.97	0.33	(–0.12 , 0.34)	
females	0.12	0.09	1.31	0.19	(–0.06 , 0.29)	
num_kids	–0.09	0.13	–0.69	0.49	(–0.34 , 0.17)	
education	–0.15	0.08	–1.80	0.08	(–0.32 , 0.02)	.
income	–0.04	0.04	–1.02	0.31	(–0.11 , 0.04)	
hours_tv	0.00	0.01	–0.20	0.84	(–0.03 , 0.03)	
computers	0.01	0.03	0.41	0.69	(–0.05 , 0.08)	
vehicles	–0.08	0.08	–1.09	0.28	(–0.24 , 0.07)	
quiz_total	0.03	0.03	1.23	0.22	(–0.02 , 0.09)	
pv	0.94	0.06	16.33	$<$ 2.20E-16	(0.83 , 1.06)	***
bayes	–0.10	0.08	–1.22	0.22	(–0.27 , 0.06)	
ev	–1.00	0.00	–574.48	$<$ 2.20E-16	(–1.00 , -0.99)	***
greenbuilt	0.00	0.09	–0.01	0.99	(–0.18 , 0.18)	
retrofit	–0.01	0.12	–0.12	0.91	(–0.25 , 0.22)	
smart_therm	–0.38	0.18	–2.10	0.04	(–0.75 , -0.02)	*
pv:greenbuilt	–0.84	0.11	–7.93	0.00	(–1.06 , -0.63)	***
ev:greenbuilt	0.51	0.15	3.50	0.00	(0.22 , 0.80)	***

χ^2 = 32.98, n = 103, Significance codes: 0 '***' 0.001 '**' 0.01 '*' 0.05 '.' 0.1 ' ' 1

For the winter clusters, the variables *pv*, *ev*, *smart_therm*, and the interaction terms *pv:greenbuilt* and *ev:greenbuilt* were significant using a confidence interval of 95% and the variables *workday* and *education* were significant using a confidence interval of 90%. In the winter profiles, the shape is less driven by thermal loads than in other seasons and more driven by appliances and, in this case, electric vehicles. Home with solar PV were highly correlated with being in cluster 1 (94%) while homes with electric vehicles were highly correlated with not being in cluster 1 (~100%). However, both interaction terms associated with the homes being green-built were also significant and thus reduced (*pv:greenbuilt*) or increased (*ev:greenbuilt*) the chances of being in cluster 1. Also, homes with a learning thermostat (*smart_therm*) were 38% less likely to be in cluster 1. The variable *workday* was positively associated with being in cluster 1, while the variable *education* was negatively associated with being in cluster 1. The model was able to correctly predict cluster identification about 82% of the time and has a χ^2 value of 32.98.

The results for the spring probit regression are given in Table 3.5.

For the spring clusters, the variables *workday*, *education*, and *income* were significant using a confidence interval of 95% and the variables *hours_tv*, *bayes*, and *retrofit* were significant using a confidence interval of 90%. Thus, if a home contains a person that regularly works from home (*workday*), that home is 28% more likely to be in cluster 1, each additional level of education and income were negatively correlated with cluster 1 with a 23% and 11% reduction in probability, respectively. The variables *hours_tv*, *bayes*, and *retrofit* were all positively correlated with being in cluster 1, again with less certainty. The model was able to correctly predict cluster identification about 79% of the time and has a χ^2 value of 31.9.

All of the models found *workday* to be significant, at least to the 90% confidence interval and associated with cluster 1 of each season. Cluster 1 for the summer,

Table 3.5: Probit regression results for spring profiles showing marginal effects (dF/dx) of each explanatory variable (β) on the probability of being in cluster 1, at the average of all the others. Spring cluster 1 is the left box of Figure 3.10.

Explanatory Variable	Coefficient (dF/dx)	Robust Std. Error	z-value	Two-tailed P-test	95% Confidence Interval	
workday	0.28	0.12	2.40	0.02	(0.05 , 0.51)	*
males	0.14	0.16	0.90	0.37	(–0.18 , 0.47)	
females	0.21	0.17	1.26	0.21	(–0.12 , 0.55)	
num_kids	–0.15	0.18	–0.82	0.41	(–0.51 , 0.21)	
education	–0.23	0.11	–2.10	0.04	(–0.45 , -0.01)	*
income	–0.11	0.05	–2.26	0.03	(–0.21 , -0.01)	*
hours_tv	0.05	0.03	1.99	0.05	(0.00 , 0.10)	.
computers	0.04	0.05	0.76	0.45	(–0.07 , 0.14)	
vehicles	0.00	0.11	–0.03	0.98	(–0.23 , 0.22)	
quiz_total	–0.05	0.04	–1.28	0.20	(–0.12 , 0.03)	
pv	–0.40	0.27	–1.47	0.15	(–0.94 , 0.14)	
bayes	0.28	0.16	1.70	0.09	(–0.05 , 0.60)	.
ev	–0.40	0.37	–1.09	0.28	(–1.14 , 0.34)	
greenbuilt	0.28	0.22	1.25	0.21	(–0.17 , 0.73)	
retrofit	0.24	0.13	1.84	0.07	(–0.02 , 0.49)	.
smart_therm	–0.01	0.25	–0.02	0.98	(–0.50 , 0.49)	
pv:greenbuilt	0.51	0.35	1.46	0.15	(–0.19 , 1.21)	
ev:greenbuilt	–0.22	0.44	–0.49	0.62	(–1.10 , 0.66)	

$\chi^2 = 31.9$, n = 103, Significance codes: 0 '***' 0.001 '**' 0.01 '*' 0.05 '.' 0.1 ' ' 1 fall, and spring seasons is marked with an earlier daily rise in energy use than cluster 2. The variable *hours_tv* was positively correlated with the summer, fall, and spring season's cluster 1 and *education* was negatively correlated with the same three seasons' cluster 1. The variables *retrofit* and *computers* were positively associated with summer and spring's cluster 1 while *income* was negatively correlated with the same season's cluster 1.

Variables such as *workday, hours_tv*, and *computers* are likely associated with higher relative electricity use during the day based on the behavioral impacts of being at home and the use of multiple pieces of technology. Plug loads are increasing as a share of the total energy use in the home [103], and these results indicate that this extra electricity draw might be during times of higher wholesale electricity prices. As expected, the variable *workday* was strongest during the summer as space cooling during the day would be desired by someone at home during the hot summers.

Surprisingly, the variable *retrofit* was positively associated with cluster 1 in both the summer and spring seasons, this might indicate either some sort of rebound effect in not only magnitude of energy use, but in the temporal aspect of that energy use as well. More study is needed in both the classical rebound effect and the temporal aspect that this analysis might have observed.

Residential customers typically pay a flat fee, on a $/kWh basis, for electricity. While some pricing structures are tiered based on total consumption and some utilities offer time-of-use rates, currently most rates in Texas are not dynamically tied to market conditions. Electric utilities act as a buffer for the market and attempt to charge a price that, over a fiscal year, will account for market fluctuations. There seems to be a distinct group of customers that typically use electricity when the price is higher, possibly narrowing the utilities' profit margins. However, homeowners do not typically have a financial reason to care about this situation as they are not subject to the temporal fluctuations in price, but might indirectly be so when utilities consider rates cases (changing electric pricing structures). This analysis shows that there are markers of homes that typically use higher priced (normalized) electricity and thus utilities might be able to target such customers with incentives that would reduce or shift electricity usage to less expensive times, possibly increasing profit margins and keeping rates lower overall. However, this could raise some equity issues associated with giving larger rebates to some households than others, but also give insights as to how the introduction of time-of-use or real-time electricity price structures might disproportionately affect lower income homes. These results could inform policies that could be put into place to correct for possible equity imbalances.

3.5 Conclusions

This analysis employed a data-driven approach to 1) determine the shape of seasonally-resolved residential demand profiles, 2) determine the optimal number of normalized representative residential electricity use profiles within each season, and 3) draw correlations to the different profiles based on survey data for over 100 homes in Austin, TX. This analysis determined that, for homes in a southern U.S. location, there are two main groups of temporal profiles, representing residential electricity demand in each season. Temporal and magnitude differences in the summer profiles are significant with one group typically demanding more power during higher wholesale electricity price times than the other. Finally, probit regression analysis determined that explanatory variables such as whether someone worked at home, the number of hours of television watched per week, and education were significant determiners of inclusion in a given cluster. These results point to markers of households that might be more impacted by time-of-use or real-time pricing electricity rates and can act as predictors as to how evolving demographics can change electricity demand patterns.

This analysis could also serve as a starting point for utilities looking to reduce electricity use during peak times. The drivers of the temporal shape of residential use could allow for policies that target load shifting and efficiency upgrade rebates to homes that would benefit the utility the most, such as homes with persons who work from home. This work and the methods herein could be used to predict how changing demographics of neighborhoods could influence local distribution grid conditions. Also, further work is needed to assess the possible temporal rebound effect of residential energy retrofits. Policy interventions (or exceptions) for lower income households in areas that switch to time-of-use or real-time electricity price structures might be necessary to ensure that lower income household's electricity bills are not disproportionately increased. These results might also inform local or regional planning organization's policies on incentives for likely household demographic targets or changes with a focus towards reducing volatility in an aggregate electric demand curve, which have implications for distribution and transmission line planning.

Chapter 4

A multi-objective assessment of the effect of solar placement on energy production and system economics

4.1 Introduction

This analysis considers the effect of the placement (azimuth and tilt) of fixed solar PV systems on their total energy production, peak power production, and the economic value of that energy production. Solar energy production is important for a multitude of reasons, these include reduced carbon emissions; a fuel source that is free, renewable, domestic and distributed; its contributions for energy equity, and because the prices of solar panels are falling. While solar energy production is zero carbon at time of generation, lifecycle analyses indicate that over the energy production lifetime, solar power emits 50 – 100 g CO_{2-eq}/kWh while natural gas and coal fired generation emit at about 550 and 850 g CO_{2-eq}/kWh, respectively [51]. This reduction in CO_{2-eq} emissions is substantial because electric power generation accounts for 40% of US CO_{2-eq} emissions [104], which is a significant contributor to global climate change [105]. Once the capital investment is made into solar power, the fuel cost is free and the operations and maintenance costs can be significantly lower [52]. Solar energy has the potential to bring a distributed energy source to many people in regions that lack significant economic capital and investment – much the same way that cellular phone technology has brought communications to many remote parts of the world that have never had any landline investment. In many ways solar energy can provide energy at remote locations without significant investment in transmission infrastructure [53]. Although the implementation of solar PV systems is not without its own set of challenges, the actual equipment price has fallen two orders of magnitude in the past 35 years [54], almost to parity with some other forms of generation [52]. Also, because the fuel source for solar energy is sunlight, the resource is distributed, albeit at different levels, throughout the world and investments in solar energy might reduce a region's need to import fuel for power generation. As a consequence of all these factors, in the US, solar installations are expected to grow significantly and outpace new fossil fuel power plants in the mid-future [106]. Thus, analytical methods – such as the one developed herein – that optimize the usefulness of those installations might offer value to developers

4.2 Background

There have been a many investigations into the optimal tilt for solar PV systems. These investigations were summarized in a recent review by Yadav and Chandel [58] and therefore will not be reproduced here. However, it is important to note that many of these analyses consider solar energy production assuming that a southern azimuth (in the northern hemisphere) is optimal for energy production. While the south-orientated rule-of-thumb might be best for completely clear skies, non-uniform, temporal meteorological conditions such as fog or clouds, environmental conditions such as smog, and geographic features such as mountains can block solar radiation and reduce solar panel output at different times of the day thereby changing the optimal orientation of the panels [57, 107]. Additionally, solar PV power output is a function of panel temperature [108], so dry bulb temperature fluctuations and wind speed (because of convective heating or cooling) alter PV electricity production. Lave and Kleissl [57] determined the optimal tilt and azimuth angles for the continental United

States using a high resolution grid (0.1° by 0.1°). They considered solar radiation effects, such as cloud cover, but not temperature effects.

Another consideration for optimal PV orientation is the value of the electricity generated. Because solar energy production does not always precisely align with maximum electricity grid load, even placements that might be non-optimal from an energy production basis might be optimal on an economic or peak power production basis [55, 56, 109]. Luoma et al. [110] used day-ahead market electricity prices to determine optimal solar PV orientations in California. Their work found that the market electricity prices shifted the optimal orientation of arrays further west of south.

This analysis extends this body of knowledge by estimating optimal solar orientations for 1,020 U.S. locations while considering the effects of dry bulb temperature, wind speed, and actual (i.e., not clear-sky) solar radiation. This analysis also considers the value of solar energy produced by using time-of-use rates throughout the continental US as a proxy for average local grid conditions.

4.3 Methods

This analysis uses available solar insolation and electricity price data to 1) determine the insolation on a given plane (with available solar radiation tools), 2) build a residential system-based solar PV production model, 3) estimate the total energy, power, and economic impacts of system azimuth and tilt (placement) for Austin, TX, 4) extend the analysis to other locations across the US, and 5) explore the peak power production and solar ramp rate implications of varying solar placements using the aforementioned datasets. The workflow is given in Figure 4.1.

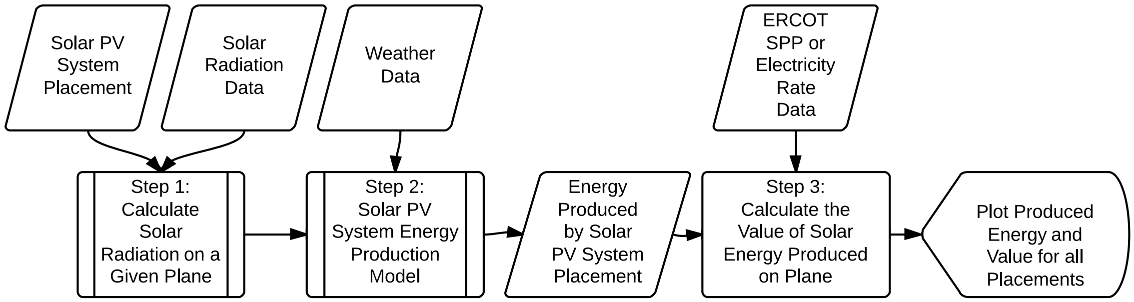

Figure 4.1: This diagram shows the process of modeling the energy and the value of energy produced from various solar placements.

4.3.1 Determining incident solar insolation on a plane

Because the goal of this analysis is to determine the value of various solar placements, it was necessary to calculate the incident solar radiation for multiple azimuths and tilts. This process requires the application of trigonometry and daily correction factors for the sun's path relative to one's location on the Earth (see Equations 4.1 and 4.2). Global horizontal, diffuse horizontal, and direct normal radiation were all directly measured, or taken from TMY weather files. These measurements allow for the calculation of solar radiation on any arbitrary plane and the basic equations for calculating the incident radiation on such a plane are given by Equations 4.1 and 4.2 [111, 112],

$$I_{Ti} = I_{B,i} R_{B,i} + I_{D,i} + V_i \tag{4.1}$$

$$R_{B,i} = \frac{cos\ \theta_i}{cos\ \theta_{z,i}} \tag{4.2}$$

where $I_{T,i}$ is the incident radiation on the tilted plane, $I_{B,i}$ is the beam radiation on the horizontal plane, $R_{B,i}$ is the ratio of beam radiation on the tilted plane (defined by tilt, azimuth, and the relative location of the sun) to that on a horizontal surface, $I_{D,i}$ is the measured diffuse radiation, V_i is the reflected ground radiation, θ_i is the angle between the beam radiation on a surface and the normal to that surface, and $\theta_{z,i}$ is the angle of incidence of beam radiation on the horizontal surface, all at time i.

4.3.2 Solar PV system energy production model

To estimate AC solar PV electricity production from solar radiation on a plane, a solar PV energy production model was built. The overall model is given in Equations 4.3 – 4.4:

$$P_{out,i} = \eta_{pv,i} \times \eta_{inv,i} \times I_{T,i} \tag{4.3}$$

$$\eta_{pv,i} = \eta_{ref}\left[1 - \beta_{ref}\left[T_{a,i} - T_{ref} + (T_{NOCT} - T_{a,i})\frac{I_{T,i}}{I_{NOCT}}\right]\right] \tag{4.4}$$

where $P_{out,i}$ is the power output of the system in W/m^2 of PV array, $\eta_{pv,i}$ is the efficiency of the solar PV panels, $\eta_{inv,i}$ is the efficiency of the (DC–AC) solar inverter, $I_{T,i}$ is the incident radiation on the tilted plane (Equation 4.1), η_{ref} is the efficacy of the PV panels (taken to be 12%), β_{ref} is the temperature coefficient of the PV panels (taken to be 0.0045 K^{-1}), T_a is the ambient temperature, T_{ref} is the reference temperature of the PV panels (25 °C), T_{NOCT} is the nominal operating cell temperature at operating test conditions, and I_{NOCT} is the incident radiation for the NOCT test, which is 800 W/m^2, for an overview of the NOCT equations, see Skoplaki and Palyvos, [113], all (besides constants) at time i. The efficiency of the modeled inverter $\eta_{inv,i}$ was modeled as a 6^{th} degree polynomial fit of a commercially available solar inverter (Power-One PVI-5000 [114]), scaled from a nominal 5 kW PV array of commercially available solar PV panels (Lumos LS250 [115]) to a per m^2 of array.

4.3.3 Calculating the value and effect of solar placement

After construction of the solar PV model based on meteorological, astronomical conditions, and assumed PV characteristics, a second model was developed to calculate the solar PV electricity produced from a solar PV system for any given placement, accommodating different tilts and azimuths. This model consisted of three steps. First, given a placement and the horizontal solar radiation values, it calculated the solar radiation on a plane. Second, using the solar PV model developed in Section 4.3.2 and weather data, it calculated the energy produced at that placement. The last step calculated the value of the energy produced using either local market conditions (ERCOT SPP) or local utility rates.

All possible combinations of azimuths ranging from 90° (due east) to 270° (due west) and tilts from 0° (horizontal) to 45° were used to calculate the solar insolation on their respective plane. These data were fed into the Solar PV Energy Production Model (Section 4.3.2), along with weather data to quantify the amount of energy produced over one year for that particular configuration. These data were then multiplied by the temporally corresponding ERCOT electricity market price (for the Austin specific analysis) or TOU rate data (for the national analysis) and summed to calculate the value of the solar energy produced as per Equation 4.5:

$$Value = \sum_{i}^{1year} P_{out,i} \times \Delta t \times Price_{1,i} + P_{out,i} \times Price_{2,i} \tag{4.5}$$

where $P_{out,i}$ is the power output of the solar PV system in W, Δt is the time-step, $Price_{1,i}$ is the economic price (ERCOT SPP or TOU rate, \$/kWh), and $Price_{2,i}$ is the price associated with reduction in overall demand charges for a commercial or industrial consumer that has the solar PV system behind the meter, all at time i. For industrial solar power plants, $Price_{2,i}$ could also be used to estimate ancillary service value or a capacity payment. For this analysis $Price_{2,i}$ was considered to be fixed at 0 (because Texas has an energy-only market), but it could be considered in another analysis that looked at markets with capacity payments or the ability of solar PV to reduce demand changes for arrays behind the meter (many commercial and industrial customers have demand changes in addition to energy charges). This price would be appropriate to consider on a case by case basis, but is beyond the scope of this more general analysis. This calculation was then completed for multiple radiation inputs (measured, TMY, and clear-sky), weather inputs (measured and TMY), and pricing inputs (market and electric rate) for Austin.

4.3.4 Optimal solar placement on a national level

The analysis was then generalized to a national level. TMY data were gathered and processed in the same way as described in Section 4.3.3 for 1020 locations across the US [116]. The data were run through the solar placement value (Section 4.3.3) program in a similar fashion. However, to speed up the process, an optimization routine (R function *optim*, with method of Byrd et. al. [117]) was used so that each location's placements of both energy and value did not have to be directly computed.

The expanded model considered both total energy produced, power produced, and the value of that energy. The energy-only model is the same as for the more Austin-specific data. However, the value of energy model was somewhat different. In order to consider the regional differences in electricity markets, local TOU energy rates were used as a proxy for the temporal value of energy, as it was assumed that these rates would be designed such that times of higher costs would be typically associated with times of higher grid stress/demand. An attempt was made to obtain an electric utility TOU rate for each state from the OpenEI database [118]. Of the 50 US states, at least 37 states had TOU rates for at least one customer class. When each simulation was run, the amount of energy produced during a given interval was multiplied by the rate for that hour. For all locations within a given state, a single representative rate from a large city in that state was used, for states without TOU rates, the closest (shortest Euclidian distance) to the nearest rate (by the latitude and longitude of the largest city in each state) was used.

4.3.5 Optimal Placement for Summer Peak Reduction

The last step of the analysis was to explore the effects of solar placement on summer peak power reduction and the solar ramp rate. The summer peak times are defined as June – August, from 14:00 – 20:00 CST for Austin, TX [119]. These times are typically associated with high wholesale electricity prices and grid stress, mainly due to residential air-conditioning load [7]. For this analysis the same approach was taken as with Equation 4.5, except the $Price_{1,i}$ was given a value of 1 during summer peak hours and 0 otherwise.

4.4 Results and Discussion

The following section discusses the results of the model and presents a discussion of the results and implications of this analysis for solar energy production.

4.4.1 Calculating the value and effect of solar placement

The model was used to calculate both the total amount of energy (kWh) produced per m^2 of panel, the economic value of that energy produced, and when the power (kW) was produced. The value of the placement was determined by summing each minute's value of solar production for the entire year as discussed in Section 4.3.3 (Equation 4.5).

To verify that the entire process was running correctly, the model was first executed with clear-sky radiation. Clear-sky radiation is the solar radiation that would reach the earth's surface if there were not any clouds or other objects to block or amplify it. Clear-sky radiation curves are similar everyday, except taller and wider during the summer. Because there is no clear-sky equivalent weather information available, TMY weather data (temperature, wind speed) were used. Using clear-sky as the radiation input should cancel out all weather effects to solar panel production and should indicate an optimal energy azimuth of due south and a tilt related to (in this case slightly less than) the local latitude (about 28° for Austin). The model provided just that result, shown in Figure 4.2. Figure 4.2 shows the total number of kWh per year produced (normalized for 1 m^2 of array) for every combination of azimuth and tilt, 90°–270° and 0°–45°, respectfully using clear-sky radiation and TMY weather data.

Figure 4.3 shows the effect of using TMY radiation and weather on optimal placement. The number of kilowatt-hours overall are reduced compared to Figure 4.2 because this data include the effect of clouds on the amount of solar radiation that reaches the earth's surface. It is interesting to note that using 'typical meteorological' data for Austin indicates that shifting the array west 11° and 5° towards the horizontal (from the 180°/28° rule-of-thumb) produces the most amount of energy, about 0.5% more than the rule-of-thumb. These results would suggest that meteorological events such as cloud cover in the mornings and winter typically block the sun more than in the afternoon and summer.

Figures 4.4 and 4.5 show the optimal azimuth for the value ($/$m^2$/year) of

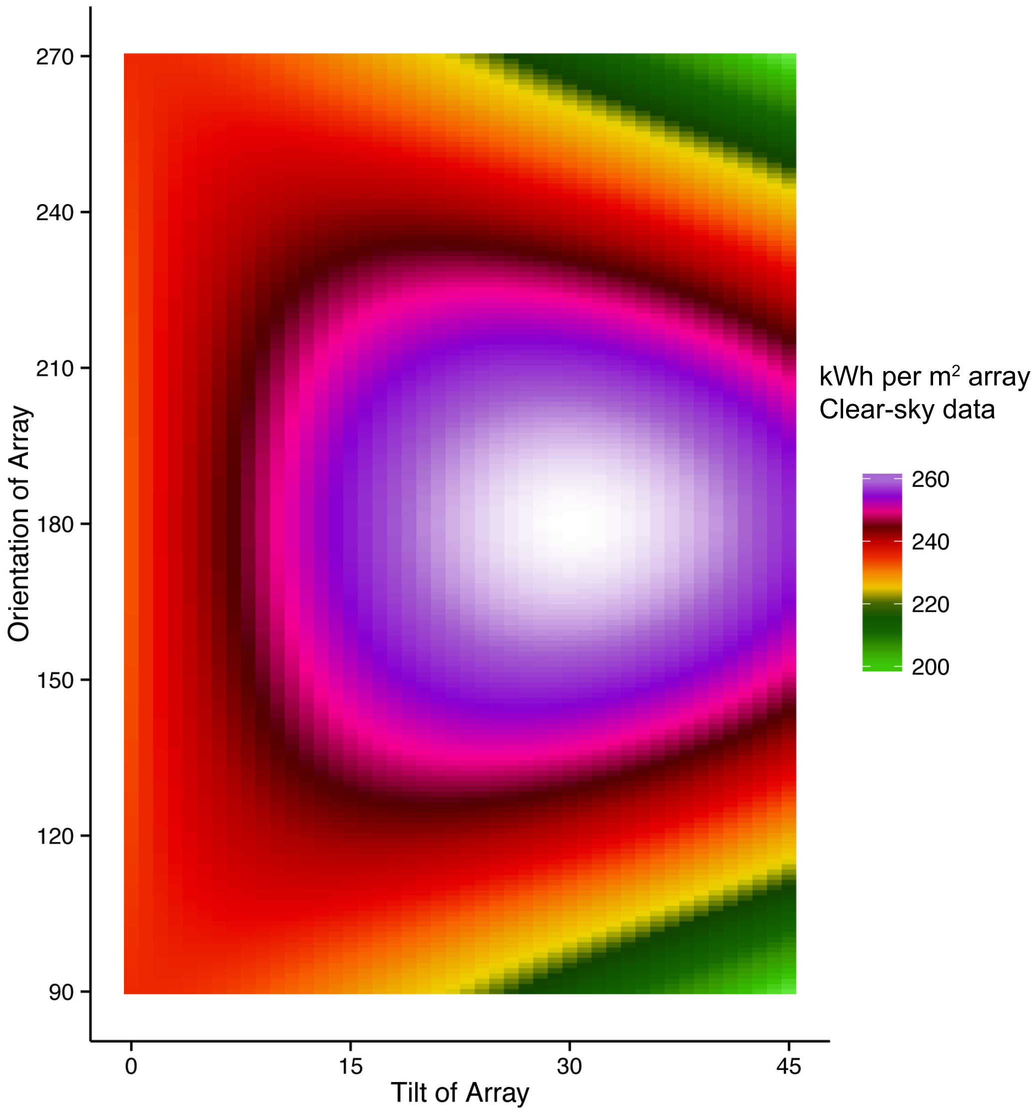

Figure 4.2: Heat map of model results for clear-sky radiation and TMY weather showing an optimal energy azimuth of 180° and 30° tilt, as expected for Austin, TX.

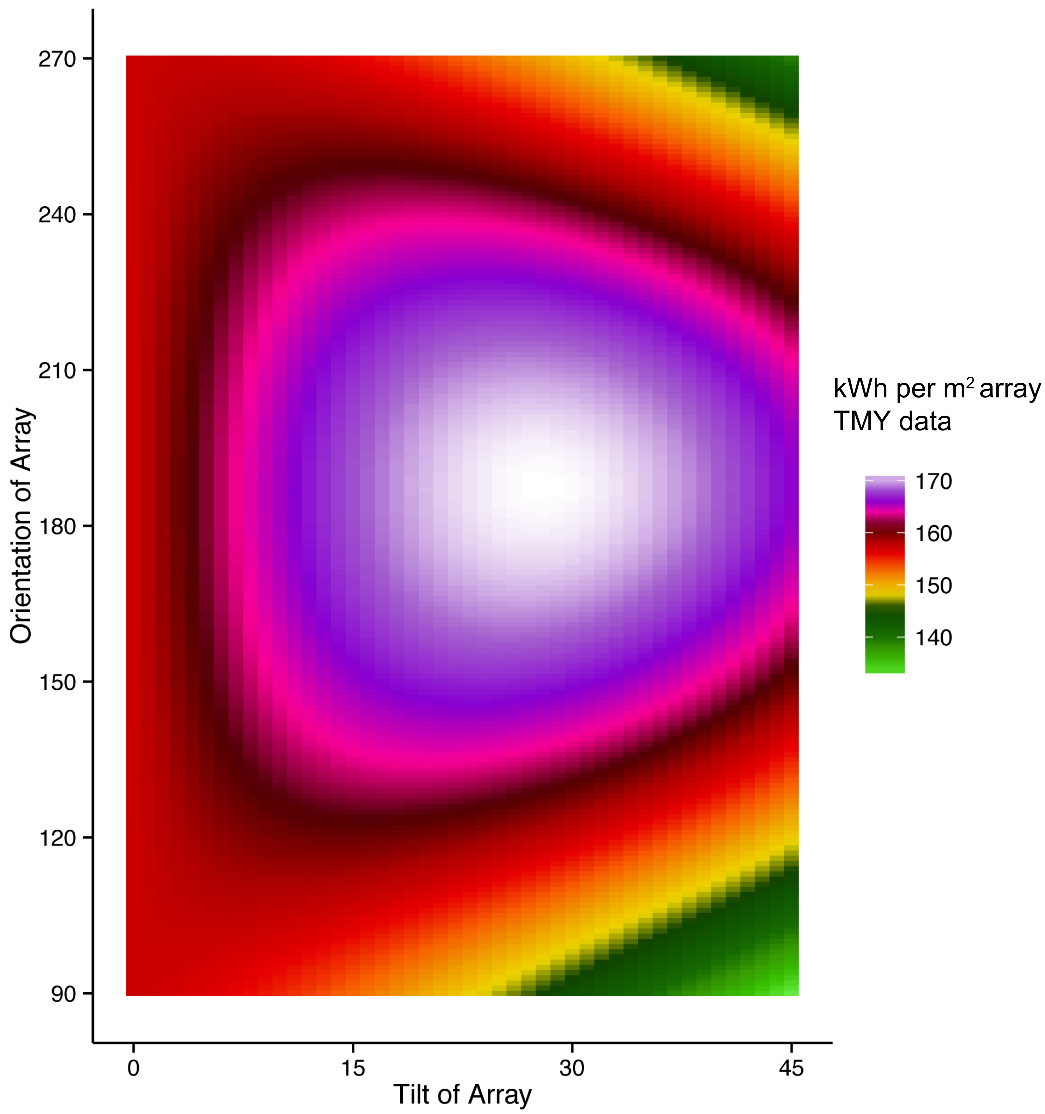

Figure 4.3: Heat map of model results for TMY radiation and TMY weather showing an optimal energy azimuth of 188° and 28° tilt, indicating the due south azimuth might not be optimal for total energy generation in Austin, TX when typical meteorological conditions are considered.

electricity produced (Equation 4.5) for the 2012-2013 measured data and coincident ERCOT prices and the TMY data with average ERCOT prices, respectfully. Both figures show that placement is shifted west when optimizing based on market value.

Figure 4.6 shows the values associated with Austin TMY solar radiation and weather with Austin Energy's residential TOU rate and also shows shows how azimuth and tilt are related under the TOU rate. For example, if a solar PV array's azimuth were constrained to 150°, its optimal tilt is not the 25° associated with the unconstrained array, but 18°, a 0.5% ($\$/m^2/year$) difference.

Table 4.1 summarizes the results of the various cases for both total energy production and the value of the energy produced in Austin, TX. For the cases where the placement was optimized for maximum total energy generated, the TMY and measured case seemed to shift the arrays about 7° west of south. For the cases where the placement was optimized for maximum total economic value of the energy generated, the cases seemed to shift the arrays about 20 to 50° west of south, depending on the price considered. While the increase in the amount of energy generated in the optimal cases was negligible, the increased values for shifting the solar PV arrays west of south were on the order of 1–7%.

In general, higher summer electricity prices drive azimuth west and tilt towards the horizontal [57], as is seen in the Austin + TOU rate case. However, the later and the higher the electricity prices, the further the sun has dipped in the sky and the steeper the tilt will need to be to capture the incident radiation as seen in the TMY + ERCOT AVG and TMY + ERCOT 2011 cases. The TMY + ERCOT 2011 case is taken to be a scarcity pricing scenario as that year the price cap ($3000/MWh) in ERCOT was hit for 54 15-minute periods, most after 16:00 local time, versus just once in 2012 and twice in 2013. However, the current price cap in ERCOT has been raised

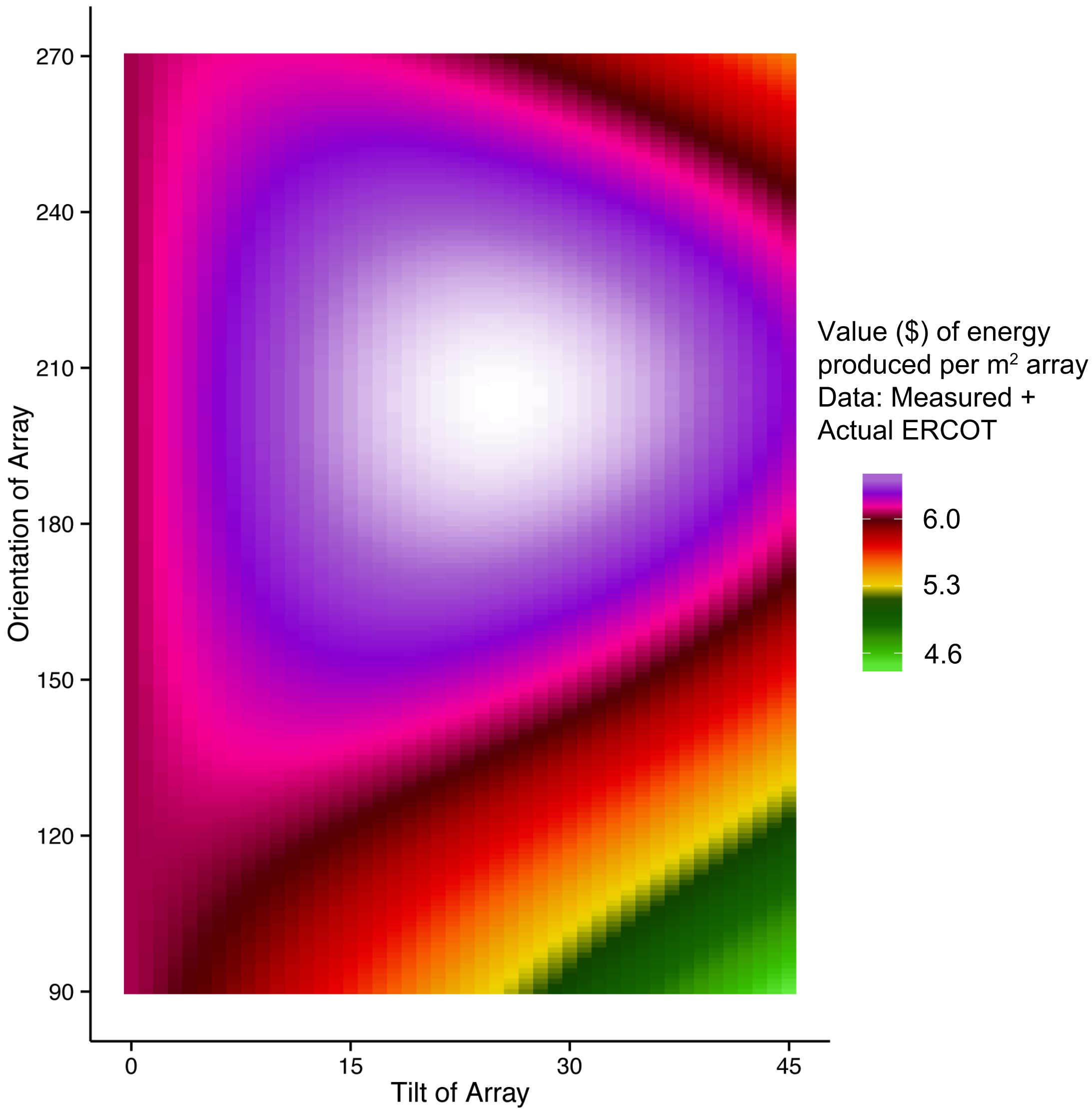

Figure 4.4: Heat map of model results for measured 2012-2013 radiation and weather with coincident ERCOT prices showing an optimal value ($\$/\mathrm{m}^2$/year) azimuth of 204° and 25° tilt for Austin, TX.

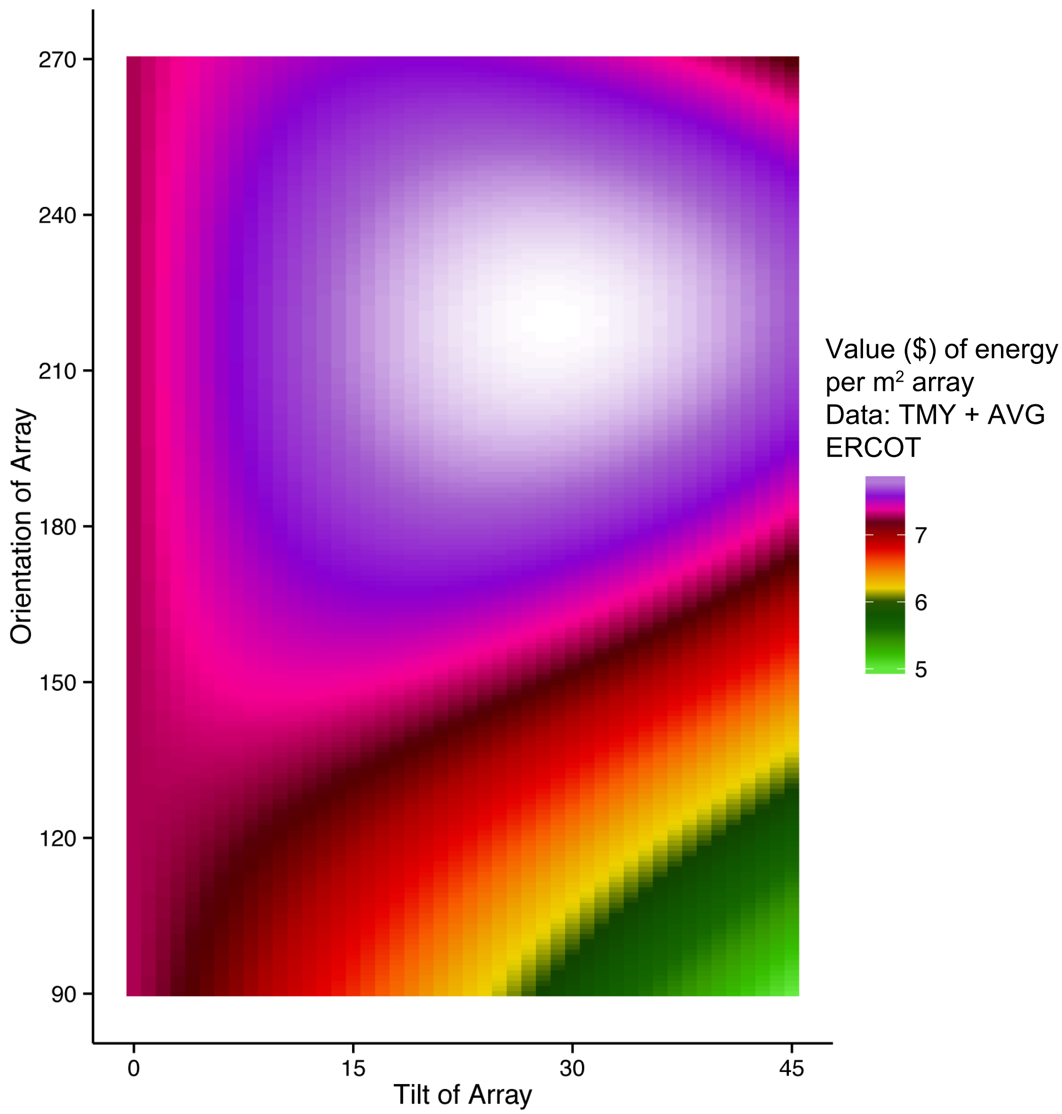

Figure 4.5: Heat map of model results for TMY radiation and weather with average ERCOT prices showing an optimal value ($\$/m^2/year$) azimuth of 219° and 29° tilt for Austin, TX.

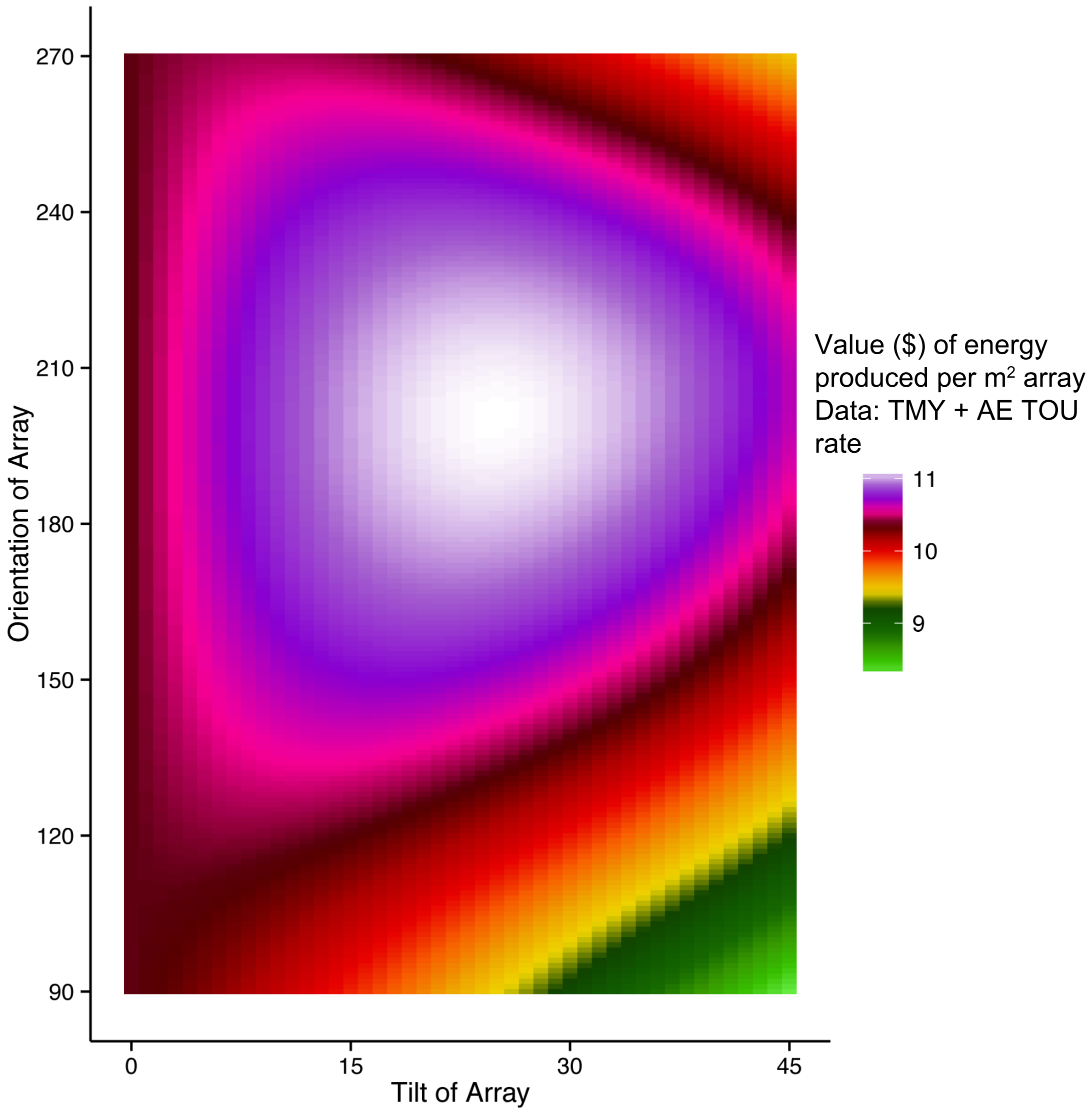

Figure 4.6: Heat map of model results for TMY radiation and weather with Austin Energy Residential TOU rate showing an optimal value ($\$/m^2/year$) azimuth of 200° and 25° tilt for Austin, TX.

Table 4.1: Cases for for analysis of multiple radiation, weather, and economic data inputs for Austin, TX.

Radiation Inputs	Weather Inputs	Pricing Data	Optimal Placement	Units	Optimal Value	Value at 180°/30°	Percent Change
Clear Sky	TMY	–	180°/30°	kWh/m^2/year	264.3	264.3	0.0
TMY	TMY	–	188°/28°	kWh/m^2/year	171.4	171.1	0.2
Measured	Measured	–	186°/27°	kWh/m^2/year	194.6	194.3	0.2
TMY	TMY	ERCOT 2011	231°/30°	\$/m^2/year	11.28	10.53	7.1
TMY	TMY	ERCOT AVG	219°/29°	\$/m^2/year	7.97	7.67	3.9
TMY	TMY	AE TOU Rate*	200°/25°	\$/m^2/year	11.07	10.96	1.0
Measured	Measured	ERCOT AUCT	204°/25°	\$/m^2/year	6.53	6.43	1.7

*Austin Energy residential time-of-use rate

to \$5000/MWh with plans to further raise to \$9000/MWh. A high price cap and more instances of scarcity pricing (during historically consistent times of the day) could have an impact on the optimal placements of fixed solar PV installations, namely further west with a steeper tilt. Utilities could incentivize these solar placements as a hedge towards a more volatile wholesale electricity market.

These results have the potential to be significant for solar PV installations. Large ground-mounted and flat roof arrays that require fixtures can take advantage of an optimal placement (or perceived future optimal placement) at little to no additional cost than due south installations. For a building of fixed orientation, a cost-benefit analysis would have to consider possibly less capacity (due to solar PV installations not being aligned with the building lines) verses temporal generation revenue. Utilities can encourage this optimal placement (which could be further west than arrays designed to maximize energy production) by structuring rates that offset their highest wholesale cost times and net-metering. Also, these results could be used to influence roof azimuth and pitch in new construction or retrofits to maximize the ability of installed solar PV systems to generate energy. Further, these results could also be useful for calculating the true cost/value of solar in non-optimal placements.

4.4.2 Optimal solar placement on a national level

4.4.2.1 Optimal azimuth

The same analysis was performed on data from 1020 locations in the US that have TMY data. The model was extended to consider both the total amount of energy produced, as well as the value of that energy produced. Figure 4.7 shows the results of the energy-only analysis.

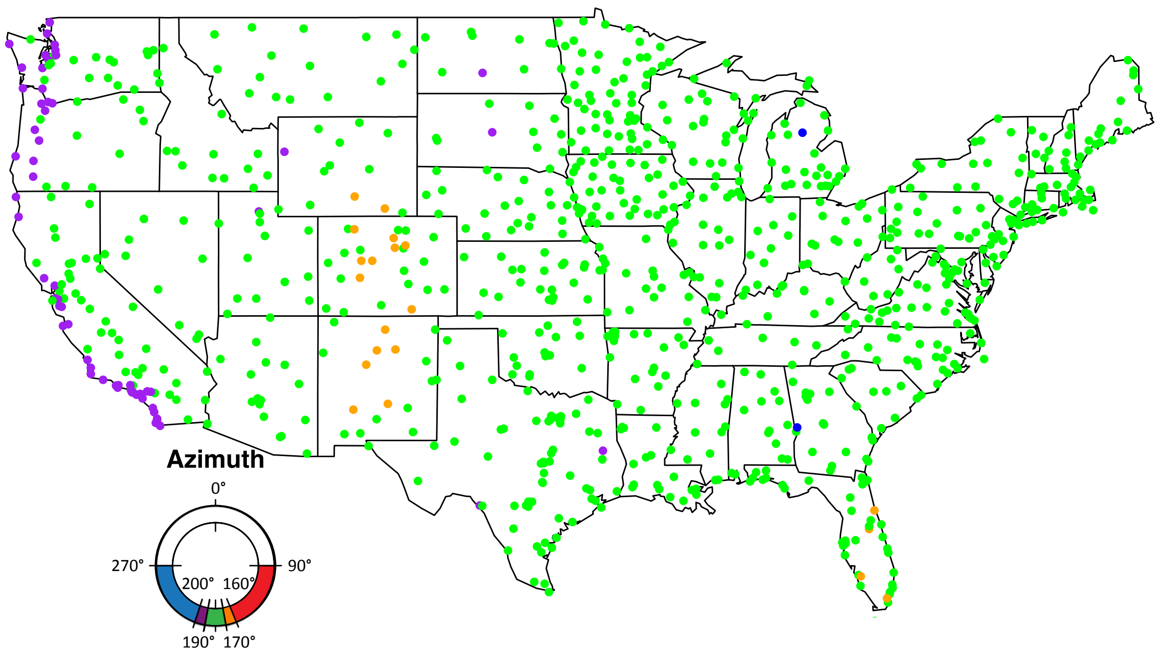

Figure 4.7: Map of continental US showing the energetically optimal azimuth of of solar PV systems. The red points indicate optimal solar azimuths east of south (less than 160°), orange points indicate slightly east of south optimal solar azimuths (160° – 170°), green points indicate southerly optimal solar azimuths (170° – 190°), purple points indicate slightly west of south optimal solar azimuths (190° – 200°) and blue points indicate optimal azimuths west of south (greater than 200°).

Most of the locations in the US fall within the south-facing band (170° – 190°) indicating that the rule-of-thumb approach might work for most of the country. However there are some notable exceptions. The results indicate that a band of locations from Wyoming, through Colorado, and into New Mexico have optimal azimuths that face slightly east of south. This result is probably explained in that these locations are along the Rocky Mountains and the mountains block the sun as it sets to the west, along with prevailing summer afternoon thunderstorms. Another location of interest the US west coast, where the model indicates an optimal slightly west-facing azimuth for almost the entire length of the coast. This effect is probably explained by persistent cloudiness in the early part of the day, higher morning humidity ratios, or additional shading from west coast mountain ranges.

These findings are significant because Colorado ranks 10^{th} (130 MW) in the US for installed solar capacity and California ranks 1^{st} at 2,051 MW (Texas ranks 7^{th} at 174 MW) [120]. While data on the actual placements of solar PV systems are not readily available, if roughly half of California's small scale ($<$ 25 kW capacity) solar output could be improved 1% via an optimal placement, the result would be an additional production of approximately 15 million kWh/year at current capacity levels – about the total annual electricity consumption of 2,200 California homes [121].

Figure 4.8 shows the results when considering the maximum economic value of the solar energy produced for all considered solar placements. Again, the value of the electricity produced is approximated by the structure of a utility TOU pricing structure that is either in the state of the TMY data location, or if the state doesn't have a TOU rate available, the closest location with a TOU rate was chosen.

Overall the economic consideration shifts the number of optimally south-facing (170°–190°) array locations from 921 (pure energy analysis) to 476 locations. The number of optimally west-facing (>190°) array locations increased from 63 to 499 and the number of optimally east-facing (<170°) array locations increased from 36 to

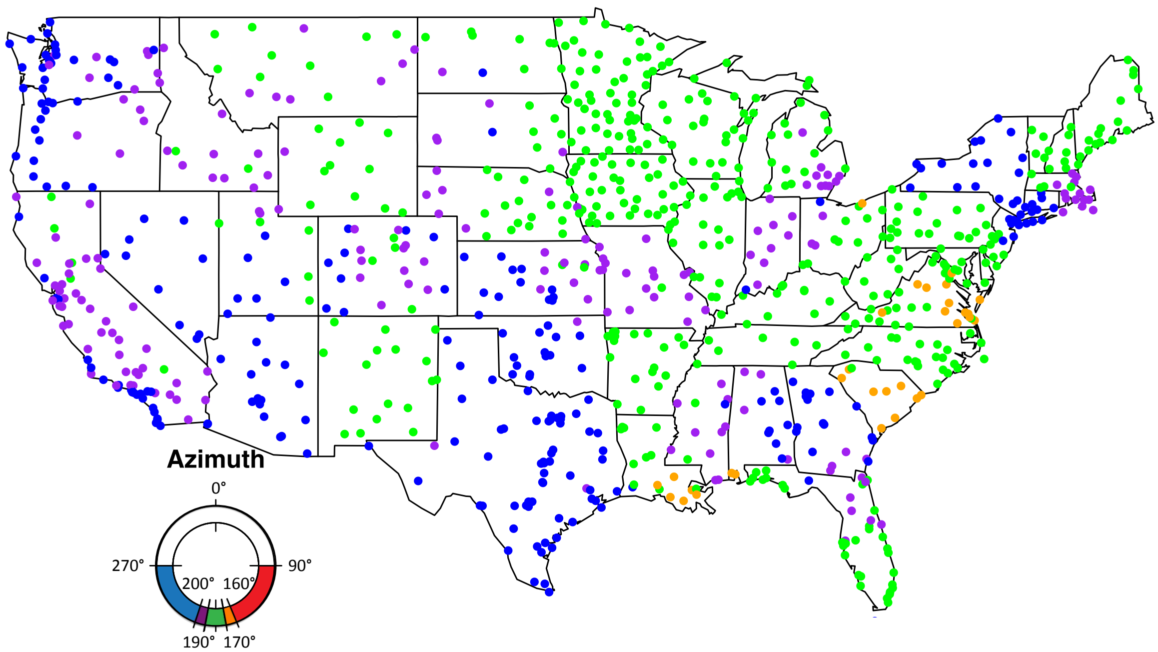

Figure 4.8: Map of continental US showing optimal azimuth of solar PV systems when considering the value of the solar energy produced. The red points indicate optimal solar azimuths east of south (less than 160°), orange points indicate slightly east of south optimal solar azimuths (160° – 170°), green points indicate southerly optimal solar azimuths (170° – 190°), purple points indicate slightly west of south optimal solar azimuths (190° – 200°) and blue points indicate optimal azimuths west of south (greater than 200°).

45. However, because the rates were not the same, the change of optimal economic placement is different for different locations. A significant portion of the western half of the US, including Texas shifted varying degrees west of south. Even some arrays that had an optimal energy placement east of south in Colorado trended west. The eastern half of the US, which for energy only was almost all south-facing is more mixed. For example, the TOU rates of Virginia and South Carolina, while they have higher summer afternoon prices, also have high morning prices in the winter months, presumably due to a morning grid peak from electrical heating or activity demand. Other states, such as New York, had rate structures that reflect higher afternoon grid demand.

4.4.2.2 Optimal tilt

While best practices would have tilts of solar systems determined by local solar data as is attempted in this analysis, many times the tilt is decided based on the local latitude alone [58]. Figure 4.9 shows the band of rule-of-thumb tilts for solar PV systems in the US for comparisons purposes. Figure 4.10 shows a map of optimal solar placement tilts as determined by maximum total energy produced.

Figure 4.10 suggests that while accurate for parts of the southwest US, the optimal energy tilt is typically lower than the local latitude, especially in the states surrounding Tennessee and Kentucky. Lower optimal tilts would indicate the prevalence of more sunny days when the sun is higher in the summer sky. Figure 4.11 shows a map of optimal solar placement tilts as determined by the maximum value ($\$/m^2$/year based on local TOU electric rates) of the solar energy produced.

Figures 4.10 and 4.11 are very similar, except in situations where the local rates incentivize either more summer or winter production. For example, in California, high summer afternoon electricity prices force the optimal tilt lower to produce more

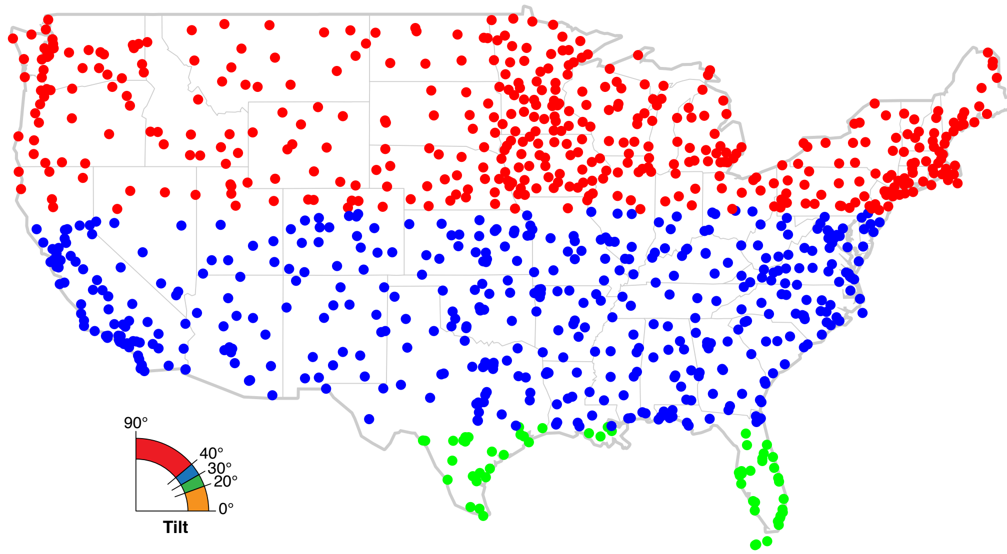

Figure 4.9: Map of continental US showing the approximate tilt for rule-of-thumb solar placements in US based on latitude alone.

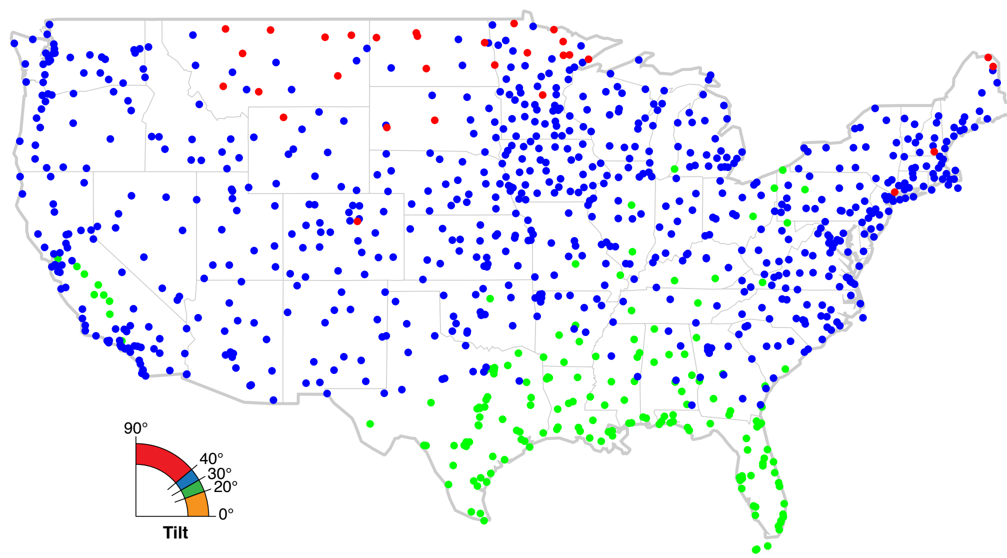

Figure 4.10: Map of continental US showing the optimal tilt for solar placements based on total energy production.

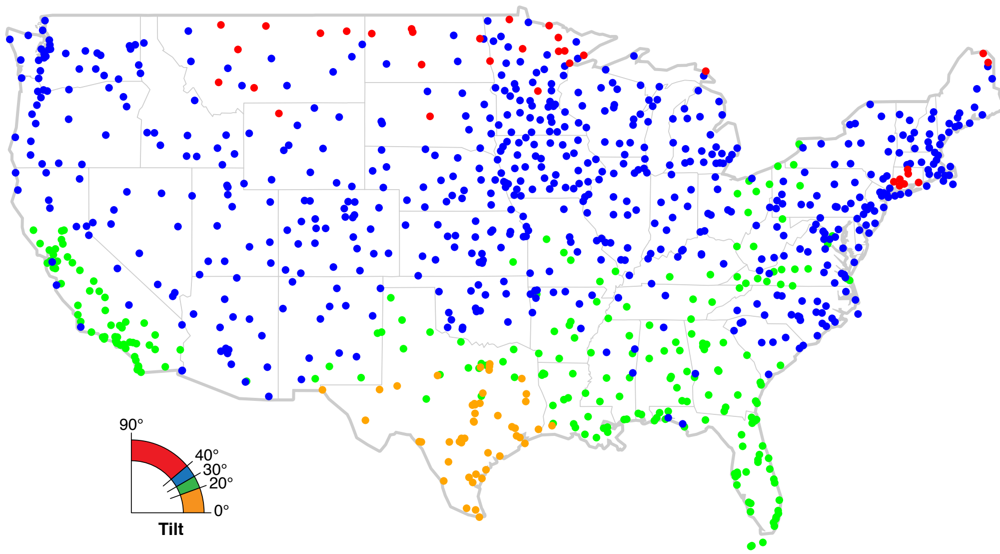

Figure 4.11: Map of continental US showing the optimal tilt for solar placements based on the value of solar energy production.

during the summer peak.

While the solar tilt rule-of-thumb for total energy production might be a good approximation for most of the US, it does not apply everywhere. Notable examples include some locations east of the front range (Rocky Mountains) and the majority of the west coast. Using local TOU electricity rates as a proxy for local grid conditions further changes the optimal tilt. In many locations, the optimal tilt is shifted down, particularly in locations that have TOU rates with higher summer afternoon prices. Although in some cases, rates shift the tilt steeper – particularly in places where TOU rates are high in winter times.

4.4.3 Optimal Azimuth and Tilt to Align with Summer Peak Demand

To understand how solar PV systems should be placed if the goal were to generate as many kWh during summer peak hours as possible, the analysis was run again where the value of solar was only considered during the afternoon summer hours. This portion of the analysis restricted the time of interest to June through August, and between 14:00 to 20:00 – a time period typically associated with high electric grid stress times and higher wholesale electricity prices. For Austin, as well as for most of the US, the optimal peak array placement was shifted due west. The average peak optimal azimuth was 266° with a standard deviation of 6.4° and the average optimal peak tilt was 51° with a standard deviation of 4.6°. Figure 4.12 shows the average generation curves for various solar placements in Austin using TMY data, including optimal peak placement. The top part of Figure 4.12 shows the generation curves for the entire year and the lower part shows the curves for only the summer months (June – August).

Table 4.2 summarizes the differences in energy produced (area under the curves) from the placements shown in Figure 4.12.

Table 4.2: Percent change in amount of energy generated by various solar PV placements as compared to a south facing (180°/30°) array for an entire year, only the summer months (July – August), and for just the peak hours during the summer months (14:00 – 20:00) for Austin, TX.

Placement	Full Year	Summer Only	Summer Peak Hours Only
South-Facing (180°/30°)	0.00	0.00	0.00
Optimal Energy (188°/28°)	0.32	1.30	5.56
Optimal Value Placement (219°/29°)	-1.28	1.53	21.16
West-Facing Placement (270°/30°)	-10.68	0.52	33.25
Optimal Peak Placement (270°/40°)	-14.68	-4.87	35.19

For Austin, the optimal energy and optimal value placements do not differ

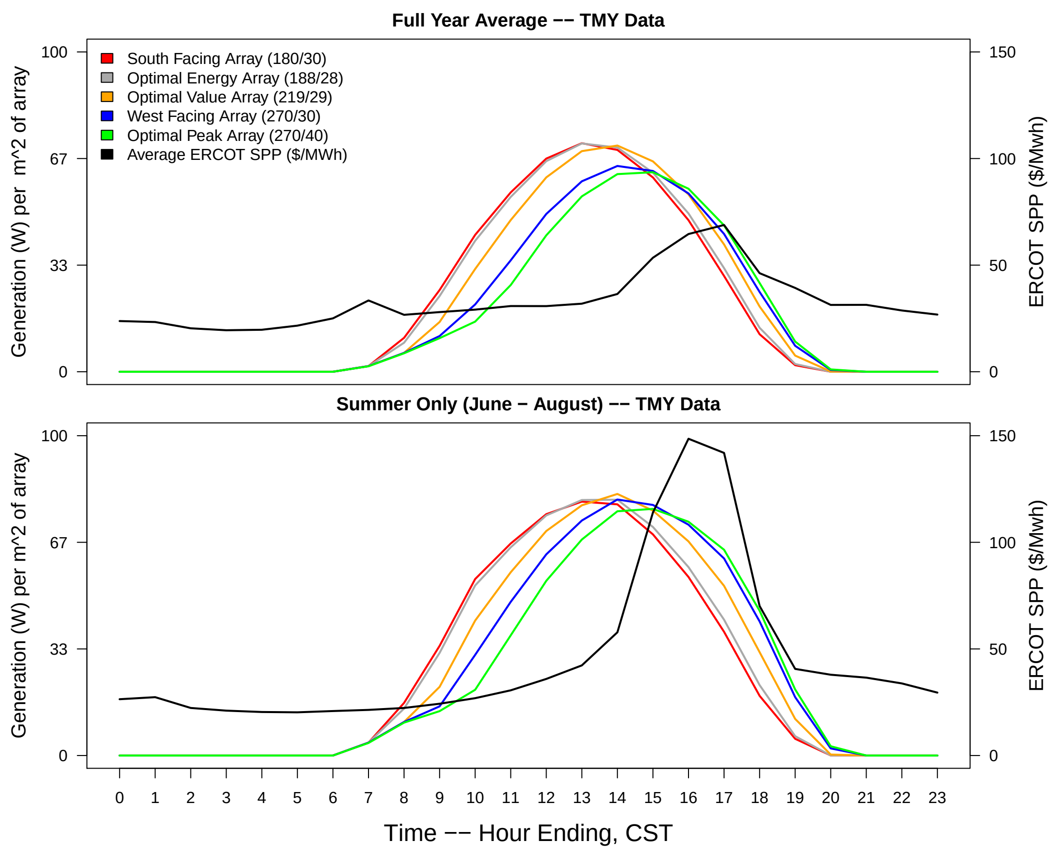

Figure 4.12: Plot showing the average generation profiles of solar PV systems at various placements in Austin, TX and the average ERCOT SPP for the same time period.

much from south placements in terms of energy use. However, west-facing and optimal peak placement generate about 11 and 15% less energy throughout the year. In the summer, the optimal energy, optimal value, and the west-facing array generate about the same amount of energy as the south-facing array with the optimal peak array generating less. During the summer peak demand hours, all placements generate more energy than south-facing arrays with west and optimal peak placements generate 33 and 35% more energy during peak hours, respectfully.

4.5 Conclusions

This analysis considers the the effect of various placements (azimuth and tilt) of solar PV systems on energy generation and value of that energy generation for a yearly period with various environmental and economic inputs in Austin, TX. Using clear-sky, typical meteorological year (TMY), and real, measured solar radiation data we find that the rule-of-thumb placement (due south and a tilt slightly less than the local latitude) might not be optimal for total energy production. Both TMY and measured data indicate a 7-8° shift west (187-188°) and a few degrees towards the horizontal (from the rule-of-thumb 30°) might be a better azimuth and tilt for energy production. Clear sky radiation data reinforce the energy rule-of-thumb as expected. Considering the value of energy produced, the optimal azimuth was pushed further west ($\approx$ 20-50°) based on wholesale electricity market prices that are typically higher in the mid to late afternoon hours. While the resulting improvements might might seem small, ($< 1 - 7\%$ difference), the improvement is free to implement during construction, and over the 25 year lifespan the excess energy produced and revenue earned could be significant.

For most of the US, the rule-of-thumb for total energy production might be a good approximation, but it does not apply everywhere. In many locations, the optimal economic placement is shifted west, particularly in locations that have TOU rates with higher afternoon prices. Although in some cases, rates shift the placement east. Placements that maximize generation during peak times shift placements further west and energy might incentivize otherwise non-optimal placements. However, shifting solar placements to maximize revenue as opposed to energy produced could have some tradeoffs in terms of possible forgone carbon reductions – if all else were held the same. On the other hand, it is reasonable to expect that if revenue were maximized, more capacity might get built and thus offset more carbon emissions. Though beyond the scope of this analysis, temporal carbon emissions could be considered either as an objective or tax and the model could optimize for maximum carbon reductions or maximum value with the tax. The same analysis could also be considered with minimizing water use for thermal generation as well.

This analysis complements the direction of the smart grid towards a more localized, temporal understanding of how energy is created and consumed. Ubiquitous computing power and localized data allow for smarter systems, including stationary systems such as solar PV installations. Just like energy use, the optimal solar placement might not be the same for all locations and the efficiencies that stand to be gained from smarter local placements should not be ignored.

Chapter 5

Other residential energy studies – residential natural gas fuel cells and residential energy use regression analysis

This chapter includes two smaller preliminary analyses that 1) consider the impacts of using small scale fuel cells on end point electric and thermal energy use in residential buildings in Austin and 2) regression results detailing the explanatory variables for total energy use within the home and the effect of energy retrofits on daily energy use*.

*Part of the analysis in this chapter has been published as a journal article [36]:

Rhodes, J.D., Charles R. Upshaw, Colin M. Meehan, David A. Walling, Paul A. Navratil, Ariane L. Beck, Chioke B. Harris, Kazunori Nagasawa, Robert L. Fares, Wesley J. Cole, Harsha Kumar, Roger D. Duncan, Chris L. Holcomb, Thomas F. Edgar, Alexis Kwasinski, Michael E. Webber, "Experimental and Data Collection Methods for a Large-Scale Smart Grid Deployment: Methods and First Results," Energy 65 (2014) 462471, DOI: 10.1016/j.energy.2013.11.004

and part as a conference paper [84]:

Rhodes, J.D., Kazunori Nagasawa, Charles R. Upshaw, and Michael E. Webber, The role of small distributed natural gas fuel cell technologies in the smart grid, ASME 2012 6th International Conference on Energy Sustainability, July 23-26, 2012, San Diego, CA, USA.

Co-authors included Charles R. Upshaw, Colin M. Meehan, David A. Walling, Paul A. Navratil, Ariane L. Beck, Chioke B. Harris, Kazunori Nagasawa, Robert L. Fares, Wesley J. Cole, Harsha Kumar, Roger D. Duncan, Chris L. Holcomb, Thomas F. Edgar, Alexis Kwasinski, Michael E. Webber (supervisor) – their contributions included editing the manuscript.

5.1 The role of small distributed natural gas fuel cell technologies in the smart energy grid

5.1.1 Introduction

Recent concerns about the stability and carbon intensity of the electricity grid have lead to the development of various scenarios for the grid of the future, often bundled under one vague umbrella coined as the 'smart grid'. Roughly speaking, the smart grid includes resource flow, such as electricity, natural gas, and water, from the provider to the end user, along with flows of information. The smart grid allows for otherwise passive parties to play a more active role in their resource use. One example of this type of active role is end-user owned generation, sometimes also called distributed generation. Distributed generation does not have to be end-user owned, but this type is considered in this analysis. Common types of distributed generation include rooftop solar PV and small wind electric power generation. These types of generation, while carbon friendly, are not dispatchable, meaning that the amount of power they produce is not controllable like a typical power plant. Therefore, a grid that relies more on distributed generation of these types would benefit from electricity storage or firming power (such as from dispatchable generating units on stand-by), to provide continuous service even with the added variability. This paper analyzes one type of distributed firming power: home-level natural gas fuel cells.

5.1.2 Background

Micro-grids and homes with local energy production, such as rooftop solar PV, have traditionally relied on the macro-grid for stabilization in the event of local interruptions in generation. These interruptions can last from just a few minutes, in the event of a passing cloud, to weeks in the event of extended cloudy skies. Fuel cells can be desirable as distributed firming power to local renewables because of their availability/reliability, relatively high efficiency, low emissions, and low noise [59]. Numerous computer models and prototype units have been built to test the ability of small-scale fuel cells to perform in residential-specific situations [59–63]. While simulations and prototypes have demonstrated the utility of small-scale fuel cell systems to operate in residential environments, a range of efficiencies has been reported. Electrical efficiencies range from 18% [63] to 56% [122], however, fuel cells also produce waste heat that can increase the total efficiency to over 90% when used in a combined heat and power (CHP) mode [60]. When operated in a CHP mode, small-scale fuel cells can produce heat for other uses such as domestic hot water, space heating, thermoelectric generation, or absorption refrigeration. Figure 5.1 presents a schematic of a possible residential fuel cell setup.

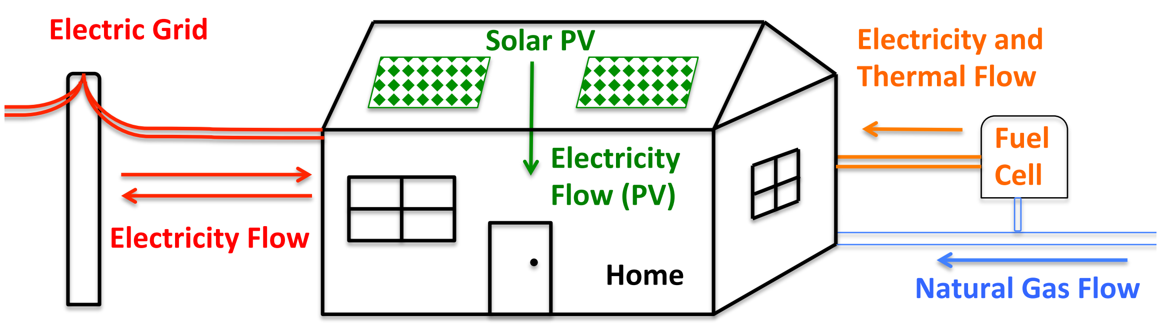

Figure 5.1: Schematic of a residential building interacting with multiple energy sources, including small-scale fuel cells.

Figure 5.1 demonstrates the possibilities of a home that is connected to more than one source of energy. The home can interact with the electric grid by buying and selling electricity. The home can produce electric power from solar when available and use that power, or sell it to the grid. The home can use natural gas directly, or could convert the natural gas to electricity and heat using the fuel cell. This electricity could be used by the home or sold to the grid and the heat, since local to the home, could be used for the purposes mentioned above.

5.1.3 Pecan Street smart grid demonstration project data

The data considered for this analysis are from the Pecan Street Smart Grid Demonstration Project [36]. The dataset used in this analysis consists of fourteen single-family detached homes that have solar PV generation installed on site. These homes were constructed to Austin Energy's Green Building standard [123]. The homes range in size from 116 m^2 to 281 m^2, averaging 214 m^2. The data acquisition equipment reports whole home consumption, total solar generation, and total demand from the grid. The data are aggregated to the average power draw for each minute for each home.

The time span chosen for this analysis is from Sunday August 28, 2011 to Saturday September 3, 2011. This span of data was chosen because it included the summer peak power demand for Austin, which was registered at 2,714 MW between 15:00 and 16:00 on Monday August 29, 2011 (during this hour the temperature spiked to 41.2 °C). This dataset allows for an analysis of one of the most demanding weeks for the grid in Austin. Figure 5.2 shows the average values for all the homes for Sunday August 28, 2011.

In Figure 5.2, the blue solid line represents the whole home demand, the red dashed line represents the solar power generation, the green dotted line represents the power drawn from the grid, and the purple dash-dot line is the outdoor temperature. The green dotted "Power from Grid" line is the difference between the blue solid whole home demand line and the red dashed solar production line. When the green dotted line is negative, the home is producing more power than it is consuming. The blue, red, and green lines correspond with the left axis and the dashed purple temperature

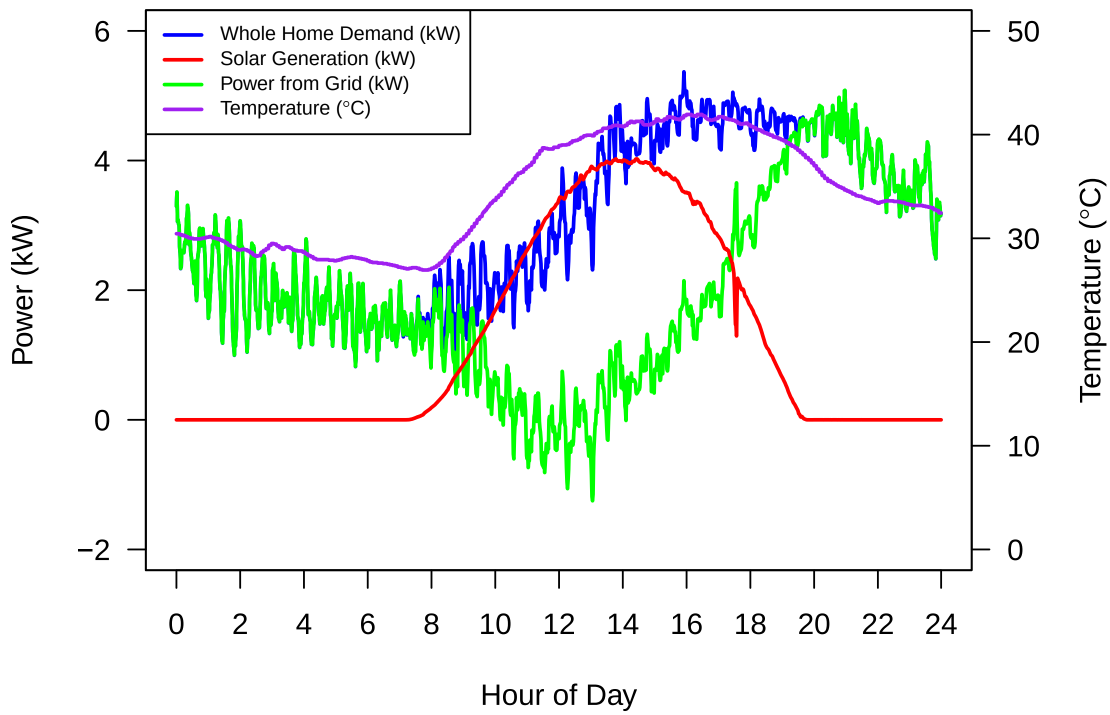

Figure 5.2: Average whole home power demand, solar generation, grid demand, and outdoor temperature for all 14 homes in the database for Sunday, August 28, 2011. The demand and grid lines are indicative of homes demand fluctuating independently and the smooth solar curve is indicative of a clear, cloudless day.

line corresponds with the right axis.

5.1.4 Methods and results

Over this entire time period, August 28 to September 3, the average maximum demand for the homes is about 5.5 kW_e (electrical power), while the average maximum power draw from the grid was 5.1 kW_e. The actual demand for a single home can be much higher; the maximum demand realized in the dataset was 13.6 kW_e for a period of two minutes. Of the 141,134 data points collected, only 9.7% were above 5.5 kW_e. During the grid peak hours of 15:00 to 19:00, 21.4% of 23,618 data points collected were greater than 5.5 kW_e. Homes may individually peak outside of the "peak hours" but the aggregate peak for the homes in the dataset also fell between 15:00 to 19:00. The maximum average solar production for the homes was 5.0 kW_e with a maximum generation value of about 6.2 kW_e. Homes in the dataset generated solar power from about 7:00 to about 19:30. During this timespan (08/28 – 09/04), the average home consumed 467 kWh_e (electrical energy), produced 189 kWh_e, and consumed an average of 278 kWh_e from the grid.

5.1.4.1 Air-conditioner run times

Air-conditioning is one of the greatest energy consuming appliances in buildings, particularly so in residences in hot and humid climates such as Austin, Texas [8]. The air-conditioning circuit was not explicitly monitored in the dataset, so the amount of time that the air-conditioner was operating was estimated. Each home's demand profile was examined for the entirety of the week monitored. Figure 5.3 shows an example of one house, for one day.

Similar to Figure 5.2, in Figure 5.3 the blue solid line represents the whole home demand, the red dashed line represents the solar power generation, the green

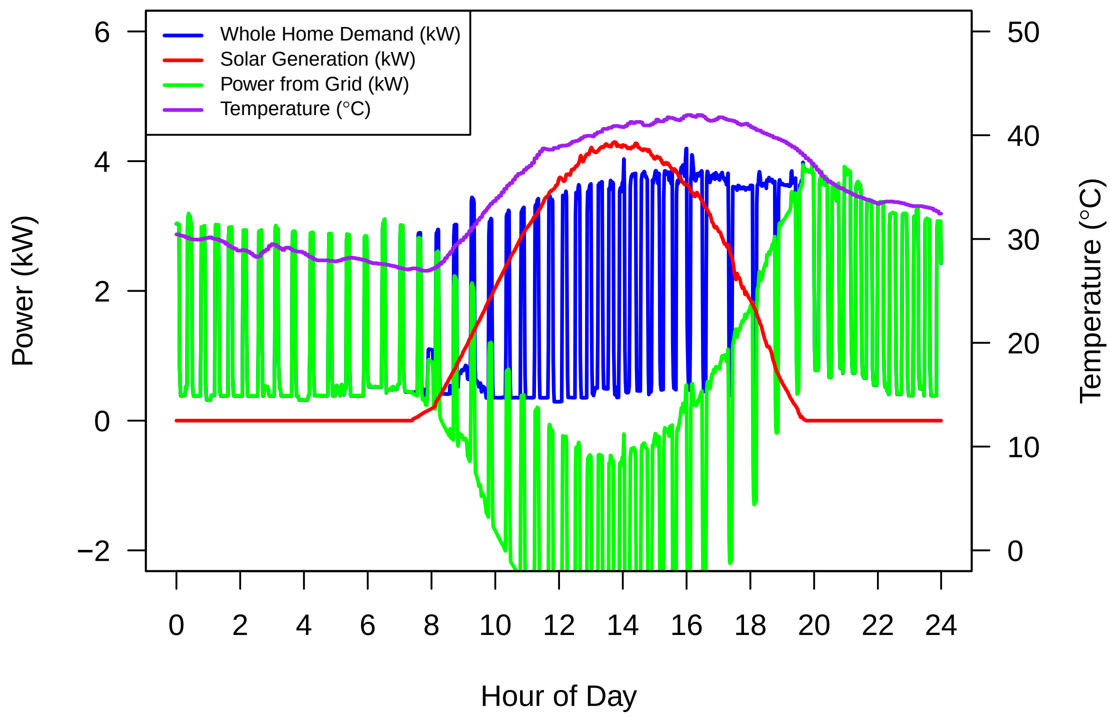

Figure 5.3: Example of whole home demand, solar generation, grid demand, and temperature for one home for Sunday, August 28, 2011.

dotted line represents the power drawn from the grid, and the purple dash-dot line is the outdoor temperature. The green dotted "Power from Grid" line is the difference between the blue solid whole home demand line and the red dashed solar production line. When the green dotted line is negative, the home is producing more power than it is consuming. The blue, red, and green lines correspond with the left axis and the dashed purple temperature line corresponds with the right axis.

Using the highly granular data and knowledge of the cycling electrical power signal of air-conditioners, combined with inspection of the data for each house for each day, it was estimated that, on average, air-conditioners were operating 54% of the time. Similarly for the peak hours between 15:00 and 19:00, air-conditioners were estimated to be operating about 85% of the time. For non-peak hours, air-conditioning runtimes averaged about 48% of the time.

Given that the average home is about 214 m^2 in size, and using an air-conditioner sizing method of about 1 kW_c (capacity) per 18.9 m^2 of flooring area [8] for a well-built home in Austin, Texas, it was estimated that the average home could use an air-conditioning system with a capacity of about 11.3 kW_c. Equipped with a standard vapor compression air-conditioner with a Coefficient Of Performance (COP is kW_c/kW_e) of 3.5, the estimated power draw would be about 3.2 kW_e, which aligns well with inspected values. The homes in this database, as part of the Austin Green Built building codes, were required to install cooling equipment with a minimum efficiency of COP 3.5. Using the average air-conditioner runtime of 54%, and the average air-conditioner power draw of 3.2 kW_e, 290 kWh_e of electricity was estimated to be used for air-conditioning during the entire week, or 62% of total use. Similarly for on-peak hours it was estimated that the air conditioner consumed approximately 76 kWh_e, or 66% of total peak use, for off-peak times air-conditioners are estimated to be operating for 213 kWh_e or 61% of off peak times.

5.1.4.2 Using the fuel cell in a combined heat and power (CHP) mode to match cooling demand

Because the fuel cell would nominally be local to the home (for this analysis), the opportunity arises to not only use the local electricity produced, but the waste heat as well. This would increase overall efficiency of the unit. Considering an absorption air-conditioner system with a COP of 0.65 [124], the system would require a thermal input of about 17.4 kW_t (heat) in order to provide the necessary amount (11.3 kW_c) of cooling capacity. Using the mid-range electrical (0.3) and thermal efficiencies (0.9) for fuel cells given above, and using the equations given in [60]:

$$\eta_{electric} = \frac{\dot{W}_e}{\dot{W}_{natgas}} \tag{5.1}$$

$$\eta_{CHP} = \frac{\dot{W}_e + \dot{W}_{thermal}}{\dot{W}_{natgas}} \tag{5.2}$$

where $\eta_{electric}$ is the electrical efficiency of the fuel cell, W_e is the electrical output of the fuel cell, W_{natgas} is the power delivered to the fuel cell from the natural gas, η_{CHP} is the efficiency of the fuel cell in combined heat and power mode, and $W_{thermal}$ is the heat produced by the fuel cell during operation. To produce 17.4 kW_t of thermal output, the electrical output of the fuel cell would be 8.7 kW_e. This value is above the average maximum power draw for the homes even when the air-conditioning load is included. This is further exacerbated by the fact that the cooling demand of the home is now met with a mostly non-electrical device. Typically, electric pumps are incorporated into absorption chillers, but the power draw is minimal when compared to the power demand of a compressor in a vapor compression refrigeration system.

This thermal and electrical output corresponds to a power input from the natural gas of about 29 kW_{ch} (chemical) of continuous input, or about 3.0 m^3 (LHV of 34.6 MJ/m^3) of natural gas per hour. Thus, sizing the fuel cell to meet the thermal demand of the home directly might be a sub-optimal approach.

5.1.4.3 Fuel cells as distributed power in the smart grid

Major market barriers to the use of residential fuel cells include high capital cost and the current residential electricity pricing structures. Current residential electric pricing structures do not typically incentivize a net producing home, i.e. one that produces more energy than it consumes. Net producing homes are sometimes given a credit towards future electricity use, but are not typically paid if they are overall net producers. This section will consider some fuel cell size and electricity pricing scenarios.

Without fuel cells. At \$0.12/kWh_e [125] the average home in Austin without solar would have paid about \$56.04 for electricity for this period; with solar production the cost is reduced to about \$33.36. Considering a simple residential time of use (TOU) pricing scheme consisting of \$0.20/kWh_e for electricity use during peak hours of 15:00 to 19:00, and \$0.05/kWh_e for all other times, the average home without solar would pay \$40.75 for electricity during this week, and homes with solar would pay an average of \$20.20.

Fuel cells meeting average building maximum load. If the average house, with solar PV, were fitted with a 5.5 kW_e fuel cell running at full load over this week, the fuel cell would have produced 924 kWh_e of electricity, almost double the consumption of the home and over triple the average consumption from the grid. For this time period, there would be a net production of about 646 kWh_e. Using Equation 5.1, the fuel cell would require 18.3 kW_{ch} of continuous power input from natural gas, or about 1.9 m^3/hr. If the utility were to buy the electricity at the retail price of \$0.12/kWh_e and assuming that natural gas cost \$0.38/m^3 [126] the energy cost (gas and electric) for the time period would be about \$43.78. This is comparable to the electricity bill without any fuel cells, however this does not take into consideration the capital cost of the fuel cells.

At home demand. If the fuel cell were to operate at more or less the demand of the average home, the fuel cell would produce about 278 kWh_e of electricity, or the same amount that is currently pulled from the grid. The cost of producing electricity solely from natural gas to bring the home to a net zero pull from grid would cost about \$36.14 for this time period, as compared to \$33.36 for buying electricity from the grid. In this analysis, the cost of electricity produced from the natural gas fuel cell, considering only fuel costs, is approximately \$0.13/kWh_e, which is close to the retail cost of electricity. However, this cost would be higher if maintenance, financing, and estimated capital cost (approximately 4,000 \$/kW [127]) were considered.

Fuel cells meeting building cooling load at flat rate electricity pricing. Implementing a strategy to couple the home cooling demand and fuel cell power and heat production as described above would result in the over production of electricity during the time period. When combined with solar production, the home would produce about 801 kWh_e of excess energy for the week. This over production is large because the electricity consumption of the air-conditioner has been eliminated and replaced with the absorption chiller, which requires far less electricity to operate. The natural gas required to produce the required thermal output over this time would be about 253 m^3 and would cost about \$103.42. If the electric utility did not pay net producing homes for their excess electricity production, the homes electric bill would be \$0, but would result in a gas bill of \$103.42 for the week. If the electric utility bought electricity produced from homeowners at retail prices, the value of the electricity produced would be \$96.15.

Fuel cells meeting building cooling load at TOU pricing. If fuel cells were allowed to operate only during the peak demand period, and considering the same simple TOU pricing scheme as given above, the result could be quite different. In this case the fuel cell only operates during the hours of 15:00 to 19:00 meeting the building cooling load with the absorption chiller and producing electricity, and during the off-peak time, a standard air-conditioner meets the cooling demand with the traditional grid meeting the electrical demand. This scenario may even allow the air-conditioner to be sized smaller, as the cooling loads could possibly be less outside of the peak times. This scenario finds that the average home over this time period is a net producer during peak, producing about 241 kWh_e. During the off-peak, the average home consumes 236 kWh_e. Allowing power to be bought at retail TOU prices during peak, which may be more agreeable to utilities especially during peak demand events, thus the average home would get paid about \$37.12 for electricity production and would pay about \$27.13 in natural gas cost, resulting in a net profit of about \$9.99 for the entire period.

Optimal sizing of fuel cells to meet building cooling load and have the house at net-zero electric energy. Optimization can be used to find the size of the fuel cell and absorption chiller combination with a small traditional air-conditioner such that the home is net zero electric energy over the time period. Not considering solar production, the optimal system consists of a 3.85 kW_e fuel cell in conjunction with a 5 kW_c absorption chiller aided by a 6.3 kW_c traditional air-conditioner or heat pump. Over this time period, the system is capable of meeting the cooling demand of the home while having the home be net zero in terms of electricity use. However, the cost of natural gas for this time period would be about \$47.55. An interesting result of this scenario is that even when the absorption chiller and the air-conditioner (COP 3.5) are running at full capacity, the fuel cell is still able to produce an extra 1.5–2 kW_e of excess power to feed to the grid, presumably when the grid needs the extra power the most.

Considering the energy produced by the solar panels and setting the same objective function as above, the optimal configuration includes a 2.35 kW_e fuel cell, a 3.1 kW_c absorption chiller, and a 8.2 kW_c standard air conditioner or heat pump. The size of the fuel cell decreases because the energy demand for the time period is lower, but the combined capacity of the cooling system must remain the same, so the air-conditioner size increases. With increased air-conditioner size comes increased energy use, and the optimization routine finds the balance. The cost of natural gas for this time period would be about \$29.14. In this case, the fuel cell electrical output would be approximately the power demand of the air-conditioner.

One major advantage of this dual setup is that the systems, if smart, would have the ability to operate independently. For example, the systems could choose to produce as much power as possible and only meet part of the cooling load if user input allowed and pricing structures produced proper incentives.

5.1.5 System efficiency

Distributed generation, including fuel cells at the home level, has the potential to increase the entire energy delivery system efficiency [128]. The end goal of energy delivery to the home or any building is for energy services, not the energy itself. While the efficiency of the grid varies somewhat from time of day and year, the average efficiency is around 27% [129]. While there is room for efficiency improvements, such as use of the waste heat at centralized generation facilities, the Carnot efficiency of heat engines will always limit the plant's electrical generation efficiency. Transmission losses can vary as well, but can be on the order of about 10% [128]. While the true efficiency of distributed fuel cell generation should include natural gas transmission losses, these data are not readily available. Considering the ability to use local generation in a CHP mode, the energy delivery efficiency to the home could possibly more than double. While beyond the scope of this analysis, other offsetting uses of local waste heat certainly include domestic hot water heating, local space heating, and even thermoelectric generation.

5.1.6 Conclusions

This work presents the possible use of distributed natural gas fuel cells, especially in cooling climates. This analysis revealed that local electricity utility policies will play a role in the financial incentive to switch to this type of local electric generation and waste heat utilization. At this point, the capital cost associated with a fuel cell-absorption chiller system for residential applications would most likely be cost prohibitive [127]. However, the major utility of such a system lies in its flexibility of outputs. The economics of the decisions would also be directly tied to the prices of two energy sources, electricity and natural gas, and dual smart systems may play an active role in this future.

This analysis found that given certain electric utility policies, distributed generation by natural gas fuel cells running in a CHP mode could be at parity or better with the traditional grid acquisition of electricity during high grid stress times. Multiple scenarios of fuel cell use were analyzed and it was determined that the structure of TOU pricing possibly allows for the best economic outcome.

Future work should include a robust model that could be optimized for individual homes. Also capital cost should be included in the economic analysis, but since fuel cell technology is just now becoming available in a scale suitable for residential use, these costs were not easily obtainable for this first iteration of analysis. Future iterations will include estimated costs or actual costs if available. Overall, this type of distributed generation technology could play a prominent role in the grid of the future.

5.2 Residential energy use regression analysis

5.2.1 Introduction

Two different regression analyses are presented that explore both the factors driving total energy use and the effectiveness of residential energy retrofits. In the first part of this section, data from this project are used to assess the relationship between survey and audit results and yearly residential energy use. While there are studies that have analyzed macro-level data from the Energy Information Administration (EIA) [6] to understand residential energy use [130–132], there is little analysis that has had this level of detail, particularly on homes in a hot and humid climate such as Austin, TX. This preliminary work seeks to fill this knowledge gap. The second analysis seeks to quantify the benefit of energy retrofits on homes in the study. There have been studies that have looked at the effect of residential energy retrofits on total energy use, but they have typically been limited to the billing (month) level or utilized building energy simulation software [133–136]. Most past studies have lacked the data to quantify the effect of retrofits on measured energy use at a finer granularity (daily kWh).

5.2.2 Background

Garbacz (1983) [130] examined the National Interim Energy Consumption Survey (NIECS) and found that the total price elasticity for electricity demand was lower than previous studies and that total income elasticity was also lower than previous studies. However, he cautioned against using direct comparisons because of differences in model specification. Hirst et al. (1982) [131] also summarized and analyzed the NIECS dataset finding that multivariate regression equations that contain less than 10 variables could account for roughly half of energy usage. They found that fuel price, year built, size, and heating degree days to the the most important variables. Kaza (2010) [132] used the 2005 Residential Energy Consumption Survey (RECS) dataset to preform a quantile regression for explore how different groups of energy consumers respond to changes in other explanatory variables. The analysis indicated, among many findings, that housing type (own vs. rent) matters more than size and that effects at the tails of the distributions can differ from the average by factors as large as 6.

Guiterman and Krarti (2011) [133] analyzed 30 low income Colorado housing units that received energy retrofits including new furnaces, tankless DHW heaters, programable thermostats, insulation, mechanical equipment tuning, CFL lighting, and air-sealing. They found about a 20% reduction in natural gas use using two years worth (pre/post) of utility billing data. Xu et al. (2013) [134] used a calibrated energy model of an apartment building and tenant surveys in northern China to estimate the savings associated with energy retrofits. They found that monetary incentives and metering technologies would not lead to the necessary behavior changes for sizable energy reductions. Ma et al. (2012) [135] in a review of current literature provides a systematic pathway for the analysis of energy retrofit technologies in buildings. Guler et al. (2001) [136] found that retrofits to residential façdes could reduce heating energy use by 8% in Canadian homes, but that many retrofit payback periods were beyond a reasonable time frame for the average homeowner.

5.2.3 Project data used in these analyses

The data used in the total energy use analysis consist of survey, audit, and measured energy use data [36]. Total energy use data used were gathered from a subset of 41 homes for the year 2011. The survey and audit data fields used as explanatory variables (regressors) included the home-specific data: number of levels, number of bedrooms, year built, home size, number of children and adults, thermostat set points, energy and water quiz scores, education level and income.

The data used in the retrofit analysis consist of daily electricity use (kWh) data for 28 homes for the period from January 02, 2010 to November 07, 2012 (27,532 total observations). Half of these homes received various energy retrofits during those three years. Care was taken to make sure that there was enough data (at least a spring-summer or summer-fall time period) before and after the retrofit(s) to support analysis consisting of adequate seasonal variation. Not all homes received the same mix of retrofits, nor did homes receive them at the same time. The retrofits performed were part of a municipal electric utility (Austin Energy) residential retrofit rebate program and some of the homes involved happened to be monitored by the Pecan Street Smart Grid Demonstration Project [137].

The retrofit analysis data are panel data, which consist of multiple individuals (in this case homes) where each individual also contains its own time series data [138]. Dummy variables (0 = no retrofit, 1 = received retrofit) were introduced to indicate when a home received a retrofit and weather effects were normalized by the inclusion of cooling degree days (CDD) and heating degree days (HDD) [139, 140].

5.2.4 Methods

Indicators of Total Energy Use. Multiple linear regression is "a method that summarizes how the average values of a numerical *outcome* variable vary over subpopulations defined by linear functions of *predictors*" [100]. This analysis seeks to determine how total yearly energy use is related to static values found in the surveys and audits. This model used the *lm* linear model package of the statistical analysis tool R [141]. The basic multiple linear regression model is given in Equation 5.3:

$$Y_i = \beta X_i + \alpha + \varepsilon_i, \tag{5.3}$$

where Y_i is the amount of yearly energy used (kWh) for a given home, β is the vector of fit regression coefficients, X_i is the set of explanatory variables, α is a constant or intercept, and ε_i is the error associated with the estimation of the energy use for that home.

Residential Energy Retrofit Analysis. Panel regression allows one to estimate the effect of explanatory variables on multiple individuals. This analysis used the *plm* panel data estimators package in R. Typically, panel regression analysis must check if the estimation method used is consistent with the data. Results of Hausman tests indicated that a fixed-effects estimator was the best option [142]. The fixed effects model is similar to a multiple linear regression for each home — the set of regression coefficients β will be the same, but each will have its own constant, or intercept. The basic panel regression model is given in Equation 5.4:

$$Y_{it} = \beta X_{it} + \alpha_i + \varepsilon_{it}, \tag{5.4}$$

where Y_{it} is the amount of energy used (kWh) for a given home i on a given day t, β

is the vector of fit regression coefficients, X_{it} is the set of explanatory variables, α_i is a constant associated with home i, and ε_{it} is the error associated with the estimation of the energy use for that home and day.

5.2.5 Results

The output from the first multiple linear regression model estimating the effect of explanatory variables on total yearly energy use is given in Table 5.1.

Table 5.1: Multiple regression output for the relationship between survey and audit data and total yearly energy use.

Explanatory Variable	Coefficient Estimate	Std. Error	t-value	Two-tailed P-test	Significance Level
Intercept	273,641	77209	3.54	0.001	**
Year_Built	-136	38.9	-3.51	0.001	**
Condition_Sqft	7.6	0.86	8.80	4.69E-10	***
Number_Kids	1096	748	1.47	0.153	
Number_Adults	2083	920	2.26	0.031	*
Income	-1115	776	-1.44	0.160	
Water_Knowledge_Score	-1858	783	-2.38	0.024	*
Energy_Knowledge_Score	-1540	673	-2.29	0.029	*

0 '***' 0.001 '**' 0.01 '*' 0.05 '.' 0.1 ' ' 1 Adjusted R^2: 0.7874 n = 41

In Table 5.1 *Intercept* is the constant term of the regression, however in this model its interpretation is of no real value (the "energy use" associated with zeros for all other coefficients, i.e. a home built in year 0, of 0 square foot, etc.), the *Year_Built* coefficient estimate is the effect of increasing the construction date of the home by one year, all else held constant, the *Condition_Sqft* coefficient estimate is the effect of increasing the size of the home by 1 square foot, *Number_Kids* is the effect of increasing the number of children in the home by 1, *Number_Adults* is the effect of increasing the number of adults in the home by 1, *Income* is the effect of increasing an income bracket, *Water_Knowledge_Score* is the effect of a 1 point increase in the score on the water knowledge quiz included in the survey, and *Energy_Knowledge_Score* is the effect of a 1 point increase in the score on the energy knowledge quiz included in the survey (see the [36] for a copy of the survey).

The model was built using best practices from regression texts [100]. All the regression coefficients in the final model had the expected signs even if they were not significant (*Number_Kids* and *Income*). The coefficient *Year_Built* indicates that newer homes (those built in more recent years), on average consume less energy than older homes. Home size (*Condition_Sqft*) also has a positive relationship with energy use, as do the number of children and adults (*Number_Kids* and *Number_Adults*). Interestingly, higher scores (*Water_Knowledge_Score* and *Energy_Knowledge_Score*) on the water and energy quiz in the survey (indicating more knowledgeable participants) were correlated with reduced energy use. This finding suggests that education might be effective in reducing in residential energy usage, however there is not enough information to deduce causality.

The output from the residential energy retrofit panel regression model is given in Table 5.2.

Table 5.2: Panel regression output for fixed-effects model showing the estimated impact of energy use retrofits on daily energy use using the whole time period.

Explanatory Variable	Coefficient Estimate	Std. Error	t-value	Two-tailed P-test	Significance Level
HDD	1.57	0.03	51.66	< 2.2E-16	***
CDD	2.68	0.02	156.61	< 2.2E-16	***
Solar.Shading	-0.53	1.02	-0.52	0.602	
Air.Seal	-1.56	0.63	-2.46	0.014	*
Attic.Insul	-1.70	0.66	-2.57	0.010	*
HVAC	-4.09	1.02	-4.02	5.91E-05	***
Other.System	3.78	1.19	3.19	0.001	**

0 '***' 0.001 '**' 0.01 '*' 0.05 '.' 0.1 ' ' 1 Adjusted R^2: 0.5099 n = 28

In Table 5.2, the coefficient estimate of *HDD* is the estimated effect of an additional heating degree day on daily energy use, *CDD* is the estimated effect of an additional cooling degree day on daily energy use, *Solar.Shading* is the estimated effect of upgrading solar shading of windows, *Air.Seal* is the estimated effect of reducing the outdoor air infiltration rate of the home (weatherstripping and sealing cracks in the façade), *Attic.Insul* is the estimated effect of increasing the amount of attic insulation, *HVAC* is the estimated effect of upgrading the home's HVAC equipment, and *Other.System* is the estimated effect of upgrading some non-HVAC appliances to Energy Star versions or acquiring new Energy Star appliances.

All the coefficient estimates have the expected sign with the exception of *Other.System*. The data did not indicate if the appliance in question was an upgrade or a new addition to the home. The data simply stated when an Energy Star appliance was purchased. Since the coefficient is positive and significant, it would seem to imply that the purchases, on average, were for new additions to the homes' set of appliances. A possible scenario being that as an older, less efficient refrigerator was replaced by a new Energy Star unit, the former was moved to the garage where it continued to be used as a 'beer fridge' [143]. The energy efficiency rebate might have offset a larger increase in energy use associated with the purchase of a less efficient appliance, but the data do not allow us to test this hypothesis. The only variable that was not significant was *Solar.Shading*. The sign of the coefficient is as expected and according to regression texts, it is convention to leave such variables in the model [100].

There were three retrofits that showed significant energy reductions: *Air.Seal*, *Attic.Insul*, and *HVAC*. Holding all else constant, the retrofits showed, on average, daily reductions of 1.56, 1.70, and 4.09 kWh, respectively. These retrofits are expected to last 30, 40, and 15 years, respectively [144].

Data from Austin Energy's rebate program [137] indicate that the average rebate associated with air sealing is \$241 for an estimated rebate-cost to the utility of \$0.014/kWh (over the expected lifetime of the retrofit). This rebate-cost was calculated using Equation 5.5:

$$C_{rebate} = \frac{R_{avg}}{\beta_{retrofit} \times 365 \times L_{retrofit}}, \tag{5.5}$$

where C_{rebate} is the "rebate-cost" to the utility (\$/kWh), R_{avg} is the average rebate of the retrofit (\$), $\beta_{retrofit}$ is the coefficient of the retrofit given in the panel regression (kWh/day), and $L_{retrofit}$ is the lifetime of the retrofit (years). Data from Austin Energy also revealed that the average capital cost of the retrofit *Air.Seal* was approximately \$744 for a final (to-homeowner) capital costs of \$503. This final capital cost leads to a homeowner-cost of \$0.029/kWh. This homeowner-cost was calculated using Equation 5.6:

$$C_{homeowner} = \frac{FC_{avg}}{\beta_{retrofit} \times 365 \times L_{retrofit}}, \tag{5.6}$$

where $C_{homeowner}$ is the "homeowner-cost" (\$/kWh), FC_{avg} is the average final capital cost to the homeowner (\$), $\beta_{retrofit}$ is the coefficient of the retrofit given in the panel regression (kWh/day), and $L_{retrofit}$ is the lifetime of the retrofit (years).

Austin Energy also offers rebates for increasing attic insulation up to R-38. Data from Austin Energy indicate that the average rebate associated with increasing attic insulation is \$163 for an estimated rebate-cost to the utility of \$0.007/kWh. The average capital cost of the retrofit was \$1,037 leading to a final homeowner capital cost of \$874 and a homeowner-cost of \$0.035/kWh.

The highest reduction in daily energy use came from upgrading the HVAC system, which is not surprising given the local cooling dominated climate. Austin Energy has a tiered rebate system with increasing rebates for higher efficiency HVAC units. Data from Austin Energy's rebate program indicate that the average rebate associated with upgrading HVAC equipment is $450 for an estimated rebate-cost to the utility of $0.020/kWh. The average capital cost of the retrofit was $6,517 leading to a final homeowner capital cost of $6,067 and a homeowner-cost of $0.271/kWh. However, this result might not be fully accurate if the HVAC unit were in need of replacement and code required a unit of higher efficiency than the unit being replaced.

Table 5.3: Summary of costs and rebates associated with residential energy retrofits and Austin Energy's retrofit rebate program.

Retrofit	Average Capital Cost	Average Rebate	Average Final Cost	Energy Saved (kWh)	Rebate Cost ($/kWh)	Homeowner Cost ($/kWh)
Air.Seal	$744	$241	$503	17,082	$0.014	$0.029
Attic.Insul	$1,037	$163	$874	24,820	$0.007	$0.035
HVAC	$6,517	$450	$6,067	22,393	$0.020	$0.271

5.2.6 Conclusions

Results from both regression analyses reveal some interesting results. While most of the results from the first regression are somewhat intuitive, the significant correlation of reduced energy use with increased energy and water knowledge is interesting and worthy of further investigation. Survey questions about residential and national resource use were deployed to assess the homeowner's knowledge with the hypothesis that it would significantly effect choices and behavior related to energy use [36]. This result might lend some support for increased energy and water education campaigns.

The retrofit analysis provided results that utilities can use to assess the value of residential retrofit rebates as compared to the cost of acquiring energy on the wholesale market. Average yearly wholesale electricity costs for 2011–2012 were \$0.037/kWh. The model indicates that the current level of rebates is cost effective for the utility for all three retrofits, and could possibly be increased. Austin Energy has a five-tiered residential electricity rate structure based on consumption, partitioned by summer and non-summer seasons [145]. The realized residential rate (per kWh costs) increases as one uses more energy in a month from \$0.065/kWh for winter use less than 500 kWh to \$0.161/kWh for all use in excess of 2500 kWh in the summer. Considering an average of \$0.113/kWh for residential electric service, both the air-sealing (*Air.Seal*) and added attic insulation (*Attic.Insul*) seem to make economic sense for the homeowner. It is difficult to infer much about the value of the homeowner cost associated with HVAC replacements as it is not known if the HVAC system was at its end of life at the time of the upgrade.

Chapter 6

Summary

This dissertation addressed the following four objectives:

1. *Explore the residential electricity consumption and common air-conditioner design and installation issues of homes in Austin, Texas,*
2. *Determine the key correlations between homeowners and their temporal energy use in Austin, Texas,*
3. *Determine the optimal placement of residential-based solar PV systems for Austin and the greater US, and*
4. *Explore the efficiencies associated with firm distributed generation and residential energy retrofits.*

The following sections summarize the major conclusions from these studies.

6.1 Using energy audits to investigate the impacts of common air-conditioning design and installation issues on peak power demand and energy consumption in Austin, Texas

Chapter 2 analyzed a database of 4971 energy audits on single-family homes in Austin, Texas. The analysis led to a conclusion similar to previous studies: residential air-conditioning systems are generally operating in poor condition. The inefficiencies associated with poor residential air-conditioning performance aggregated across a city can be significant, especially during peak periods. Single-family residential air-conditioning systems are estimated to account for approximately 17–18% of peak summer electricity demand in Austin. Furthermore, the analysis concludes that efficiency improvements alone (upgrading all systems to EER 14, COP 4.1) could reduce peak power demand by as much as 205 MW, which would achieve almost 26% of Austin's Climate Protection Plan's goal of an 800 MW peak reduction by 2020. Similarly, this analysis suggests that accurately sizing residential air-conditioning equipment could displace as much as 41 MW of peak demand, or nearly the equivalent of one natural gas peaking plant. Additionally, replacing oversized units with higher efficiency units (EER 14, COP 4.1) could increase those peak savings to 81 MW. This research also indicates that Austin Energy could substantially increase energy efficiency rebate levels for home energy retrofits and still be at parity with the cost of building new generating capacity.

6.2 Clustering analysis of residential electricity demand profiles

Chapter 3 employed a data-driven approach to 1) determine the shape of seasonally-resolved residential demand profiles, 2) determine the optimal number of normalized representative residential electricity use profiles within each season, and 3) draw correlations to the different profiles based on survey data for over 100 homes in Austin, TX. This analysis determined that, for homes in a southern U.S. location, there are two main groups of temporal profiles, representing residential electricity demand in each season. Temporal and magnitude differences in the summer profiles are significant with one group typically demanding more power during higher wholesale electricity price times than the other. Finally, probit regression analysis determined that explanatory variables such as whether someone worked at home, the number of hours of television watched per week, and education were significant determiners of inclusion in a given cluster. These results point to markers of households that might be more impacted by time-of-use or real-time pricing electricity rates and can act as predictors as to how changing demographics can change electricity demand patterns.

6.3 A multi-objective assessment of the effect of solar placement on energy production and system economics

Chapter 4 considered the the effect of various placements (azimuth and tilt) of solar PV systems on energy generation and value of that energy generation for a yearly period with various environmental and economic inputs in Austin, TX. Using clear-sky, typical meteorological year (TMY), and real, measured solar radiation data the analysis finds that the rule-of-thumb placement (due south and a tilt slightly less than the local latitude) might not be optimal for total energy production. Both TMY and measured data indicate a 7–8° shift west (187–188°) and a few degrees towards the horizontal (from the rule-of-thumb 30°) might be a better azimuth and tilt for energy production. Clear sky radiation data reinforce the energy rule-of-thumb as expected. Considering the value of energy produced, the optimal azimuth was pushed further west ($\approx$ 20–50°) based on wholesale electricity market prices that are typically higher in the mid to late afternoon hours. While the resulting improvements might might seem small, ($<$ 1–7% difference), the improvement is free to implement during construction, and over the 25 year lifespan the excess energy produced and revenue earned could be significant. For most of the US, the rule-of-thumb for total energy production might be a good approximation, but it does not apply everywhere. In many locations, the optimal economic placement is shifted west, particularly in locations that have TOU rates with higher afternoon prices. Although in some cases, rates shift the placement east. Placements that maximize generation during peak times shift placements further west and energy might incentivize otherwise non-optimal placements.

6.4 Other residential energy studies – residential natural gas fuel cells and residential energy use regression analysis

Chapter 5 considered the possible use of distributed natural gas fuel cells to increase the primary energy efficiency of residential buildings, residential predictors of total electricity use, and the the observed electricity use reduction effect of residential energy retrofits.

The analysis indicates that given certain electric utility policies, distributed generation by natural gas fuel cells running in a CHP mode could be at parity or better with the traditional grid acquisition of electricity during high grid stress times. Multiple economic scenarios of fuel cell use were analyzed and it was determined that the structure of TOU pricing allows for the best economic outcome.

Results from both regression analyses reveal some interesting results. While most of the results from the first regression are intuitive, the significant correlation of reduced energy use with increased energy and water knowledge is interesting. Survey questions about residential and national resource use were deployed to assess the homeowner's knowledge with the hypothesis that it would significantly effect choices and behavior related to energy use. This result might lend some support for increased energy and water education campaigns.

The retrofit analysis provided results that utilities can use to assess the value of residential retrofit rebates as compared to the cost of acquiring energy on the wholesale market. Average yearly wholesale electricity costs for 2011–2012 were \$0.037/kWh. The model indicates that the current level of rebates is cost effective for the utility for all three retrofits, and could possibly be increased. Considering an average of \$0.113/kWh for residential electric service, both the air-sealing and added attic insulation make economic sense for the homeowner given current rebate structures, while all studied retrofit rebate costs are economical to Austin Energy.

6.5 Overall considerations of the work in this dissertation

The lessons learned in the analyses within this dissertation could be used together in the following succinct way: Chapter 3 provides insights to which homes use more expensive electricity than others and whose energy reductions from energy retrofits might be worth more to utilities than others. Utilities could use this information to provide more rebates to those from whom they then receive the greatest benefit. Chapter 2 gives insights as to how much energy reductions could be achievable in Austin from increasing energy retrofits to residential buildings and Chapter 5 provides insights as to the value of the energy retrofits to both the utility and the homeowner. Chapter 2 also concludes that rebates could be increased and still be at parity with acquiring more generation capacity. Chapter 4 extends the idea of additional generation capacity by optimizing the placement of fixed solar PV systems in response to prices and grid stress versus the total amount of energy produced. Chapter 5 provides optimal sizing and analysis for distributed firm generation that could also be used to reduce distributed demand by producing energy but also utilizing waste heat for space conditioning services.

Taken together, this body of work points towards a holistic approach to optimizing residential energy use. Intelligent efficiency measures coupled with smart generation, control, and prediction could produce a more versatile and cleaner future.

6.6 Future work

Recommended future work includes extended analysis on many of the aspects of this dissertation. Recent interactions with Austin Energy (AE) have resulted in AE providing a dataset of over 1,700 homes that have participated in their energy retrofit programs. These data include basic home characteristics, what retrofits occurred and when, and at least a year of daily energy use data before and after the retrofit. Costs, including total retrofit costs, rebate cost, and total costs paid by homeowners are also included. Using techniques from Chapter 2, 5 and Appendix A these data could be used to better predict the effect of energy efficiency retrofits on energy use and compare the parity of rebates per reduction in energy use to acquisitions on wholesale markets. These data will also allow for the comparisons of engineering calculations of energy use reductions to actual reductions for an assessment of rebound effects.

In the future, a set of 12,000 energy audits recently supplied by AE for the purpose of increasing the effectiveness of the audits to spur investment in energy efficiency retrofits could be analyzed. Currently, less than 10% of persons who receive these audits act on the recommendations. Using the lessons learned in Chapter 2, 3, 5, and Appendix A, building energy models could be built (directed by results from the above analysis) that will enable an energy retrofit optimization for individual homes and recommend retrofits that will reduce overall energy costs. The percentage of households that act on the recommendations could then be tested against the base of 10%. Before and after energy use data could be compared for feedback to the ability of the models to make recommendations.

Also, analysis from Chapter 4 could be extended to consider the ability of various solar placements and other renewable energy systems geographically distributed throughout Texas to offset fossil fuel generation in ERCOT. Optimal solar and wind deployments could be then used in unit commitment models of the ERCOT grid to assess their feasibility and impacts on price, grid stability, carbon emissions, and water use for electricity production.

Appendix A

Comparison of Simulated and Measured Energy Use using Energy Audits

A.1 Introduction

Many different building energy simulation models have been developed over the last 50 years to help users predict specific building performance characteristics [146]. Recently, residential energy use modeling has become popular to provide homeowners feedback about their homes energy performance [147]. One platform for building energy simulation, EnergyPlus was developed by the US Department of Energy (DOE) and was released in 2001, with a focus on commercial buildings. Recently, a residential front-end to EnergyPlus, BEopt, was developed by the National Renewable Energy Laboratory to provide easier and better modeling of residential homes [148]. However, modeling residential buildings can lead to systematic errors that need to be understood to evaluate the applicability of the models results in the real world [147,149–152]. Thus, it is valuable to assess the accuracy of modeling programs. This work seeks to do that by use of 1) a database of residential home energy audits, and 2) data from a smart grid demonstration project. Understanding how these models predict actual energy usage in Austins hot and humid climate under different design considerations can lead to better simulations and retrofit recommendations.

A.2 Datasources Used in this Analysis

In this analysis, a sample of 57 single-family homes with energy audits and metered electricity use data, provided by Pecan Street Inc., a smart grid demonstration project that is based in Austin, was used to test the accuracy of home energy profiles generated by the EnergyPlus simulation software [36]. These audits are similar to a citywide program, The Energy Conservation Audit and Disclosure (ECAD) ordinance in Austin, which mandates that an energy audit be performed on a home before it can be sold [74]. Table A.1 summarizes the key audit data that were used to build the models in BEopt.

Table A.1: Residential Home Characteristics Utilized for Energy Simulation

Parameter	Unit	Mean	Standard Deviation	Median
Year Built	–	1965	18.2	1964
Conditioned Area	ft^2 [m2]	1,780.6 [165.4]	904.9 [84.1]	1,617.5 [150.2]
House Volume	ft3 [m3]	15,062.8 [426.3]	8,829.6 [250]	12,960 [367]
Total Window Area	ft^2 [m2]	218.1 [20.3]	130.2 [12.1]	206.0 [19.1]
Attic R Value	hr-ft^2-°F/BTU [RSI]	23.3 [4.1]	10.7 [1.9]	22.5 [4]
Home Duct Leakage	%	14.3	9.6	12
Duct R Value	hr-ft^2-°F/BTU [RSI]	4.3 [0.76]	1.9 [0.34]	4.0 [0.71]
Conditioner Capacity	BTU [kW]	36,766.7 [10.7]	11,492.6 [3.4]	36,000 [10.5]
System Efficiency	EER [COP]	10.2 [3]	2.3 [0.67]	10.0 [2.9]
Furnace Capacity	BTU [kW]	66,388.9 [19.5]	21,560.3 [6.3]	66,000 [19.3]
Furnace	AFUE	80.3	1.7	80
ACH50	–	11.7	5.2	10.8

In addition to the data on residential home characteristics, electricity use data were retrieved from two sources: 1) Austin Energy and 2) Pecan Street Inc. Austin Energy provided daily kWh smart meter reads from the homes electricity meter, and Pecan Street provided energy demand data (1-min) for each home which allowed for temporal comparisons between modeled and measured values. Finally, demographic data on the occupants of each of the 57 single-family homes were also available and were used in the BEopt simulations to adjust the thermostat set points of the air conditioning systems in each of the respective models. The BEopt simulations used for this work do not account for behavioral patterns that might arise due to specific demographic information such as miscellaneous large loads. This issue will be discussed further in the results section of this report. Recent upgrades to BEopt (version 2.1), released after this analysis, accommodate a better characterization of homeowner behavior but were not considered in this analysis.

A.3 Methods

A.3.1 Construction of the BEopt models.

In this analysis, 4 different scenarios, utilizing 57 home energy models, were constructed. The main performance criterion used in this analysis is a comparison of the models predicted yearly electricity use to measured utility and smart metered electricity data. The process for developing the 57 home models for the four scenarios is shown in Figure A.1. The home models were constructed using BEopt, a graphic user interface that provides functionality to build a residential homes geometry and indicate specific features of each individual home (e.g. home insulation values, duct leakage, AC efficiency, etc). The BEopt software can use either the DOE2/TRNSYS or the EnergyPlus simulation engine, and for this analysis, we utilized the EnergyPlus engine because it includes more flexibility in simulations. Furthermore, BEopt contains three main interface screens to enter information that will be used by the simulation engine to calculate a homes energy profile: the geometry screen, the options screen (insulation levels, window types, etc.), and the site screen (location, weather files, utility rate structures, etc.).

Information on the specific functionality for each screen can be found in prior literature [148]. The BEopt default values were used in cases where the energy audit did not provide specific details of the building (e.g. wall insulation, miscellaneous

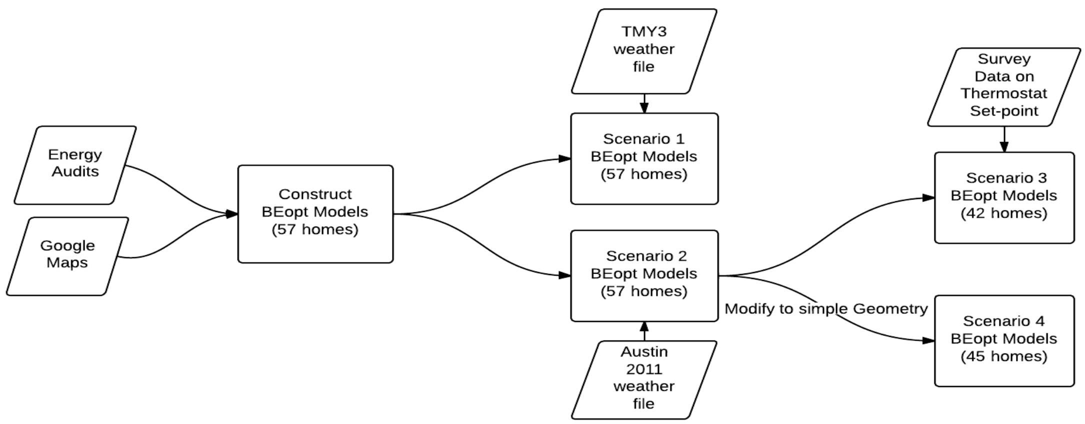

Figure A.1: Flowchart for creating and analyzing the 57 residential homes using BEopt and EnergyPlus.

electric load, floor insulation, refrigerator, cooking range, dishwasher, and lighting information). The data that were updated due to availability of audit data were building orientation, neighbor spacing, exterior finish, unfinished attic type and insulation, roof material, radiant barrier, window areas, window type, home air leakage, clothes dryer and water heater fuel, central AC and furnace efficiency and size, duct insulation, and duct leakage.

In part of our analysis, we compare the outputs of models run with TMY3 weather data along with real measured weather data for Austin in 2011, a particularly hot year for Austin. The 2011 weather file was created by modifying the TMY3 weather file used by BEopt for energy simulation. All fields for which local, temporally-resolved weather data, including temperature, humidity, wind speed, wind direction, etc., were available were modified. However, solar radiation data for 2011 were not available, so the TMY values were used instead.

A.3.2 Scenarios Considered for Analysis

In total, four different model scenarios (Figure A.1) were developed in order to compare the 57 homes in different situations to monitor the effect of certain changes on the output of the EnergyPlus simulation. The first scenario involved the utilization of a TMY3 weather file and the second scenario involved the utilization of an Austin 2011 weather file. No home properties were changed between these two scenarios. The third scenario involved the application of thermostat set-point information that was obtained from the surveys given out to the homeowners. This scenario was developed to observe the effect of thermostat behavior on the models overall performance. The fourth scenario simplified the geometry of the homes to test the effect of geometry on the home electricity use. In total, nine generalized geometries existed before modification for the 57 modeled homes. These geometries are shown in Figure A.2. To determine the extent to which complicated geometries influence electricity consumption, each complex home geometry was simplified to geometry A. For comparison purposes, special attention was given to ensure that the percent change of the new square footage to the square footage of the original model remained within 1%.

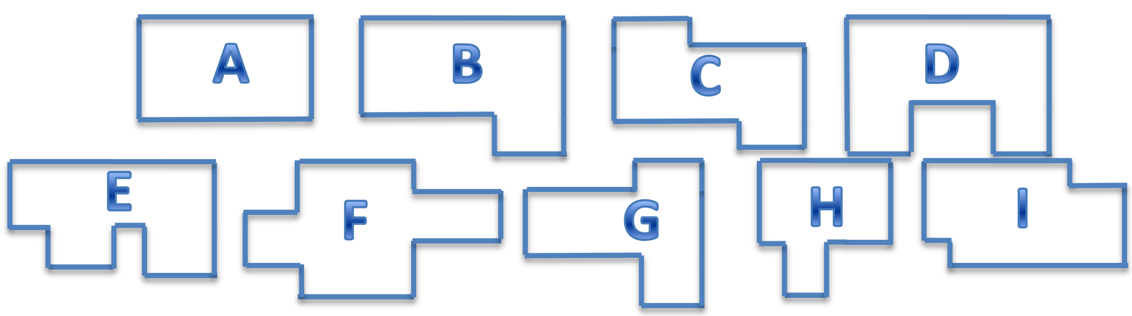

Figure A.2: Depiction of the main floor geometries used to estimate energy consumption of the residential homes.

To observe the effect of the different scenarios, the model output was compared to actual electricity use data (daily kWh reads from smart meters). First, electricity use measured by the local utility was compared to simulated electricity consumption from the model over an entire year. Error was calculated for each individual BEopt model by Equation A.1:

$$Percent\ \ Error = \frac{E_{BEopt} - E_{Utility}}{E_{Utility}} \times 100 \tag{A.1}$$

where *Percent Error* is the percent difference between the BEopt-modeled and utility-measured consumption data, E_{BEopt} is the electricity consumption predicted by the BEopt model for one home (kWh), and $E_{Utility}$ is the electricity consumption provided by Austin Energy, the local utility company (kWh). To compute aggregate BEopt model error for the entire group of 57 homes, each model's electricity consumption in kWh over the entire year was summed and compared with the summation of each individual homes utility data in kWh over the entire year via Equation A.2:

$$Aggregated\ \ Percent\ \ Error = \frac{\sum E_{BEopt} - \sum E_{Utility}}{\sum E_{Utility}} \times 100 \tag{A.2}$$

where *Aggregated Percent Error* is the error when all 57 homes model values are summed and compared with the sum of the utility data for the 57 homes.

Finally, hourly temporal profiles produced by the BEopt model were compared with hourly electricity use data to determine whether certain time periods throughout the day or seasons throughout the year affected the performance of the BEopt model. To generate the temporal profiles in BEopt, modeled electricity demand data for August 30th 2011 were averaged for 5 modeled homes. This modeled average daily profile was compared to an average profile generated from the same homes actual usage on August 30th 2013. These days were compared because the temperature data for August 30th 2011 was similar to temperature data for August 30th 2013 (the high-fidelity data were only available for 2013). The same procedure was followed to produce a winter temporal profile comparison.

A.4 Results

During the construction of the models, the pool of available homes for each scenario changed due to availability of data. Fifteen homes did not have thermostat set-point data, and therefore, only 42 homes of the available pool of 57 homes were modified with temperature set-back information for scenario 3. Furthermore, 12 of the 57 homes were initially modeled with a simplified geometry, and therefore, only 45 homes of the available pool of 57 homes could be analyzed for scenario 4.

A.4.1 BEopt Simulation Results

Figure A.3 presents the histograms of the 57 individual homes percent error values for scenarios 1, 2 and 3. Scenario 4 was not included in this analysis since it was not being compared to measured electricity data but rather to its deviation from an original model due to a modification of geometry parameters. The average percent error for the individual homes was 6.78% (s.d. 37%), 22.3% (s.d. 42%), and 19.1% (s.d. 36%) for scenario 1, 2, and 3 respectively. While a decrease from scenario 2 to 3 is expected due to the improved data quality with temperature set-back information, the increase from scenario 1 to 2 is unexpected. We hypothesize that the BEopt model tends to over predict energy usage. For this reason, when the 2011 weather file was used for Austin, the model increased its over-prediction because 2011 was a much hotter year than the average TMY3 data.

To explore the hypothesis that BEopt over predicts electricity consumption for

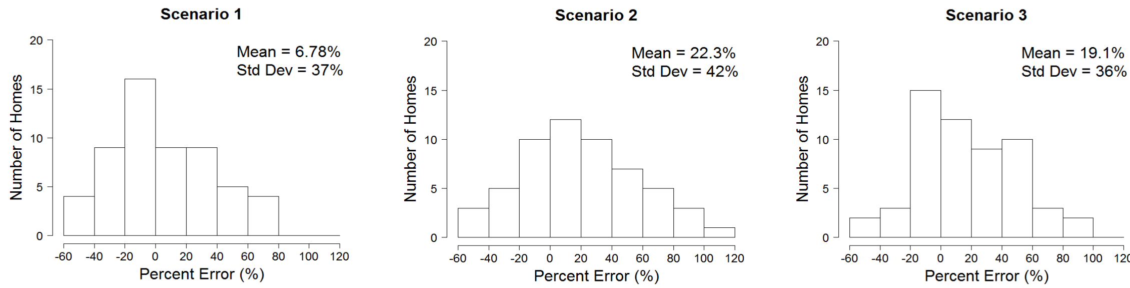

Figure A.3: Histograms of Percent Errors for scenarios 1–3 of model construction showing changes in predictability of model with TMY3 weather data for Austin (Scenario 1), Austin 2011 weather data (Scenario 2), and Austin 2011 weather data including temperature set-back data for 42 homes (Scenario 3) with one outlier (the same home) removed for each scenario for clarity.

certain homes, we looked at Energy Information Agency (EIA) data on residential homes energy consumption normalized over square footage. The EIA data indicate that the average value is 12.9 kWh/ft^2/year for Texas [6]. However, a number of the homes modeled in this study exhibited much smaller values for their site energy consumption per square foot with an average value of 6.85 kWh/ft^2/year. This analysis might suggest either that some of the utility data may be missing some values, the homes are more efficient than the average Texas home, or that BEopt has difficulty modeling homes that consume less energy on average per square foot. For example, 31 homes had average utility consumption values below 7 kWh/ft^2, and when these homes are removed from the calculation, the percent error for each individual home drops significantly to -16.1% (s.d. 22%), -3.7% (s.d. 24%), and -2.6% (s.d. 23%) for scenarios 1, 2, and 3 respectively. These results follow the expected progression from scenario 1-3 as data quality improved, and this analysis is graphically depicted in Figure A.4.

However, analysis involving simple percent error calculations on individual homes might unjustifiably put more weight on the percent errors of smaller homes that consume less electricity compared to the aggregate electricity consumption of

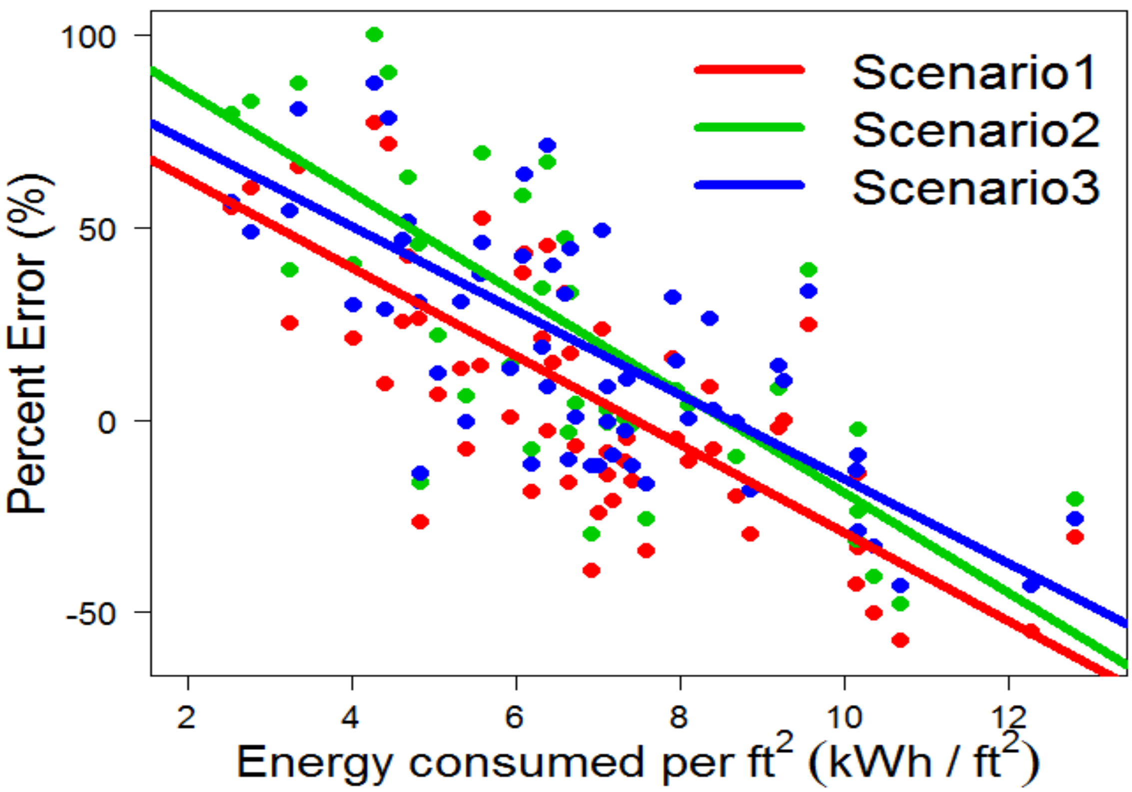

Figure A.4: Graph comparing percent errors for scenarios 1-3 to their energy consumption per square foot showing that the BEopt models perform worse over certain bounds (below 5 kWh/ft^2/year and above 10 kWh/ft^2/year) and that in general percent error has an inverse relationship with energy consumed per ft^2.

the 57 homes. For this reason, to assess the BEopts ability to predict electricity consumption in a community, an aggregated percent error for the 57 homes was calculated using Equation 2 that is explained above. This type of aggregated error is an appropriate tool to use for studies where modeled communities are used for analysis rather than individual homes [153]. For the 57 homes, the aggregate errors were -11.0%, 2.6%, and 1.7% for scenario 1, 2 and 3, respectively. As the input data quality increased from scenarios 1 to 3 so did the models performance. Including the accurate weather file in scenario 2 led to overall improvements in aggregate model performance and including behavioral data in scenario 3 led to further improvements in model performance, though smaller relative to the improvement from scenario 1 to 2. These results are summarized in Table A.2. Further improvements could most likely be made by more information about the behavioral patterns of homeowners. The effect of the lack of behavioral data on BEopt model performance is best observed by analysis of the temporal consumption profiles in the next section.

Table A.2: Summary of Results from Scenarios 1 – 4

Calculations	Scenario 1	Scenario 2	Scenario 3	Scenario 4
Percent Error (%)	6.78	22.29	19.07	–
w/ homes > 5 kWh/ft^2	–4.81	9.07	8.18	–
w/ homes > 7 kWh/ft^2	–16.17	-3.69	–2.6	–
Absolute Percent Error (%)	28.24	34.39	30.24	1.22
w/ homes > 5 kWh/ft^2	21.77	24	22	–
w/ homes > 7 kWh/ft^2	21.79	18.45	18.11	–
Aggregated Percent Error (%)	–11	2.56	1.74	–

A.4.2 Temporal Electricity Profile Comparison: Modeled vs. Measured

In this analysis, hourly consumption data were taken from the BEopt output file and compared with hourly data taken from a smart grid demonstration project in

Austin, TX. Figure A.5 shows the differences between the metered data that and the BEopt generated daily consumption profile for the summer and winter seasons. In the summer month (Figure A.5, left side), this analysis shows that the BEopt model over predicted average electricity demand fairly significantly between 6 AM and 2 PM for these five homes. Even though BEopt was running with the thermostat set-point data provided by the surveys, it did not reduce the energy demand enough during the peak time in the middle of the day. There might be a number of reasons for this, but potentially, homeowners did not provide accurate temperature set-back data, which limited the prediction ability of the BEopt model in this analysis. Also, other behavioral patterns, such as times of leaving/returning home, that were not reported by homeowners could be driving the homes' lower energy consumption compared to the model. It also could be the case that the model has trouble simulating home performance in a hot and humid climate such as that of Austin.

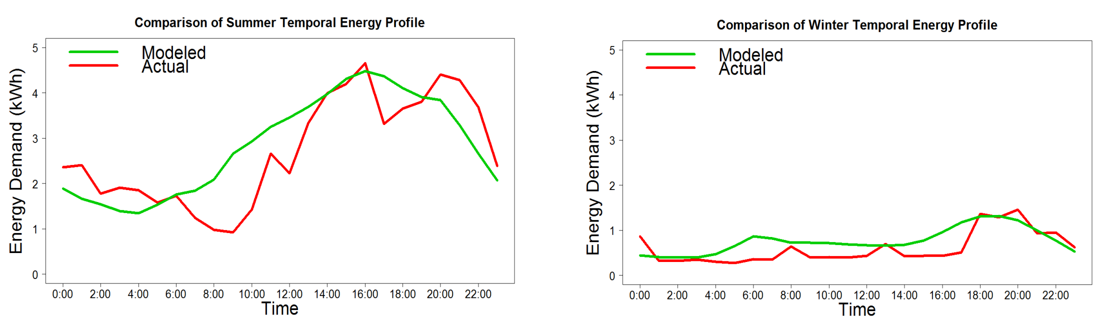

Figure A.5: Temporal graph comparing hourly consumption patterns between simulation and measurement for an August day and a February day showing that the model is over predicting electricity use most of the day in the summer time and slightly over predicts electricity consumption most of the day in the winter but follows trends relatively well.

The winter graph shows that the BEopt model did a fairly good job following the consumption profile for the 5 smart metered homes selected for analysis. While it does appear that the model over predicts consumption between 6 AM and 6 PM, the overall trends aligns quite well. Nevertheless, spikes and offsets are still present and suggest that BEopt will continue to have difficulty predicting temporal profiles due to the fact that behavior becomes such an important factor once the model is analyzed at the daily time scale. For this reason, maybe these models, in their current form, ought to be used sparingly to predict daily electricity demand profiles for individual homes.

A.4.3 BEopt Geometry Modification Analysis.

Scenario 4 involved the modification of home geometry of the scenario 2 models in order to determine whether home geometry characteristics drive energy consumption profiles in BEopt. Overall, the analysis showed that a simplified geometry does not change model performance significantly. In total, 32 home geometries were changed from a complex geometry (B-I in Figure A.3) to the A geometry type, and 13 of the homes were modified from a combination of complex two-storied construction to a two storied construction with different A geometry shapes placed on top of each other. Twelve of the models already were constructed with the A geometry shape and therefore were excluded from this portion of the analysis. Overall, for the one-story changes, the homes only deviated by 1.31% from the original model values, and the two story changes only deviated by 1.07% from their original models. Furthermore, since square footage could not be maintained precisely when the simplified geometries were created, some of these differences could be explained simply by the change in ft^2. On average, the one-storied models in scenario 4 changed by less than 5 ft^2, and the two-storied models changed by 7.4 ft^2. Results indicate that even without accurate geometry information for a real home, the BEopt simulation can produce plausible results. This result might become more important if home modeling is automated and extended to a large number of homes and complex home geometries need to be simplified for the automated process. Confirming that model output is not affected significantly should allow energy modelers to simplify their geometries or select geometries from a pre-defined list.

A.5 Conclusions

Given the integration and close comparison of two unique data sets including information about single-family homes and their hourly and yearly consumption data, we were able to quantify the performance of the BEopt simulation software under various conditions. While model results for an individual home can have a wide range of significant absolute error values, when considered in aggregate, the model performed much better. Furthermore, the analysis indicates that models of small homes or homes that have low values of energy consumed per square foot, do not perform as well, especially for homes well below the EIA average. Comparisons of temporal patterns of energy consumption showed that the model might be able to predict temporal energy use trends in the summer and winter times, though it has difficulty predicting exact values at specific times of the day. Finally, we determined that geometry adjustments do not significantly contribute (1%) to a homes overall energy results, at least within the BEopt model.

Bibliography

[1] J. B. Cummings, J. J. Tooley, N. A. Moyer, and R. Dunsmore, "Impacts of duct leakage on infiltration rates, space conditioning energy use, and peak electrical demand in Florida homes," in *ACEEE 1990 Summer Study*, American Council for an Energy Efficient Economy, 1990.

[2] D. A. Jump, I. S. Walker, and M. P. Modera, "Field Measurements of Efficiency and Duct Retrofit Effectiveness in Residential Forced Air Distribution Systems," in *ACEEE Summer Study*, 1996.

[3] "Energy Perspectives 1949–2010," tech. rep., U.S. Energy Information Administration, Oct. 2010.

[4] M. R. Shammin, *Greenhouse Gases - Emission, Measurement and Management*. InTech, Mar. 2012.

[5] "2011 Buildings Energy Data Book," report, US Department of Energy, 2011.

[6] "Residential Energy Consumption Survey (RECS) - Energy Information Administration," 2013.

[7] T. Doggett, "Overcoming Barriers to Smart Grids & New Energy Services Electric Reliability Council of Texas," in *UT Smart Grid Conference*, (Austin), Apr. 2011.

[8] J. D. Rhodes, B. Stephens, and M. E. Webber, "Using energy audits to investigate the impacts of common air-conditioning design and installation issues on

peak power demand and energy consumption in Austin, Texas," *Energy and Buildings*, vol. 43, pp. 3271–3278, Nov. 2011.

[9] J. D. Rhodes, B. Stephens, and M. E. Webber, "Energy Audit Analysis of Residential Air-Conditioning Systems in Austin, Texas," *ASHRAE Transactions*, vol. 118, pp. 143–150, May 2012.

[10] Y. Phillips, "Landlords versus tenants: Information asymmetry and mismatched preferences for home energy efficiency," *Energy Policy*, vol. 45, pp. 112–121, June 2012.

[11] S. B. Sadineni, T. M. France, and R. F. Boehm, "Economic feasibility of energy efficiency measures in residential buildings," *Renewable Energy*, vol. 36, pp. 2925–2931, 2011.

[12] D. Talavera, E. Muñoz Cerón, J. de la Casa, M. Ortega, and G. Almonacid, "Energy and economic analysis for large-scale integration of small photovoltaic systems in buildings: The case of a public location in Southern Spain," *Renewable and Sustainable Energy Reviews*, vol. 15, pp. 4310–4319, Dec. 2011.

[13] T. Downey and J. Proctor, "What Can 13,000 Air Conditioners Tell Us?," in *ACEEE Summer Study on Energy Efficiency in Building*, Proctor Engineering Group, Ltd., 2002.

[14] B. Stephens, J. a. Siegel, and A. Novoselac, "Operational characteristics of residential and light-commercial air-conditioning systems in a hot and humid climate zone," *Building and Environment*, vol. 46, pp. 1972–1983, Oct. 2011.

[15] B. Stephens, J. A. Siegel, and A. Novoselac, "Energy Implications of Filtration in Residential and Light-Commercial Buildings," *ASHRAE Transactions*,

vol. 116, pp. 346–357, 2010.

[16] B. Stephens, A. Novoselac, and J. Siegel, "The Effects of Filtration on Pressure Drop and Energy Consumption in Residential HVAC Systems (RP-1299)," *HVAC&R Research*, vol. 16, pp. 273–294, May 2010.

[17] J. J. Erinjeri, N. M. Witriol, and M. Katz, "Measurement of Return Leaks in Residential Buildings in North Louisiana," *Journal of Building Physics*, vol. 32, pp. 261–280, Jan. 2009.

[18] R. Hendron, S. Farrar-Nagy, R. Anderson, P. Reeves, and E. Hancock, "Thermal Performance of Unvented Attics in Hot-Dry Climates: Results from Building America," *Journal of Solar Energy Engineering*, vol. 126, p. 732, May 2004.

[19] D. S. Parker, "Research highlights from a large scale residential monitoring study in a hot climate," *Energy and Buildings*, vol. 35, pp. 863–876, Oct. 2003.

[20] F. Nemry, A. Uihlein, C. M. Colodel, C. Wetzel, A. Braune, B. Wittstock, I. Hasan, J. Kreiß ig, N. Gallon, S. Niemeier, and Y. Frech, "Options to reduce the environmental impacts of residential buildings in the European UnionPotential and costs," *Energy and Buildings*, vol. 42, pp. 976–984, July 2010.

[21] L. Gustavsson and A. Joelsson, "Life cycle primary energy analysis of residential buildings," *Energy and Buildings*, vol. 42, pp. 210–220, Feb. 2010.

[22] C. Neme, J. Proctor, and S. Nadel, "Energy Savings Potential From Addressing Residential Air-conditioner and Heat Pump Installation Problems," Report A992, American Council for an Energy Efficient Economy, Washington, DC, 1999.

[23] N. Djuric and V. Novakovic, "Correlation between standards and the lifetime commissioning," *Energy and Buildings*, vol. 42, no. 4, pp. 510–521, 2010.

[24] W. Pan and H. Garmston, "Compliance with building energy regulations for new-build dwellings," *Energy*, p. (In Press), 2012.

[25] E. L. Vine, "Residential building code compliance: Implications for evaluating the performance of utility residential new construction programs," *Energy*, vol. 21, no. 12, pp. 1051–1058, 1996.

[26] H. Rutkowski, *Residential Load Calculation: Manual J.* Arlington, VA: Air-conditioning Contractors of America, 2004.

[27] *2009 ASHRAE Handbook - Fundamentals*. 2009.

[28] T. F. Sanquist, H. Orr, B. Shui, and A. C. Bittner, "Lifestyle factors in U.S. residential electricity consumption," *Energy Policy*, vol. 42, pp. 354–364, Mar. 2012.

[29] T. Warren Liao and T. W. Liao, "Clustering of time series data – a survey," *Pattern Recognition*, vol. 38, pp. 1857–1874, Nov. 2005.

[30] T. A. Reddy, "Chapter 8: Classification and Clustering Methods," in *Applied Data Analysis and Modeling for Energy Engineers and Scientists*, pp. 231–251, 2011.

[31] G. Chicco, "Overview and performance assessment of the clustering methods for electrical load pattern grouping," *Energy*, vol. 42, pp. 68–80, June 2012.

[32] Y.-I. Kim, J.-M. Ko, and S.-H. Choi, "Methods for generating TLPs (typical load profiles) for smart grid-based energy programs," in *2011 IEEE Symposium*

on Computational Intelligence Applications In Smart Grid (CIASG), pp. 1–6, IEEE, Apr. 2011.

[33] T. Räsänen, D. Voukantsis, H. Niska, K. Karatzas, and M. Kolehmainen, "Data-based method for creating electricity use load profiles using large amount of customer-specific hourly measured electricity use data," *Applied Energy*, vol. 87, pp. 3538–3545, Nov. 2010.

[34] K.-l. Zhou, S.-l. Yang, and C. Shen, "A review of electric load classification in smart grid environment," *Renewable and Sustainable Energy Reviews*, vol. 24, pp. 103–110, Aug. 2013.

[35] I. P. Panapakidis, M. C. Alexiadis, and G. K. Papagiannis, "Electricity customer characterization based on different representative load curves," in *2012 9th International Conference on the European Energy Market*, pp. 1–8, IEEE, May 2012.

[36] J. D. Rhodes, C. R. Upshaw, C. B. Harris, C. M. Meehan, D. A. Walling, P. A. Navrátil, A. L. Beck, K. Nagasawa, R. L. Fares, W. J. Cole, H. Kumar, R. D. Duncan, C. L. Holcomb, T. F. Edgar, A. Kwasinski, and M. E. Webber, "Experimental and data collection methods for a large-scale smart grid deployment: Methods and first results," *Energy*, vol. 65, pp. 462–471, Feb. 2014.

[37] "The Laredo Pilot Program," tech. rep., Central Power & Light Company, Mar. 1998.

[38] D. Ndiayea and K. Gabriel, "Principal component analysis of the electricity consumption in residential dwellings," *Energy and Buildings*, vol. 43, pp. 446–453, 2011.

[39] M. Toledano-Ayalaa, E. A. Rivas-Araizaa, G. Herrera-Ruiza, G. M. Soto-Zarazua, J. A. Montoya-Sotob, S. Castanedab, and T. Contreras, "Water, gas and electric power monitoring system for residential developments: A technological approach," *Building Serv. Eng. Res. Technol.*, vol. 32, no. 2, pp. 183–197, 2011.

[40] R. H. Socolow, "The Twin Rivers Program on Energy Conservation in Housing: Highlights and Conclusions," *Energy and Buildings*, vol. 1, no. 3, pp. 207–242, 1978.

[41] G. Verbeeck and H. Hens, "Energy savings in retrofitted dwellings: economically viable?," *Energy and Buildings*, vol. 37, no. 7, pp. 747–754, 2005.

[42] D. S. Parker, "Very low energy homes in the United States: Perspectives on performance from measured data," *Energy and Buildings*, vol. 41, no. 5, pp. 512–520, 2009.

[43] R. Rüther, P. J. Knob, C. da Silva Jardim, and S. H. Rebechi, "Potential of building integrated photovoltaic solar energy generators in assisting daytime peaking feeders in urban areas in Brazil," *Energy Conversion and Management*, vol. 49, pp. 1074–1079, May 2008.

[44] S. B. Sadineni, F. Atallah, and R. F. Boehm, "Impact of roof integrated PV orientation on the residential electricity peak demand," *Applied Energy*, vol. 92, pp. 204–210, Apr. 2012.

[45] G. E. Palomino, J. Willes, J. Stevens, and F. Goodman, "Performance Of a Grid Connected Residential Photovoltaic System with Energy Storage," in *26th PVSC*, (Anaheim, CA), Institute of Electrical and Electronics Engineers, 1997.

[46] M. P. McHenry, “Are small-scale grid-connected photovoltaic systems a cost-effective policy for lowering electricity bills and reducing carbon emissions? A technical, economic, and carbon emission analysis,” *Energy Policy*, vol. 45, pp. 64–72, June 2012.

[47] J. D. Mondol, Y. G. Yohanis, and B. Norton, “Optimising the economic viability of grid-connected photovoltaic systems,” *Applied Energy*, vol. 86, pp. 985–999, July 2009.

[48] J. Hernández, P. Vidal, and G. Almonacid, “Photovoltaic in grid-connected buildings, sizing and economic analysis,” *Renewable Energy*, vol. 15, pp. 562–565, Sept. 1998.

[49] T. Meyer and J. Luther, “On the correlation of electricity spot market prices and photovoltaic electricity generation,” *Energy Conversion and Management*, vol. 45, pp. 2639–2644, Oct. 2004.

[50] n. M. R. Frank Sensfußa and M. Genoese, “The merit-order effect: A detailed analysis of the price effect of renewable electricity generation on spot market prices in Germany,” *Energy Policy*, vol. 36, pp. 3086–3094, 2008.

[51] “Carbon Footprint of Electricity Generation,” tech. rep., UK_POST, 2011.

[52] EIA, “Updated Capital Cost Estimates for Utility Scale Electricity Generating Plants,” tech. rep., U.S. Department of Energy, Washington, DC, 2013.

[53] A. K. Singh and S. K. Parida, “Need of Distributed Generation for Sustainable Development in Coming Future,” in *IEEE International Conference on Power Electronics, Drives and Energy Systems (PEDES 2012)*, (Bengaluru, India), IEEE, 2012.

[54] J. Salvatore, “Sustainable Energy in America 2013 Factbook.” 2013.

[55] B. McCracken, G. Fisher, A. Hersey, J. Shead, and K. Sokolic, “Residential solar systems reduce summer peak demand by 58 percent in Texas research trial.” 2013.

[56] I. H. Rowlands, B. P. Kemery, and I. Beausoleil-Morrison, “Optimal solar-PV tilt angle and azimuth: An Ontario (Canada) case-study,” *Energy Policy*, vol. 39, no. 3, pp. 1397–1409, 2011.

[57] M. Lave and J. Kleissl, “Optimum fixed orientations and benefits of tracking for capturing solar radiation in the continental United States,” *Renewable Energy*, vol. 36, no. 3, pp. 1145–1152, 2011.

[58] A. K. Yadav and S. Chandel, “Tilt angle optimization to maximize incident solar radiation: A review,” *Renewable and Sustainable Energy Reviews*, vol. 23, pp. 503–513, 2013.

[59] V. Dorer, R. Weber, and A. Weber, “Performance assessment of fuel cell micro-cogeneration systems for residential buildings,” *Energy and Buildings*, vol. 37, pp. 1132–1146, Nov. 2005.

[60] L. Barelli, G. Bidini, F. Gallorini, and A. Ottaviano, “An energeticexergetic analysis of a residential CHP system based on PEM fuel cell,” *Applied Energy*, vol. 88, pp. 4334–4342, Dec. 2011.

[61] E. Cetin, A. Yilanci, Y. Oner, M. Colak, I. Kasikci, and H. K. Ozturk, “Electrical analysis of a hybrid photovoltaic-hydrogen/fuel cell energy system in Denizli, Turkey,” *Energy and Buildings*, vol. 41, pp. 975–981, Sept. 2009.

[62] V. Dorer and A. Weber, "Energy and CO2 emissions performance assessment of residential micro-cogeneration systems with dynamic whole-building simulation programs," *Energy Conversion and Management*, vol. 50, pp. 648–657, Mar. 2009.

[63] G. Gigliucci, L. Petruzzi, E. Cerelli, A. Garzisi, and A. La Mendola, "Demonstration of a residential CHP system based on PEM fuel cells," *Journal of Power Sources*, vol. 131, pp. 62–68, May 2004.

[64] R. Galvin, "Targeting behavers rather than behaviours: A subject-oriented approach for reducing space heating rebound effects in low energy dwellings," *Energy and Buildings*, vol. 67, pp. 596–607, Dec. 2013.

[65] L. Pérez-Lombard, J. Ortiz, and C. Pout, "A review on buildings energy consumption information," *Energy and Buildings*, vol. 40, pp. 394–398, Jan. 2008.

[66] P. W. James, J. Cummings, J. K. Sonne, R. K. Vieira, and J. F. Klongerbo, "The Effect of Residential Equipment Capacity on Energy Use, Demand, and Run-Time," *ASHRAE Transactions*, vol. 103, no. 2, pp. 297–303, 1997.

[67] J. Proctor, "Field measurements of new residential air-conditioners in Phoenix, Arizona," *ASHRAE Transactions*, vol. 103, no. 1, pp. 406–415, 1997.

[68] J. Proctor, "Monitored In-Situ Performance of residential Air-Conditioning Systems," *ASHRAE Transactions*, vol. 104, no. 1B, pp. 1833–1840, 1998.

[69] R. J. Mowris, A. Blankenship, and E. Jones, "Field measurements of air conditioners with and without TXVs," in *Proceedings of the ACEEE Summer Study on Energy Efficiency in Buildings*, 2004.

[70] L. Palmiter and P. W. Francisco, "Measured Efficiency of Forced-Air Distribution Systems in 24 Homes," in *1994 ACEEE Summer Study on Technology Research, Development and Evaluation*, 1994.

[71] D. Parker, P. Fairey, and L. Gu, "Simulation of the effects of duct leakage and heat transfer on residential space-cooling energy use," *Energy and Buildings*, vol. 20, pp. 97–113, Jan. 1993.

[72] J. A. Siegel, I. S. Walker, and M. Sherman, "Delivering tons to the register: energy efficient design and operation of residential cooling systems," Paper LBNL-45315, Lawrence Berkeley National Laboratory, 2000.

[73] D. L. ONeal, A. Rodriguez, M. Davis, and S. Kondepudi, "Return Air Leakage Impact on Air Conditioner Performance in Humid Climates," *Journal of Solar Energy Engineering*, vol. 124, no. 1, p. 63, 2002.

[74] "About the Energy Conservation Audit and Disclosure (ECAD) Ordinance," 2013.

[75] Austin Energy and C. of Austin, "AN ORDINANCE ADDING A NEW CHAPTER 6-7 TO THE CITY CODE RELATING TO ENERGY CONSERVATION AUDIT AND DISCLOSURE REQUIREMENTS; CREATING AN OFFENSE AND IMPOSING PENALTIES UP TO $2,000 FOR EACH OFFENSE," 2008.

[76] T. Kisner, "Personal Correspondence," 2011.

[77] "Performance Rating of Unitary Air-Conditioning & Air-Source Heat Pump Equipment," Tech. Rep. ANSI/AHRI Standard 210/240, Air-Conditioning, Heating and Refrigeration Institute, Arlington, VA, 2008.

[78] "U.S. Climate Normals, National Oceanic and Atmospheric Administration." Online.

[79] A. Rudd, J. Lstiburek, P.Eng, and K. Ueno, "Unvented-cathedralized attics: Where we've been and where we're going," Tech. Rep. 9904, Building Science Corporation, 1999.

[80] "Home : ENERGY STAR," 2014.

[81] S. Pigg, "Central Air Conditioning in Wisconsin," Tech. Rep. 241-1, Energy Center of Wisconsin, May 2008.

[82] J. K. Sonne, D. S. Parker, and D. B. Shirey, "Measured Impacts of Proper Air Conditioning Sizing in Four Florida Case Study Homes," Tech. Rep. FSEC-CR-1641-06, Florida Solar Energy Center, 2006.

[83] G. R. Newsham and B. G. Bowker, "The effect of utility time-varying pricing and load control strategies on residential summer peak electricity use: A review," *Energy Policy*, vol. 38, pp. 3289–3296, July 2010.

[84] J. D. Rhodes, K. Nagasawa, C. Upshaw, and M. E. Webber, "The Role Of Small Distributed Natural Gas Fuel Cell Technologies In The Smart Energy Grid," in *Proceedings of the ASME 2012 6th International Conference on Energy Sustainability & 10th Fuel Cell Science, Engineering and Technology Conference*, American Society of Mechanical Engineers, July 2012.

[85] Z. Li and S. Deng, "An experimental study on the inherent operational characteristics of a direct expansion (DX) air conditioning (A/C) unit," *Building and Environment*, vol. 42, pp. 1–10, Jan. 2007.

[86] 1996 ACEEE Summer Study on Energy Efficiency in Buildings, *How contractors really size air-conditioning systems*, no. 8, (Washington, DC), 1996.

[87] "Electricity Market Module." 2011.

[88] J. McGarvey, K. Costello, R. S. Potter, M. Murphy, and P. Laurent, "What Generation Mix Suits Your State? Tools for Comparing Fourteen Technologies across Nine Criteria." 2007.

[89] D. Belzer, G. Mosey, P. Plympton, and L. Dagher, "Home Performance with ENERGY STAR: Utility Bill Analysis on Homes Participating in Austin Energy's Program." 2007.

[90] P. W. Francisco and L. Palmiter, "Field Evaluation of a New Device to Measure Air Handler Flow," *ASHRAE Transactions*, vol. 109, no. 2, 2003.

[91] G. Helcke, F. Conti, B. Daniotti, and R. Peckham, "A detailed comparison of energy audits carried out by four separate companies on the same set of buildings," *Energy and Buildings*, vol. 14, pp. 153–164, Jan. 1990.

[92] EIA, "Annual Energy Review 2010," tech. rep., Energy Information Administration, U.S. Department of Energy, 2011.

[93] W. Katzenstein and J. Apt, "Air Emissions Due To Wind And Solar Power," *Environmental Science & Technology*, vol. 43, pp. 253–258, Jan. 2009.

[94] C. M. Meehan, C. W. King, J. B. Garrison, and M. E. Webber, "The Total Impact of Wind Energy Variability on Fossil Fuel Emission Rates in Texas," in *31st USAEE/IAEE North American Conference*, pp. 1–17, USAEE, 2012.

[95] P. L. Mokhtarian and K. V. Varma, "The trade-off between trips and distance traveled in analyzing the emissions impacts of center-based telecommuting," *Transportation Research Part D: Transport and Environment*, vol. 3, pp. 419–428, Nov. 1998.

[96] "The Texas Advanced Computing Center," 2013.

[97] K. Gram-Hanssen, C. Kofod, and K. N. r. Petersen, "Different Everyday Lives: Different Patterns of Electricity Use ECEEE," in *2004 American Council for Energy Efficient Economy Summer study in Buildings, American Council for an Energy Efficient Economy*, (Washington, DC), 2004.

[98] T. Hothorn and B. S. Everitt, *A Handbook of Statistical Analyses Using R, Second Edition.* Chapman and Hall/CRC, 2009.

[99] A. Fernihough, "CRAN - Package mfx," 2013.

[100] A. Gelman and J. Hill, *Data Analysis Using Regression and Multilevel/Hierarchical Models*, vol. 625 of *Analytical methods for social research.* Cambridge: Cambridge University Press, 11 ed., 2006.

[101] R. F. Engle, "Wald, likelihood ratio, and Lagrange multiplier tests in econometrics," *Handbook of Econometrics*, vol. 2, pp. 775–826, 1984.

[102] A. K. Srivastava, R. L. Pineda, and P. Mandal, "Wind power generation impact on electricity price in ERCOT," in *2012 IEEE Power and Energy Society General Meeting*, pp. 1–7, IEEE, July 2012.

[103] "Heating and cooling no longer majority of U.S. home energy use – U.S. Energy Information Administration (EIA)," 2013.

[104] EIA, "Monthly Energy Review – May 2012." 2012.

[105] IPCC, "Climate Change 2013: The Physical Science Basis. Working Group I Contribution to the IPCC 5th Assessment Report - Changes to the Underlying Scientific/Technical Assessment." 2013.

[106] EIA, "Assumptions to the Annual Energy Outlook 2013," Tech. Rep. January, 2013.

[107] C. B. Christensen and G. M. Barker, "Effects Of Tilt And Azimuth On Annual Incident Solar Radiation For United States Locations," in *Solar Forum 2001*, (Washington, DC), 2001.

[108] J. W. Stultz, "Thermal and Other Tests of Photovoltaic Modules Performed in Natural Sunlight," *Journal of Energy*, vol. 3, pp. 363–372, Nov. 1979.

[109] A. Schroder, "Determination of annual optimal altitude and azimuth angles of fixed tilt solar collectors in the continental United States using the National Solar Radiation Database," in *Proceedings of the ASES National Solar Conference*, May 2011.

[110] J. Luoma, M. Lave, and J. Kleissl, "Optimum fixed orientations considering day-ahead market energy pricing in California," in *American Solar Energy Society Conference*, (Denver, CO), pp. 1–5, 2012.

[111] J. A. Duffie and W. A. Beckman, *Solar Engineering of Thermal Processes*. Wiley, 3rd ed., 2006.

[112] J. J. E. Hay and D. D. C. McKay, "Estimating solar irradiance on inclined surfaces: a review and assessment of methodologies," *International Journal of Solar Energy*, vol. 3, pp. 203–240, Sept. 1985.

[113] E. Skoplaki and J. Palyvos, "On the temperature dependence of photovoltaic module electrical performance: A review of efficiency/power correlations," *Solar Energy*, vol. 83, pp. 614–624, May 2009.

[114] Power-one, "AURORA UNO Photovoltaic Inverters Technical Manual," tech. rep., 2013.

[115] Lumos, "Lumos LS 250 Series," Tech. Rep. 3, 2012.

[116] S. Wilcox and W. Marion, "Users Manual for TMY3 Data Sets." 2008.

[117] R. H. Byrd, P. Lu, J. Nocedal, and C. Zhu, "A Limited Memory Algorithm for Bound Constrained Optimization," *SIAM Journal on Scientific Computing*, vol. 16, pp. 1190–1208, Sept. 1995.

[118] "Utilities — Open Energy Information," 2013.

[119] "City of Austin Electric Rate Schedules," 2013.

[120] National Renewable Energy Lab, "The OpenPV Project," 2013.

[121] EIA, "How much electricity does an American home use? - FAQ - U.S. Energy Information Administration (EIA)," 2013.

[122] M. Powell, K. Meinhardt, V. Sprenkle, L. Chick, and G. McVay, "Demonstration of a highly efficient solid oxide fuel cell power system using adiabatic steam reforming and anode gas recirculation," *Journal of Power Sources*, vol. 205, pp. 377–384, May 2012.

[123] "Austin Energy Green Building." \url{https://my.austinenergy.com/wps/portal/aegb/aegb/}, Oct. 2012.

[124] R. Wang, T. Ge, C. Chen, Q. Ma, and Z. Xiong, "Solar sorption cooling systems for residential applications: Options and guidelines," *International Journal of Refrigeration*, vol. 32, pp. 638–660, June 2009.

[125] US Energy Information Administration, "State Ranking 9. Residential Electricity Prices." On the Web, 2012.

[126] US Energy Information Administration, "NATURAL GAS." On the Web, 2012.

[127] National Fuel Cell Research Center, "Fuel Cell Information: Challenges." On the Web, 2012.

[128] T. Griffin, K. Tomsovic, D. Secrest, and A. Law, "Placement of dispersed generation systems for reduced losses," in *Proceedings of the 33rd Annual Hawaii International Conference on System Sciences*, vol. vol.1, p. 9, IEEE Comput. Soc, 2000.

[129] M. Czachorski and N. Leslie, "Source Energy and Emission Factors for Building Energy Consumption," Natural Gas Codes and Standards Research Consortium 1, American Gas Foundation, Washington, DC, Aug. 2009.

[130] C. Garbacz, "A model of residential demand for electricity using a national household sample," *Energy Economics*, vol. 5, pp. 124–128, Apr. 1983.

[131] E. Hirst, R. Goeltz, and J. Carney, "Residential energy use," *Energy Economics*, vol. 4, pp. 74–82, Apr. 1982.

[132] N. Kaza, "Understanding the spectrum of residential energy consumption: A quantile regression approach," *Energy Policy*, vol. 38, pp. 6574–6585, Nov. 2010.

[133] T. Guiterman and M. Krarti, "Analysis of Measurement and Verification Methods for Energy Retrofits Applied to Residential Buildings," *ASHRAE Transactions*, vol. 117, pp. 382–394, Oct. 2011.

[134] P. Xu, T. Xu, and P. Shen, "Energy and behavioral impacts of integrative retrofits for residential buildings: What is at stake for building energy policy reforms in northern China?," *Energy Policy*, vol. 52, pp. 667–676, Jan. 2013.

[135] Z. Ma, P. Cooper, D. Daly, and L. Ledo, "Existing building retrofits: Methodology and state-of-the-art," *Energy and Buildings*, vol. 55, pp. 889–902, Dec. 2012.

[136] B. Guler, A. S. Fung, M. Aydinalp, and V. I. Ugursal, "Impact of energy efficiency upgrade retrofits on the residential energy consumption in Canada," *International Journal of Energy Research*, vol. 25, pp. 785–792, July 2001.

[137] "Home Performance with ENERGY STARRebate Levels," 2013.

[138] B. E. Hansen, *Econometrics*. Self, 12 ed., 2013.

[139] E. Valor, V. Meneu, and V. Caselles, "Daily Air Temperature and Electricity Load in Spain," *Journal of Applied Meteorology*, vol. 40, pp. 1413–1421, Aug. 2001.

[140] R. G. Quayle and H. F. Diaz, "Heating Degree Day Data Applied to Residential Heating Energy Consumption," *Journal of Applied Meteorology*, vol. 19, pp. 241–246, Mar. 1980.

[141] "The Comprehensive R Archive Network," 2013.

[142] J. A. Hausman, "Specification Tests in Econometrics," *Econometrica*, vol. 46, no. 6, pp. 1251–1271, 1978.

[143] D. Young, "Who pays for the beer fridge? Evidence from Canada," *Energy Policy*, vol. 36, pp. 553–560, Feb. 2008.

[144] "Standard for the Calculation and Labeling of the Energy Performance of Low-Rise Residential Buildings using the HERS Index." 2013.

[145] "Austin Energy Rates," 2013.

[146] D. B. Crawley, J. W. Hand, M. Kummert, and B. T. Griffith, "Contrasting the capabilities of building energy performance simulation programs," *Building and Environment*, vol. 43, pp. 661–673, Apr. 2008.

[147] B. Polly, N. Kruis, and D. Roberts, "Assessing and Improving the Accuracy of Energy Analysis for Residential Buildings," tech. rep., National Renewable Energy Lab, Golden, CO, 2011.

[148] C. Christensen, R. Anderson, S. Horowitz, A. Courtney, and J. Spencer, "BEopt Software for Building Energy Optimization : Features and Capabilities." 2006.

[149] S. Pigg and M. Nevius, "Energy and Housing in Wisconsin." 2000.

[150] R. Judkoff and J. Neymark, "Model Validation and Testing : The Methodological Foundation of ASHRAE Standard 140." 2006.

[151] R. Judkoff, D. Wortman, B. O. Doherty, and J. Burch, "A Methodology for Validating Building Energy Analysis Simulations." 2008.

[152] B. Polly, S. Horowitz, C. Booten, N. Kruis, and C. C. Nrel, "Automated Comparison of Building Energy Simulation Engines." 2012.

[153] W. J. Cole, J. D. Rhodes, W. Gorman, K. X. Perez, and M. E. Webber, "Community-scale residential air conditioning control for effective grid management," *Under Review at Applied Energy*, 2014.